Asymptotic Analysis of Thin Plates Under Normal Load and Horizontal Edge Thrust

Thesis by
Mary Elizabeth Brewster

In Partial Fulfillment of the Requirements

for the Degree of

Doctor of Philosophy

California Institute of Technology

Pasadena, California

1987

(Submitted October 1, 1986)

Acknowledgments

I would like to thank my advisor, Professor H. B. Keller, for continually asking questions I didn't have the answers to and for putting up with my mercurial temperament. My thanks also go to Professor R. Kannan, my advisor during my master's studies at the University of Texas at Arlington, for his guidance, support and friendship. I also wish to express my appreciation to the many faculty and students of Caltech whom I have met for enriching the time I have spent here. Particularly, I would like to thank Professor D. S. Cohen for all the advice that I didn't follow and Jeff Aguilera, who deserves the credit for anything in this dissertation that looks good.

Financial support for my graduate studies has been generously provided by institute fellowships and a teaching assistantship from Caltech, research assistantships from the Department of Energy under the contract DE-AS03-76ER72012, from the Army under the contract DAAG29-85-K-0092 and a scholarship from the ARCS Foundation. Computations were performed at Caltech on the IBM 4341 and the manuscript was typeset using the HP TEX system with the aid of the THEME software written by Jeffrey A. Aguilera.

Above all my gratitude is due to my husband, John, whose never-ending love and support have made this work possible.

Abstract

We consider the radially symmetric nonlinear von Kármán plate equations for circular or annular plates in the limit of small thickness. The loads on the plate consist of a radially symmetric pressure load and a uniform edge load. The dependence of the steady states on the edge load and thickness is studied using asymptotics as well as numerical calculations. The von Kármán plate equations are a singular perturbation of the Föppl membrane equation in the asymptotic limit of small thickness. We study the role of compressive membrane solutions in the small thickness asymptotic behavior of the plate solutions.

We give evidence for the existence of a singular compressive solution for the circular membrane and show by a singular perturbation expansion that the nonsingular compressive solutions approach this singular solution as the radial stress at the center of the plate vanishes. In this limit, an infinite number of folds occur with respect to the edge load. Similar behavior is observed for the annular membrane with zero edge load at the inner radius in the limit as the circumferential stress vanishes.

We develop multiscale expansions, which are asymptotic to members of this family, for plates with edges that are elastically supported against rotation. At some thicknesses this approximation breaks down and a boundary layer appears at the center of the plate. In the limit of small normal load, the points of breakdown approach the bifurcation points corresponding to buckling of the nondeflected state. A uniform asymptotic expansion for small thickness combining the boundary layer with a multiscale approximation of the outer solution is developed for this case. These approximations complement the well known boundary layer expansions based on tensile membrane solutions in describing the bending and stretching of thin plates. The approximation becomes inconsistent as the clamped state is approached by increasing the resistance against rotation at the edge. We prove that such an expansion for the clamped circular plate cannot exist unless the pressure load is self-equilibrating.

Table of Contents

Table

List of Figures

CHAPTER 1

Introduction

The design of light-weight structures often requires the determination of the behavior of thin plates undergoing deformations greater than their thickness. Linear plate theory is valid for deformations that are small compared to the thickness; thus, a nonlinear theory is required for the study of this problem. The von Kármán theory is a nonlinear treatment valid for deformations that are small compared to the large dimensions of the plate. We study the steady states of the von Kármán equations for circular and annular plates subjected to a pressure load and a horizontal edge load in the asymptotic limit of small thickness. In particular, we are interested in constructing solutions with compressive radial stress. In the limit of small thickness, the von Kármán plate equations are a singular perturbation of the Föppl membrane equation. The main goal of this dissertation is to delineate cases where it is and is not possible to approximate compressive plate solutions in some asymptotic sense by compressive membrane solutions.

Formulation of the Problem. We take a plate with outer radius R, inner radius aR and thickness H; the dimensionless parameter a is the ratio of inner to outer radius; for the circular plate $a = 0$. The independent variables r, θ, z represent postion in the undeformed plate in polar coordinates. We assume radially symmetric deformation with the vertical and radial displacements of the midplane $z = 0$ being $w(r)$ and $\rho(r)$, respectively. A schematic of the deformation is shown in Figure (1.1). We denote by σ_r, σ_θ, and σ_z the normal

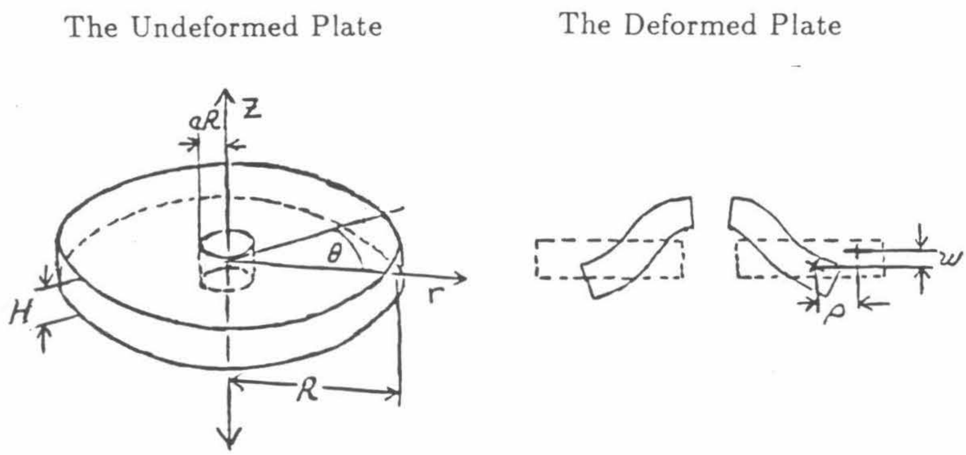

FIGURE 1.1. Deformation of an annular plate
The independent variables r, θ, and ϕ represent position in the undeformed plate. The dependent variables w and ρ measure the vertical and radial displacements in the deformed plate.

stresses in the radial, circumferential, and vertical directions; in von Kármán plate theory, shear strains and stresses are considered negligible. We let

$$\sigma_r = -\tilde{v}.$$

Note that positive $\tilde{v}$ corresponds to compressive radial stress. It may be shown that in the von Kármán plate theory the circumferential stress is given by

$$\sigma_c = -\tilde{v} - r\frac{d\tilde{v}}{dr}.$$

A normal pressure p is applied to the upper surface $z = H/2$; we assume that the pressure is positive at the inner radius aR. The normal stress in the vertical direction is given by

$$\sigma_z = \left(z + \frac{H}{2}\right)\frac{p(r)}{H}.$$

We specify $w(R) = 0$ to locate the plate in the z-direction and let

$$\tilde{u} = \frac{1}{r}\frac{dw}{dr}. \tag{1.1}$$

Clearly, then, the vertical displacement of the midplane is given by

$$w(r) = -\int_r^R s\tilde{u}(s)\,ds.$$

Also, the radial displacement is given by

$$\rho(r) = -\frac{1}{E}\left(r^2\frac{d\tilde{v}}{dr} + r(1-\nu)\tilde{v}\right)$$

where ν is Poisson's ratio. Thus, the normal stresses σ_r, σ_c, σ_z and the displacements w and ρ may be determined from the functions $\tilde{u}$ and $\tilde{v}$.

The equations of the von Kármán[1] theory are the compatibility equation

$$\frac{2}{E}\left(\frac{d^2\tilde{v}}{dr^2} + \frac{3}{r}\frac{d\tilde{v}}{dr}\right) = \tilde{u}^2, \tag{1.2}$$

and the equilibrium equation

$$\frac{E}{2}(\gamma H)^2\frac{1}{r}\frac{d}{dr}\,r\frac{d}{dr}\,\frac{1}{r}\frac{d}{dr}\,r^2\tilde{u} + \frac{1}{r}\frac{d}{dr}\,(r^2\tilde{u}\tilde{v}) = \frac{p}{hR} \tag{1.3}$$

for $r \in [aR, R]$, where $\gamma^2 = (6(1-\nu^2))^{-1}$ and E is Young's modulus. Multiplying through by r in (1.3) and integrating from the inner radius aR to r, we find

$$\frac{E}{2}(\gamma H)^2\left(r^2\frac{d^2\tilde{u}}{dr^2} + 3r\frac{d\tilde{u}}{dr}\right) + r^2\tilde{u}\tilde{v} = r^2\tilde{g}(r) + \tilde{A} \tag{1.4}$$

where $\tilde{g}$ is

$$\tilde{g}(r) = \frac{1}{Hr^2}\int_{aR}^{r} \xi p(\xi)\,d\xi$$

and $\tilde{A}$ is a constant given by

$$\tilde{A} = \frac{E}{2}(\gamma H)^2\left(a^2\frac{d^2\tilde{u}}{dr^2}(a) + 3a\frac{d\tilde{u}}{dr}(a)\right) + a^2\tilde{u}(a)\tilde{v}(a).$$

[1] Cf. J. J. Stoker, *Nonlinear Elasticity*, 1968

We obtain a dimensionless form of the equations via the transformations

$$
\begin{aligned}
h &= \frac{H}{\tau R}, & x &= \frac{r}{R}, \\
u &= \frac{R}{\tau}\tilde{u}, & v &= \frac{2}{\tau^2 E}\tilde{v}, \\
g &= \frac{2R}{\tau^3 E}\tilde{g}, & A &= \frac{2}{\tau^3 RE}\tilde{A}
\end{aligned}
$$

where

$$
\tau^3 = \frac{\gamma^3 R}{HE} \cdot p(aR).
$$

This choice of τ gives us

$$
g(x) \sim 1 - \frac{a^2}{x^2} \qquad \text{as } x \to a.
$$

We have utilized the assumption that $p(aR) > 0$ so that $\tau > 0$; the case of $p(aR) = 0$ must be normalized differently. Note also that the dimensionless parameter h may become small in a number of ways. We will refer to the parameter h as the "thickness" because it varies directly with the actual thickness H in the case of fixed outer radius and pressure load, but it should be kept in mind that h is also influenced by the magnitude of the pressure load.

Using the above transformations, the equations (1.2, 1.4) become

$$
\begin{aligned}
h^2(u'' + \frac{3}{x}u') + uv &= g(x) + \frac{A}{x^2}, \\
v'' + \frac{3}{x}v' &= u^2
\end{aligned}
\tag{1.5}
$$

for $x \in [a, 1]$. *The equations (1.5) along with suitably chosen boundary conditions constitute the von Kármán plate theory, which we employ for our study of thin radially symmetric circular or annular plates.* The von Kármán plate theory is discussed further in Appendix I.

For well-posedness, five boundary conditions are required. In the case of the circular plate, we have three conditions arising from the requirement that the solution be smooth at the origin. These are

$$A = 0, \qquad u'(0) = 0, \qquad v'(0) = 0. \tag{1.6}$$

For annular plates, we specify the radial stress at the inner edge

$$v(a) = \eta, \tag{1.7}$$

and we take the conditions corresponding to a free edge

$$au'(a) + (1+\nu)u(a) = 0, \qquad a^2 u(a)\eta = A. \tag{1.8}$$

The last two conditions are the natural boundary conditions arising from the variational formulation of the problem. Physically, the former implies that the bending moment vanishes; the latter is a joint requirement embodying the shears and rate of change of twisting moment. Note that in the case $\eta = 0$, i.e., no applied stress at the inner edge, we have $A = 0$. For specified $\eta \neq 0$, we cannot determine A *a priori*. For a given value of A, we define the function $\hat{g}(x) = g(x) + A/x^2$.

At the outer edge in the case of either circular or annular plates, we specify the stress

$$v(1) = \lambda, \tag{1.9}$$

and also we impose one of two boundary conditions:

$$u'(1) + Qu(1) = 0, \quad Q \geq 1+\nu \qquad \text{or} \qquad u(1) = 0. \tag{1.10}$$

The first case, $(1.10a)$, corresponds to the outer edge being elastically supported against rotation as described by MANSFIELD.[2] If $Q = 1+\nu$ we say

[2] *The Bending and Stretching of Plates*, p.17, 1964

that the plate is simply supported; the support against rotation vanishes. As Q increases, the strength of the support against rotation increases; in the limit $Q \to +\infty$, we obtain the clamped edge condition (1.10b).

We study each of these problems individually in the asymptotic limit as $h \to 0$, and also we consider the limiting case; the plate elastically supported against rotation passes into the clamped plate as $Q \to +\infty$.

Singular Perturbation of the Membrane Problem. The von Kármán theory of thin plates is a singular perturbation of the Föppl[3] membrane equation

$$v'' + \frac{3}{x}v' = \frac{\hat{g}^2(x)}{v^2} \tag{1.11}$$

for $x \in [a, 1]$, with boundary conditions

$$\begin{gathered} v'(0) = 0 \qquad \text{or} \qquad v(a) = \eta, \\ v(1) = \lambda. \end{gathered} \tag{1.12}$$

As in most singular perturbation problems, we cannot expect the thin plate solutions to pass uniformly into the membrane solutions as the thickness h vanishes. We wish to study compressive plate solutions; thus, we attempt to form asymptotic expansions for the plate solutions based on compressive membrane solutions.

Compressive Membrane Solutions. We will first discuss the properties of the compressive solutions of the membrane equation (1.11). The existence of a branch of compressive circular membrane solutions is demonstrated by CALLEGARI, REISS AND KELLER.[4] In this paper, phase-plane analysis is performed in the case of uniform pressure load to show the existence of a value

---

[3] *Vorlesungen über technische Mechanik*, Vol. 5, 1907

[4] *Comm. Pure Appl. Math.* **24** (1971)

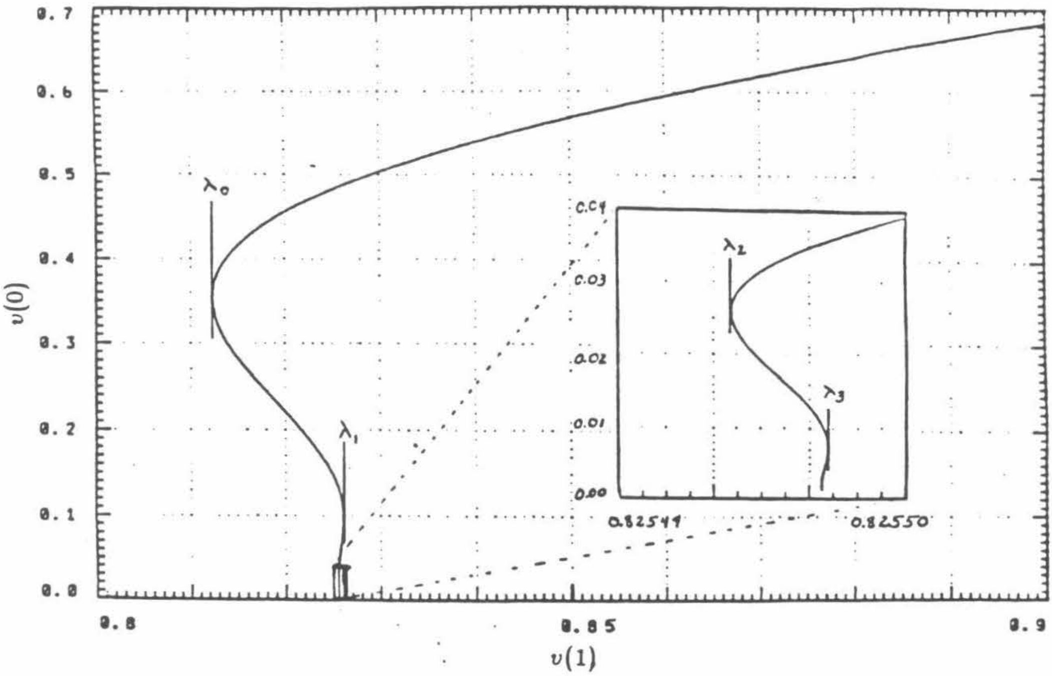

FIGURE 1.2. Continuation diagram for the circular membrane
The family of compressive circular membrane solutions for uniform pressure load $\hat{g}(x) \equiv 1$ is shown. The components of the solution plotted are the radial stress at the edge $v(1) = \lambda$ (abscissa) and the radial stress at the center $v(0)$ (ordinate). The folds λ_0 and λ_1 can be seen on the large scale plot; the inset shows the folds λ_2 and λ_3, which are closer to the limit λ_∞.

of the edge load, λ_∞, for which there are an infinite number of membrane solutions. The compressive solution branch has an infinite number of folds with respect to the edge load and the fold points converge to λ_∞. These folds are illustrated in Figure (1.2) where the compressive solution branch is shown for the case of uniform pressure load.

It is observed by CALLEGARI, REISS AND KELLER that for uniform pressure load, i.e., $\hat{g}(x) = 1$, there exists a singular solution of the circular membrane problem

$$v_\infty(x) = (\tfrac{3}{4}x)^{\frac{2}{3}}$$

which satisfies $v_\infty(1) = \lambda_\infty = (\frac{3}{4})^{\frac{2}{3}}$. This solution is compressive for $x \in (0, 1]$

but has $v(0) = 0$, while $v'(x)$ becomes unbounded as $x \to 0$. It may be shown by phase-plane analysis that in the limit $v(0) \to 0^+$ the solutions converge to this singular solution.

In the second chapter, we will present evidence that such a singular compressive solution exists for the circular membrane under arbitrary smooth pressure load and also for the annular membrane with vanishing radial stress at the inner edge. Specifically, we propose an iteration procedure

$$v_0(x) = (\tfrac{3}{4}x)^{\frac{2}{3}},$$
$$v_{n+1}(x) = \int_0^x \left(\xi - \frac{\xi^3}{x^2}\right) \frac{\hat{g}^2(\xi)}{2v_n^2(\xi)}\, d\xi,$$

which we conjecture will converge to a singular compressive membrane solution. The iterations are carried out approximately using numerical integration, and these calculations support the conjecture of convergence. For the annular membrane with $\eta = 0$, a similar iteration procedure may be defined to obtain a singular compressive solution.

We derive the asymptotic behavior of the solutions near this singular solution via perturbation analysis. The fold points λ_0, λ_1, ... alternate about the limit λ_∞. Thus we find

$$\lambda_{2m} < \lambda_\infty < \lambda_{2m+1}$$

for $m \geq 0$. It is also observed that

$$\lambda_{2m} < \lambda_{2m+2} \quad \text{and} \quad \lambda_{2m+3} < \lambda_{2m+1}.$$

The asymptotic analysis gives these results for the folds λ_m, λ_{m+1}, ... where m is sufficiently large; numerical calculations for a variety of pressure loads confirm that this property holds for $m \geq 0$. Thus, for $\lambda_{2m} < \lambda < \lambda_{2m+2}$, there are $2m+2$ distinct solutions; for $\lambda_{2m+1} < \lambda < \lambda_{2m-1}$, there are $2m+1$ solutions. For $0 < \lambda < \lambda_0$, membrane solutions do not exist.

The fold points λ_n, λ_{n+2} are called successive fold points; from the asymptotic analysis, the spacing between successive fold points is found at leading order to decrease geometrically; i.e.,

$$\frac{\lambda_{n+2}-\lambda_n}{\lambda_n-\lambda_{n-2}} \sim b^2, \qquad \frac{\lambda_{n+2}-\lambda_n}{\lambda_{n+1}-\lambda_{n-1}} \sim -b, \tag{1.13}$$

where $b = \exp(-5\pi/\sqrt{23}) \approx 0.038$. These ratios are obtained for sufficiently smooth pressure load given the assumption that the pressure does not vanish at the center of the plate. For the annular plate with $\eta = 0$, the asymptotic behavior (1.13) is also observed with the same value of the constant b as for the circular membrane provided the pressure does not vanish at the inner edge. The case where the pressure does vanish at the center or the inner edge may be treated similarly, but a different value of b is obtained. A generalized form of the circular membrane is studied by FIER[5] using phase-plane analysis, and our results agree with the asymptotic behavior obtained in those cases where both methods are applicable.

Plate Solutions—Background. Although solutions of the von Kármán plate equations with various boundary conditions have been studied using approximate methods by many investigators, few theoretical results are known concerning plate solutions with compressive radial stress. For the case of vanishing pressure, the unbuckled states corresponding to zero vertical deflection ($u \equiv 0$) can be found exactly. The radial stress v must satisfy

$$v'' + \frac{3}{x}v' = 0.$$

[5] *Ph. D. Thesis, California Institute of Technology*, 1985

For the circular plate, this state has constant radial stress; for the annular plate, the radial stress has the form

$$v = \alpha + \frac{\beta}{x^2}$$

where α and β are chosen so that the conditions $v(a) = \eta$, $v(1) = \lambda$ are satisfied. Buckled states for this problem have been studied by FRIEDRICHS AND STOKER,[6] KELLER, KELLER AND REISS,[7] and WOLKOWISKY.[8] In the first paper it is shown that for the clamped circular plate there is one pair of buckled states with no internal nodes—an internal node is a point $x \in (0,1)$, where $u(x) = 0$—for all values of λ greater than the buckling load $\lambda_1 = h^2 x_1{}^2$, where x_n is the nth positive zero of J_1; no other buckled states exist when λ is less than or equal to $\lambda_2 = h^2 x_2{}^2$. In the second paper it is shown that for every positive integer n a pair of buckled states with $n-1$ internal nodes exists when the edge load λ is slightly larger than $\lambda_n = h^2 x_n{}^2$. The pairs of buckled states differ only in the sign of u. In the third paper it is shown that these pairs of buckled states continue to exist for all $\lambda > \lambda_n$. This result is also extended to the case of the simply supported circular plate.

Fewer results are available for compressive solutions in the case of nonvanishing pressure. KEENER AND KELLER[9] have applied perturbed bifurcation theory to show that for small pressure load the bifurcations from the unbuckled state are perturbed in such a way that the solution branches separate from each other—bifurcation is no longer present. On the other hand, asymptotic analysis suggests that the perturbed solutions are asymptotic to the unper-

---

[6] *Amer. J. Math.* **63** (1941)

[7] *Q. Appl. Math.* **20** (1962)

[8] *Bifurcation Theory and Nonlinear Eigenvalue Problems*, 1969

[9] *Lecture Notes in Mathematics*, Vol. **280**, 1972

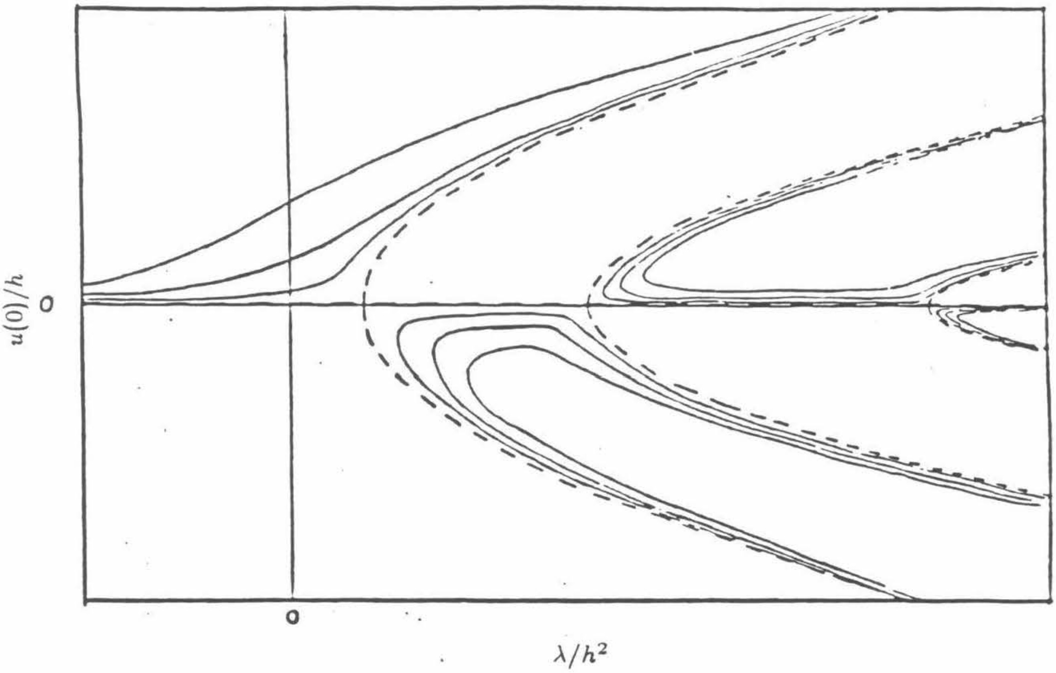

FIGURE 1.3. A sketch of perturbed bifurcation for small pressure load
The bifurcation diagram for the case of vanishing pressure load is given by the dashed lines. The solid lines represent families of solutions for the case of small pressure load. Three different loads are shown; as the load becomes smaller, the solution curve approaches the curve for zero load. Also, as the edge load λ increases for fixed pressure load, the solution curve is asymptotic to the curve for zero pressure load.

turbed buckled states for $\lambda \to +\infty$ on a particular branch. This information is presented pictorially in Figure (1.3).

Asymptotic Analysis for Compressive Plate Solutions. The compressive solution branch with its infinite number of folds is observed in the membrane problem for arbitrary smooth pressure load; however, such a branch is not apparent for the plate problem as can be seen from the continuation diagrams in Figures (1.4, 1.5). The numerical methods used to obtain these plots are described in Appendix II. The family of plate solutions consists of an infinite number of distinct branches, which are numbered as shown. The

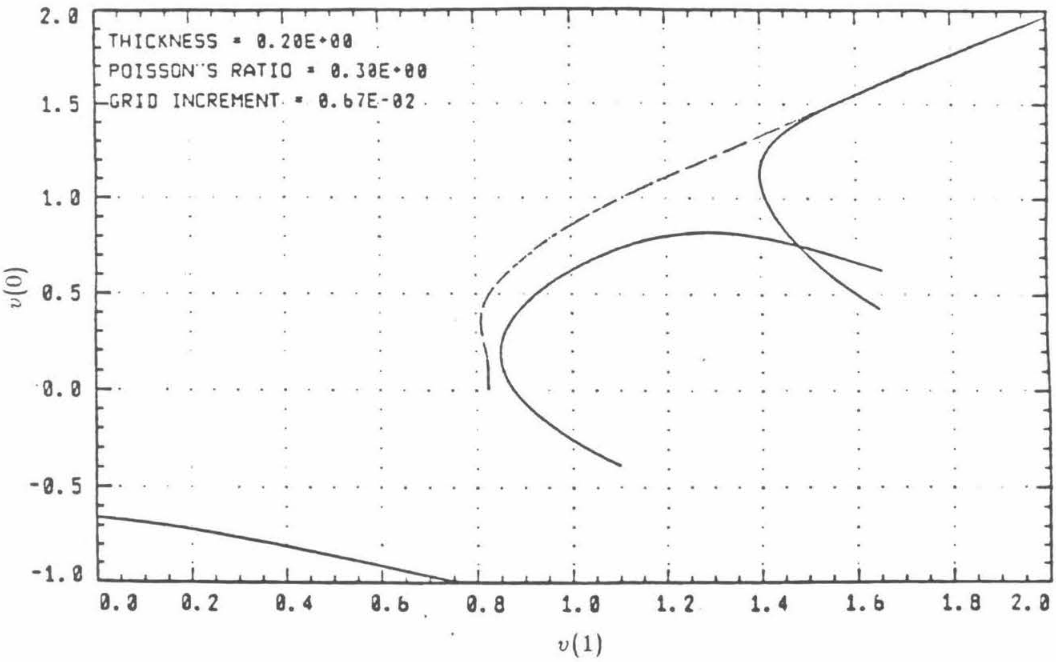

FIGURE 1.4. Continuation diagram for the simply supported circular plate, $h = 0.20$ The von Kármán plate equations for a simply supported circular plate under uniform pressure load are solved for varying edge load by continuation. The radial stress at the center $v(0)$ is plotted against the edge load $\lambda = v(1)$ for h fixed at 0.20. Several plate solution branches are shown by the solid lines. The family of compressive membrane solutions is also plotted for comparison and is represented by the dotted line.

plot indicates that some plate solutions are related to compressive membrane solutions; a segment of a branch of the plate solutions will approach a segment of the compressive membrane solution branch. As the thickness vanishes, the index of the plate branch having a point that is close to a given membrane solution tends to infinity. *We quantify this behavior by constructing asymptotic expansions for the plate solutions based on compressive membrane solutions.*

For illustrative purposes, we first discuss the known asymptotic expansions for plate solutions. Boundary layer constructions for the plate problem based on tensile membrane solutions have been developed by SRUB-

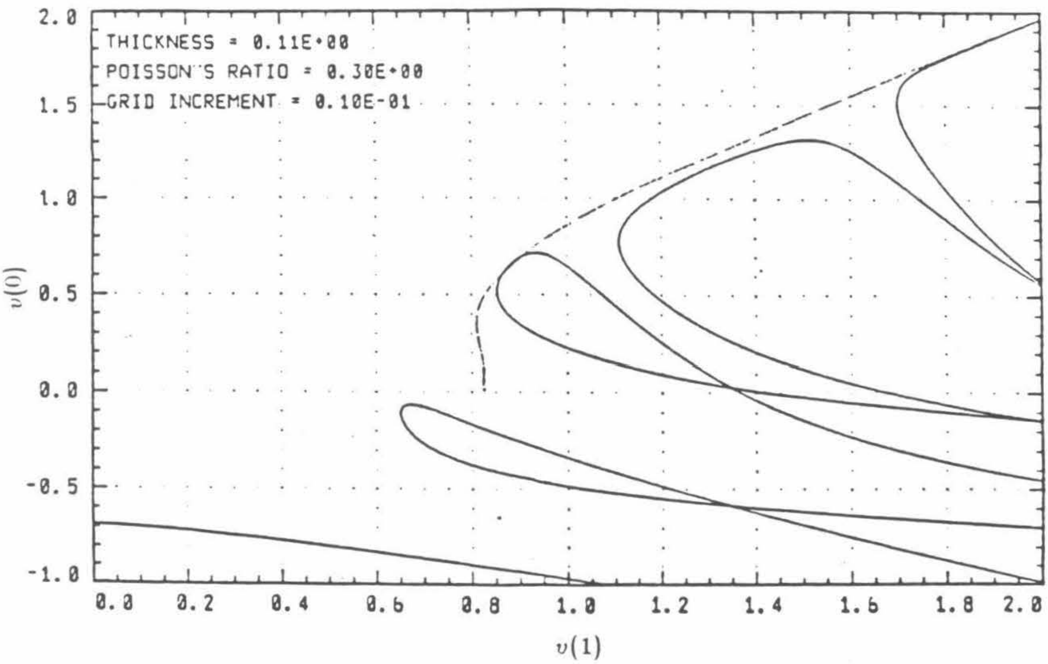

FIGURE 1.5. Continuation diagram for the simply supported circular plate, $h = 0.11$ Similar to the previous Figure but with h fixed at 0.11.

SHCHIK AND YUDOVICH[10] for the case of tensile edge load, FRIEDRICHS AND STOKER[11] and BODNER[12] for the case of compressive edge load and BROMBERG[13] for the case of vanishing edge load. In these constructions, a boundary layer appears at the edge of the plate and is necessary so that the approximation satisfies the boundary condition

$$u(1) = 0 \quad \text{or} \quad u'(1) + Qu(1) = 0.$$

To illustrate the boundary layer construction, we derive the asymptotic expansion for the circular plate whose edge is elastically supported against

---

[10] *Dokl. Akad. Nauk SSSR* **139** (1961)

[11] *Amer. J. Math.* **64** (1941)

[12] *Q. Appl. Math.* **12** (1955)

[13] *Comm. Pure Appl. Math.* **9** (1956)

rotation in the case of tensile edge load; i.e., $v(1) = \lambda < 0$. The asymptotic approximation of the solution that is presented below was derived and proven to be valid by SRUBSHCHIK AND YUDOVICH.

The outer solution for the stress v is taken to be a tensile (negative) solution v_0 of the Föppl membrane equation (1.11) satisfying the membrane boundary conditions (1.12). Letting $u_0 = g(x)/v_0(x)$, we then take u_0 as the outer solution for the displacement variable u. Only for special choices of g and v_0 does it happen that the boundary condition at $x = 1$ is satisfied by the outer solution. We will assume that this is not the case, and so we must introduce a boundary layer about $x = 1$. The boundary layer variables are chosen to be

$$\tilde{x} = \frac{1 - x}{h},$$
$$\tilde{u}(\tilde{x}) = u(x), \qquad \tilde{v}(\tilde{x}) = v(x).$$

Substitution into the plate equations (1.5) gives

$$\begin{aligned} \frac{d^2\tilde{u}}{d\tilde{x}^2} - \frac{3h}{1 - h\tilde{x}}\frac{d\tilde{u}}{d\tilde{x}} + \tilde{v}\tilde{u} &= g(1 - h\tilde{x}), \\ \frac{d^2\tilde{v}}{d\tilde{x}^2} - \frac{3h}{1 - h\tilde{x}}\frac{d\tilde{v}}{d\tilde{x}} &= h^2\tilde{u}^2. \end{aligned} \tag{1.14}$$

The boundary conditions at $\tilde{x} = 0$ are

$$\tilde{v}(0) = \lambda, \qquad h^{-1}\tilde{u}'(0) + Q\tilde{u}(0) = 0.$$

The boundary conditions for $\tilde{x} \to +\infty$, which are required for the boundary layer solution to match the outer solutions v_0 and u_0 in the overlap region, are

$$\tilde{v}(\tilde{x}) \to v_0(1) - h\tilde{x}v_0{}'(1),$$

$$\tilde{u}(\tilde{x}) \to u_0(1) - h\tilde{x}u_0{}'(1),$$

as $\tilde{x} \to \infty$. By inspection we find the boundary layer solutions to be

$$\tilde{v}(\tilde{x}) = \lambda - h\tilde{x}v_0{}'(1) + O(h^2),$$
$$\tilde{u}(\tilde{x}) = u_0(1) - h\tilde{x}u_0{}'(1) - \frac{h}{\sqrt{-\lambda}}\kappa e^{-\sqrt{-\lambda}\tilde{x}} + O(h^2)$$

where

$$\kappa = \frac{u_0{}'(1) + Qu_0(1)}{1 + \frac{hQ}{\sqrt{-\lambda}}}.$$

The uniform asymptotic expansion is thus

$$\begin{aligned} v(x) &\sim v_0(x), \\ u(x) &\sim u_0(x) - \frac{h}{\sqrt{-\lambda}}\kappa \exp\left(-\frac{\sqrt{-\lambda}}{h}(1-x)\right). \end{aligned} \tag{1.15}$$

Differentiating with respect to x, we have

$$v'(x) \sim v_0{}'(x),$$
$$u'(x) \sim u_0{}'(x) - \kappa \exp\left(-\frac{\sqrt{-\lambda}}{h}(1-x)\right).$$

Thus, we have a boundary layer in the derivative of the displacement variable, u', which has the usual exponential decay.

If the construction is attempted in the case of compressive edge load, i.e., $\lambda > 0$, we obtain a boundary layer solution of the form

$$\tilde{v}(\tilde{x}) \sim \lambda - h\tilde{x}v_0{}'(1),$$
$$\tilde{u}(\tilde{x}) \sim u_0(1) - h\tilde{x}u_0{}'(1) - \frac{h}{\sqrt{\lambda}}\kappa \cos(\sqrt{\lambda}\tilde{x} + \phi)$$

where

$$\kappa = \frac{u_0{}'(1) + Qu_0(1)}{\sin\phi + \frac{hQ}{\sqrt{\lambda}}\cos\phi}.$$

This cannot be matched asymptotically to the outer solution and therefore the boundary layer construction is inconsistent. *The oscillatory character of the rejected boundary layer solution suggests a global breakdown of the* *outer solution; that is, the outer solution must be modified throughout the interval $x \in [0,1]$ to obtain a valid asymptotic approximation. This is accomplished with multiscale analysis.*

A simple asymptotic construction related to multiscale analysis can be carried out for fixed pressure load and vanishing thickness if we allow the edge load to tend to $+\infty$. The membrane solution approaches a state of constant compression for large compressive edge load. Thus, taking $v(x;h) = v_0(x) + o(1)$, we perturb about $v_0(x) = \lambda$ under the assumption $u = o(1)$ for $x > 0$. The equation for u_0, the leading term of u, is

$$h^2\left(u_0'' + \frac{3}{x}u_0'\right) + \lambda u_0 = g(x).$$

For small thickness h and large edge load $\lambda > 0$, the solution has the asymptotic form

$$u(x) \sim \frac{g(x)}{\lambda} - \frac{h}{\lambda^{\frac{1}{2}}x} \cdot \kappa J_1(h^{-1}\lambda^{\frac{1}{2}}x) \tag{1.16}$$

where

$$\kappa = \frac{g'(1) + Qg(1)}{\lambda\left(J_1'(h^{-1}\lambda^{\frac{1}{2}}) + (h(Q-1)/\lambda^{\frac{1}{2}})J_1(h^{-1}\lambda^{\frac{1}{2}})\right)}. \tag{1.17}$$

Clearly, the assumption that $u = o(1)$ is satisfied provided $x \gg h\lambda^{-\frac{1}{2}}$. The derivative of u has the asymptotic form

$$u'(x) \sim \frac{g'(x)}{\lambda} - \kappa J_1'(h^{-1}\lambda^{\frac{1}{2}}x).$$

Note that the expansion for u' differs by an $O(1)$ amount from the estimate of membrane theory, which is $g'(x)/\lambda$. The expansion is consistent for $\lambda \gg 1$.

In the third chapter we generalize the small thickness asymptotic approximation (1.16) *to the case of* $O(1)$ *edge load for the circular or annular plate whose edge is elastically supported against rotation.* It cannot be assumed that the leading order behavior of the plate is a state of constant stress; however, the stress will vary "slowly" as compared to the $O(h^{-1})$ scale on which the oscillations occur. The multiscale expansions thus obtained are compared to the numerical calculations for the plate solutions and an estimate is made for the order of the error.

The approximation (1.16) breaks down when

$$h^{-1}\lambda^{\frac{1}{2}}J_1'(h^{-1}\lambda^{\frac{1}{2}}) + (Q-1)J_1(h^{-1}\lambda^{\frac{1}{2}}) = 0.$$

Letting x_n be the nth zero of $xJ_1'(x) + (Q-1)J_1(x)$, then for fixed h the values λ_n that satisfy this condition are

$$\lambda_n = h^2 {x_n}^2. \tag{1.18}$$

It is shown by KELLER, KELLER AND REISS[14] that the values λ_n given by (1.18) are precisely the edge loads at which bifurcation from the trivial state—or buckling—occurs in the case that the pressure load vanishes; i.e., $g(x) \equiv 0$. Asymptotically, as $h \to 0$ for $Q = O(1)$, this condition reduces to $h^{-1}\lambda^{\frac{1}{2}} = (n + \frac{3}{4})\pi$. *In the multiscale expansion derived in Chapter 3, a similar breakdown of the expansion is observed.* In particular, let v_0 be a compressive solution of the Föppl membrane equation and let $\alpha = v_0(0)$, $\lambda = v_0(1)$. If we have

$$h^{-1}K(\alpha) = (n + \tfrac{3}{4})\pi \quad \text{with} \quad K(\alpha) = \int_0^1 {v_0}^{\frac{1}{2}}(s)\, ds,$$

then the multiscale approximation for the circular plate solution derived from the assumption

$$v(x;h) \sim v_0(x) + O(h^2)$$

---

[14] *Q. Appl. Math.* **20** (1962)

is not valid for this choice of α and h. *We find that near these points an asymptotic expansion may still be constructed if a boundary layer is introduced at the center of the plate.* The boundary layer solutions were calculated numerically and the asymptotic behavior of the family of expansions constructed in this manner were studied in the limit as the stress at the center of the plate approached $-\infty$.

The expansion for the clamped circular plate may be obtained from (1.16) in the limit $Q \to \infty$. *It is shown in Chapter 3 that the expansion for the clamped circular plate is consistent provided $\lambda \gg h^{-\frac{2}{5}}$, a much stronger restriction than that for the case of the plate whose edge is elastically supported against rotation where we require $\lambda \gg 1$. For the case of the clamped circular plate, we show that the generalization of the expansion to $O(1)$ edge load is in general not consistent.*

The Clamped Circular Plate. The clamped plate may be considered as the limit where the support against rotation becomes unbounded ($Q \to +\infty$). Inspection of the multiscale expansion derived in Chapter 3 in this limit shows that the expansion is not valid for the clamped plate unless the pressure load is self-equilibrating; i.e., $g(1) = 0$. In Chapter 4, the cause of the failure of the expansion in the case of the clamped circular plate is investigated. We show that, for the clamped circular plate problem, it is not possible to find solutions that asymptotically approach a given Föppl membrane solution as the thickness vanishes.

The method of proof is motivated in part by the results of KREISS.[15]

---

[15] *SIAM J. Numer. Anal.* **16** (1979)

Consider the system

$$\begin{aligned} h\mathbf{z}_I' &= B\mathbf{z}_I + F_I(t, \mathbf{z}_I, \mathbf{z}_{II}; h), \\ \mathbf{z}_{II}' &= A\mathbf{z}_{II} + F_{II}(t, \mathbf{z}_I, \mathbf{z}_{II}; h) \end{aligned} \tag{1.19}$$

where the real matrix B has imaginary eigenvalues only, and the functions F_I, F_{II} vanish quadratically in $\mathbf{z}_I$, $\mathbf{z}_{II}$ for $\mathbf{z}_I$, $\mathbf{z}_{II} \to 0$, $h = 0$. KREISS gives sufficient conditions such that if a solution $\mathbf{z}_I$, $\mathbf{z}_{II}$ is $O(h)$ at some point $t \in [\tau_0, T_1]$, then the solution is $O(h)$ for all $t \in [\tau_0, T_1]$. *In the fourth chapter, we prove a lemma that provides sufficient conditions such that if* $\mathbf{z}_I$ *and* $\mathbf{z}_{II}$ *are bounded by some constant* δ *sufficiently small, then the solution is bounded by* 4δ *for all* $t \in [\tau_0, T_1]$.

We then obtain the result that it is not possible to find sequences $\{h_n\}$, $\{u_n\}$, $\{v_n\}$, $n = 1, 2, \ldots$, satisfying: $h_n \to 0$ as $n \to \infty$; u_n, v_n are continuous solutions of the clamped circular plate problem with thickness h_n and fixed g, $g(1) \neq 0$; for some $C > 0$ and points $\{x_n\}$, $0 < x_0 < x_n \leq 1$, the solutions u_n, v_n evaluated at x_n satisfy

$$|v_n(x_n)| + |v_n'(x_n)| \leq C, \tag{1.20}$$

$$|u_n(x_n)v_n(x_n) - g(x_n)| + |h_n u_n'(x_n)| \to 0 \tag{1.21}$$

as $n \to \infty$; for some $m > 0$, $v_n(x_n) \geq m$ for all n.

To prove this result, we show that the plate equations can be transformed into a system of the form (1.19) by subtracting the membrane approximation from the solution and performing a few changes of variables. In this formulation the condition (1.21) implies that the solution $\mathbf{z}_I$, $\mathbf{z}_{II}$ is small at some point. On the other hand, the clamped boundary condition implies that the solution is bounded away from zero at the endpoint. The hypotheses of the lemma discussed above are verified; the lemma is then used to show that a sequence of solutions with $h \to 0$ cannot be asymptotic to the membrane approximation in the sense of (1.21) and also satisfy the clamped boundary condition.

It is worthwhile to discuss just what is and what is not contained in this result. For comparison, we consider the related problem of the elastica with clamped ends under the same assumptions concerning the magnitudes of the deformations as were used in the derivation of the von Kármán equations. We obtain the equations

$$h^2 u'' + vu = g(x), \qquad v'' = 0,$$

with boundary conditions

$$\begin{aligned} u'(0) &= 0, \qquad & u(1) &= 0, \\ v'(0) &= 0, \qquad & v(1) &= \lambda. \end{aligned}$$

We may solve for v to get $v(x) \equiv \lambda$. Thus,

$$h^2 u'' + \lambda u = g(x).$$

The small thickness asymptotic expansions for u and $u'$are

$$\begin{aligned} u(x) &\sim \frac{g(x)}{\lambda} - \frac{g(1)}{\lambda} \cos \frac{\sqrt{\lambda}}{h} x, \\ u'(x) &\sim \frac{g(1)}{h\sqrt{\lambda}} \sin \frac{\sqrt{\lambda}}{h} x. \end{aligned} \tag{1.22}$$

Clearly, u differs from the "membrane" approximation $u_0 = g(x)/\lambda$ by an $O(1)$ amount; in particular, for some $\theta > 0$ we have

$$|uv - g| + |hu'| \geq \theta$$

for all $x \in [0,1]$. Thus, for the elastica, a result analogous to that for the circular plate also holds. But we must note that for the 1-dimensional problem, the asymptotic expansion (1.22) *is* valid; compressive solutions of the problem of the elastica with clamped edges do exist for $h \to 0$ such that

$$|v| + |v'| + |u| + |hu'| = O(1).$$

For the plate problem, we have the additional complication that the equation determining the stress

$$v'' + \frac{3}{x}v' = u^2$$

depends on u. This was not true for the 1-dimensional problem. Thus, if u differs from the membrane approximation by an $O(1)$ amount, we cannot expect to recover the Föppl membrane equation for the leading order term of the stress v. There is also a physical motivation for the condition that $hu' \to 0$; the von Kármán equations become invalid if this condition is not satisfied because of the breakdown of the assumption of negligible shear strain.

CHAPTER 2

Föppl Membrane Solutions

The fundamental assumption of membrane theory that distinguishes it from plate theory is that the bending stresses are negligible. The membrane equations can then be obtained[1] by analyzing the stresses and strains on the structure, independent of the more complicated plate theory, which takes bending stresses into account. Alternatively, setting the thickness to zero in the plate theory may give rise to the same governing equations as the membrane theory. For the problems we discuss—circular or annular plates under radially symmetric loading and deformations—the von Kármán plate equations (1.5) reduce to the Föppl membrane equations when the thickness vanishes.

The von Kármán theory of thin plates is a singular perturbation of Föppl membrane theory, and thus we cannot expect the thin plate solutions to pass uniformly into the membrane solutions as the thickness vanishes. In Chapter 3, we construct asymptotic expansions for the plate solutions based on compressive membrane solutions. (It is possible to obtain compressive solutions because the membrane does resist radial or circumferential compression.) It is therefore necessary to know something about the behavior of these membranes.

In the first section of this chapter, we discuss results from the literature, including existence and uniqueness proofs for the case of tensile edge load, proofs of nonexistence or nonuniqueness for the case of compressive edge load

---

[1] See, for example, A. Föppl, *Vorlesungen über technische Mechanik*, Vol. **5**, 1907

as well as characterization of the singular solutions that appear in the cases of zero radial or circumferential stress either at the edges or at the center of the membrane. The second section is devoted to a singular perturbation analysis about the singular compressive solution in the case of arbitrary smooth pressure load. The near-singular membrane solutions have been studied primarily by phase-plane analysis in special cases where it is possible to transform the equations into an autonomous system of ODE's.

2.1 Background

Recall from (1.11, 1.12) that the the FÖPPL membrane is the second-order nonlinear equation

$$v'' + \frac{3}{x}v' = \frac{\hat{g}^2(x)}{v^2} \tag{2.1}$$

with boundary conditions

$$\begin{gathered} v'(0) = 0 \qquad \text{or} \qquad v(a) = \eta, \\ v(1) = \lambda. \end{gathered} \tag{2.2}$$

CALLEGARI AND REISS[2] give existence and uniqueness results for solutions of the circular membrane problem where $\lambda < 0$, the case where the radial stress is tensile at the edge. GRABMÜLLER AND WEINITSCHKE[3] have shown existence and uniqueness for tensile solutions of the annular membrane problem with $\eta = 0$, that is, vanishing radial stress at the inner edge, and tensile edge load $\lambda < 0$. For zero edge load, $\lambda = 0$, SRUBSHCHIK[4] has shown the existence of a unique circular membrane solution that is tensile for $x \in [0, 1)$; if the pressure load is not self-equilibrating, i.e., $\hat{g}(1) \neq 0$, then the derivative v' becomes unbounded at the edge.

---

[2] *Arch. Rat. Mech. Anal.* **31** (1968)

[3] *J. Elast.*, to appear

[4] *Prikl. Mat. Mekh.* **30** (1966)

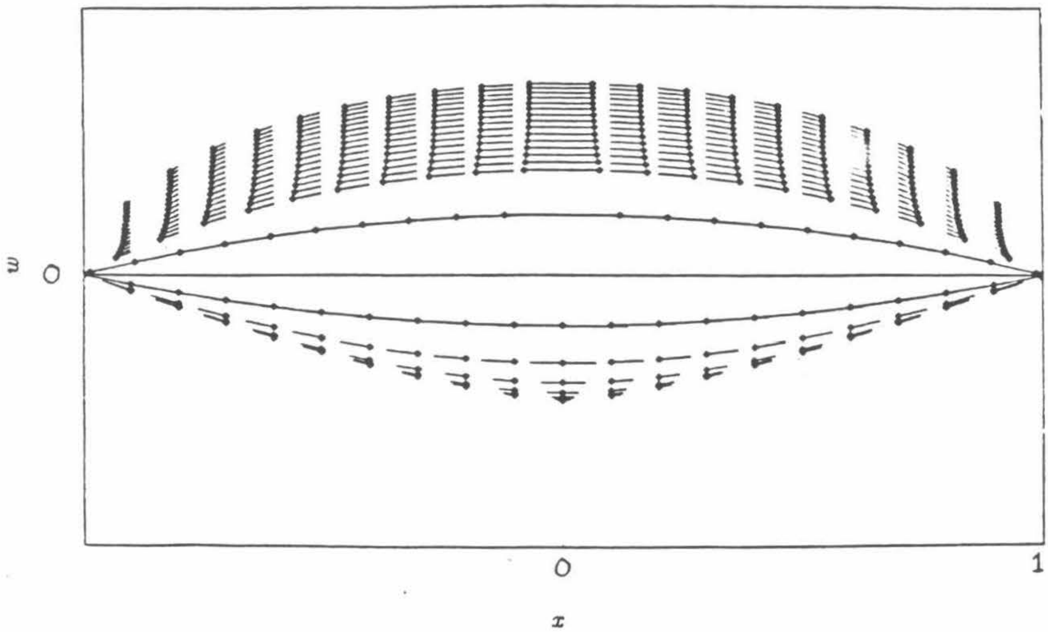

FIGURE 2.1. Solutions of the membrane equation
The vertical deflection w of the circular membrane under uniform pressure load is plotted against the radial distance r. The pressure load is in the upward direction. Vectors representing the radial stress are also plotted; those pointing towards the edge of the membrane represent tensile stress.

The existence of a branch of compressive circular membrane solutions is demonstrated by CALLEGARI, REISS AND KELLER.[5] In this paper it is shown that specifiying $v(0) = \alpha > 0$ provides a unique characterization of the nonsingular compressive membrane solutions. In Figure (2.1), we show some circular membrane solutions for uniform pressure load. The numerical methods used to obtain these solutions are discussed in Appendix II. Note that tensile solutions are deflected in the same direction as the pressure, while compressive solutions are deflected in the opposite direction. Also, phase-plane analysis is performed in the case of uniform pressure load to

[5] *Comm. Pure Appl. Math.* **24** (1971)

show the existence of a value of the edge stress, λ_∞, for which there are an infinite number of membrane solutions. The compressive solution branch has an infinite number of folds with respect to the edge load and the fold points converge to λ_∞. These folds are illustrated in the continuation diagram (1.2), where the compressive solution branch is shown for the case of uniform pressure load. The phase-plane analysis is generalized to a class of problems with variable pressure load in the thesis of KOSECOFF.[6]

It is observed by CALLEGARI, REISS AND KELLER that for uniform pressure load, i.e., $\hat{g}(x) \equiv 1$, there exists a singular solution of the circular membrane problem

$$v_\infty(x) = (\tfrac{3}{4}x)^{\frac{2}{3}}.$$

This solution is compressive for $x \in (0,1]$ but has $v(0) = 0$, while $v'(x)$ becomes unbounded as $x \to 0$. It may be shown by phase-plane analysis that in the limit $v(0) \to 0^+$ the solutions converge to this singular solution. Similarly, for the class of problems studied by KOSECOFF, there exist singular solutions that are obtained in the limit $v(0) \to 0^+$. To our knowledge the existence of such singular solutions for the case of general pressure load has not been established in the literature.

2.2 Perturbation Analysis for General Pressure Load

The asymptotic behavior of circular membrane solutions near a singular solution—a solution that is not twice continuously differentiable for $x \in [0,1]$—having zero radial stress at the origin is obtained by singular perturbation. The small parameter is taken to be the radial stress at the origin. The ratio of the spacing between successive folds is found to asymptotically

[6] *Ph. D. Thesis, California Institute of Technology*, 1975

approach a constant value. Similar results may be obtained for the annular membrane with vanishing radial stress at the inner edge. In this case the small parameter is $v'(a)$, which is related to the circumferential stress at the inner edge.

Singular Solution. In the case that $\hat{g}(x)$ is analytic, a series expansion valid for x sufficiently small may be obtained for a singular solution of the form

$$v_\infty(x) = \left(\tfrac{3}{4}x\right)^{\frac{2}{3}}\left(1 + \sum_{n=1}^{\infty} a_n x^n\right).$$

This solution is singular because $v'(x)$ becomes unbounded as $x \to 0$. The recursion relations for the coefficients a_n are

$$\frac{32 + (3n+2)(3n+8)}{16} a_n = b_n - r_n$$

where b_n is the nth Taylor series coefficient for $\hat{g}^2$ expanded about $x = 0$ and

$$r_n = \sum_{k=1}^{n-1} \frac{(3k+2)(3k+8)}{16} a_k \sum_{m=0}^{k} a_m a_{n-k-m} + a_0 \sum_{m=1}^{n-1} a_m a_{n-m}.$$

It is not hard to show that

$$a_n \leq \frac{K}{n^2 \rho^n} \qquad \text{for } n \geq 1$$

with K and ρ appropriately chosen.

In the more general case where $\hat{g}$ is only assumed to be continuous, we propose the following iterations: let

$$\begin{aligned} v_0(x) &= \left(\tfrac{3}{4}x\right)^{\frac{2}{3}}, \\ v_{n+1}(x) &= \int_0^x \left(\xi - \frac{\xi^3}{x^2}\right) \frac{\hat{g}^2(\xi)}{2v_n^2(\xi)}\, d\xi. \end{aligned}$$

We conjecture that these iterations converge to the singular solution v_∞ for $x \leq \hat{x}$ sufficiently small; similar iterations are used by CALLEGARI, REISS

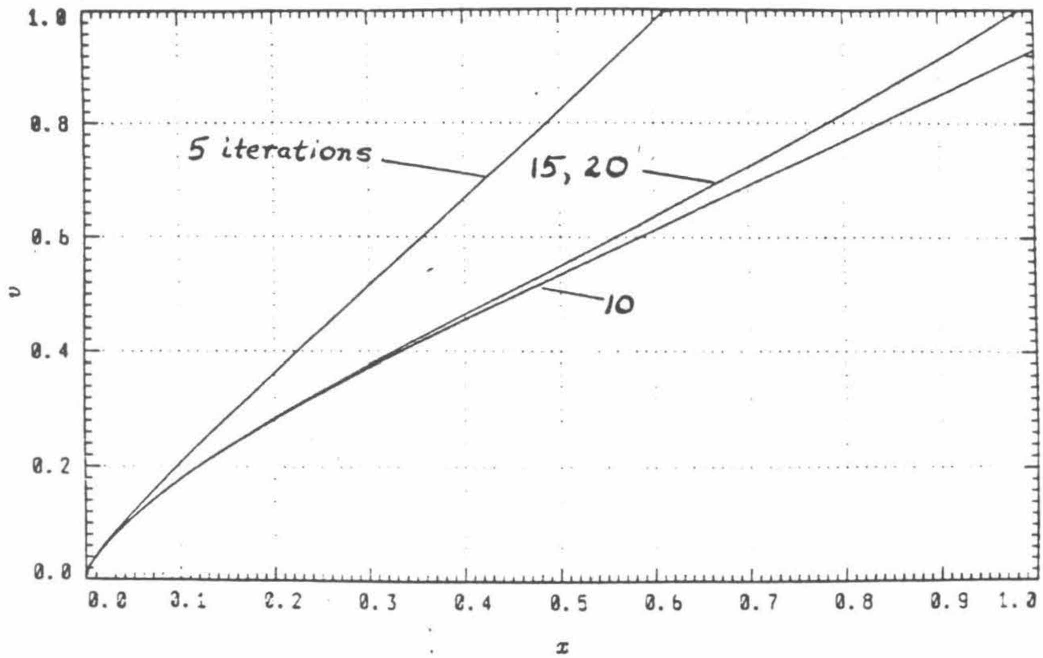

FIGURE 2.2. Iterations for the singular solution

The approximate compressive singular solutions for the circular membrane are shown for the case of $\hat{g}(x) = 1 + x^2$. The stress v is plotted against the radial distance x for the iterates 5, 10, 15, and 20.

AND KELLER to show existence of nonsingular membrane solutions. Note that as $x \to 0$

$$v_n(x) \sim \left(\tfrac{3}{4}x\right)^{\frac{2}{3}}$$

for all n and hence,

$$v_\infty \sim \left(\tfrac{3}{4}x\right)^{\frac{2}{3}} \qquad \text{as } x \to 0.$$

The iterations were performed numerically for several choices of $\hat{g}$ and were observed to converge in every case. The iterations for $\hat{g}(x) = 1 + x^2$ are shown in Figure (2.2). That this singular solution is obtained in the limit $v(0) \to 0^+$ is supported by the perturbation analysis that follows.

The case of the annular membrane with vanishing radial stress at the

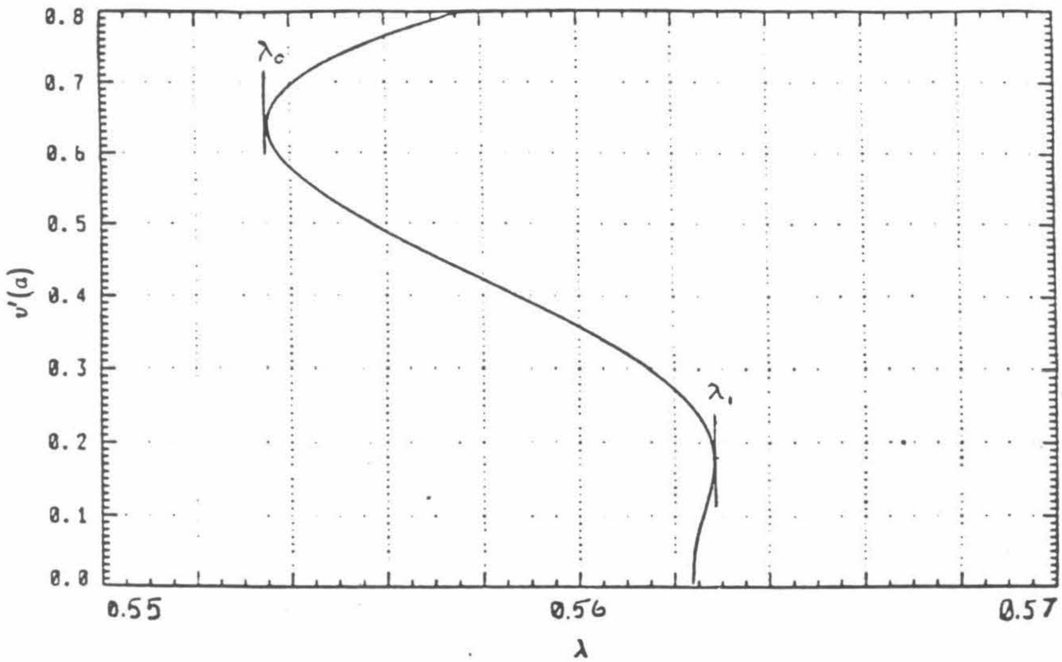

FIGURE 2.3. Continuation diagram for the annular membrane
The family of compressive annular membrane solutions for uniform pressure load is shown. The components of the solution plotted are the radial stress at the edge $v(1) = \lambda$ (abscissa) and $v'(a)$ (ordinate), which is related to the circumferential stress at the inner edge. The folds λ_0 and λ_1 can be seen on this plot.

inner edge ($\eta = 0$) is similar. We have $\hat{g}(a) = 0$ in this case. The compressive solution branch for the annular membrane under uniform pressure load with $a = 0.5$ is shown in Figure (2.3). Local analysis about $x = a$ suggests the existence of a singular solution of the form

$$v_\infty(x) \sim \left(\frac{3}{a}\right)^{\frac{2}{3}} (x-a)^{\frac{4}{3}} \quad \text{as } x \to a.$$

In fact, letting

$$\hat{g}(x) = \frac{2}{a}(x-a)\sqrt{1 + \frac{9}{x}(x-a)}\,,$$

we obtain the exact solution

$$v_\infty(x) = \left(\frac{3}{a}\right)^{\frac{2}{3}} (x-a)^{\frac{4}{3}}.$$

An iteration procedure may be defined for a singular solution of the annular membrane problem, which is similar to the iterations obtained for the circular membrane case.

Outer solution. Linearizing the membrane equation (2.1) about the singular solution v_∞ for the circular membrane problem gives rise to the linear second order equation

$$z'' + \frac{3}{x}z' + \frac{2\hat{g}^2(x)}{{v_\infty}^3(x)}z = 0. \tag{2.3}$$

Using $\hat{g}(0) = 1$, we have for $x \ll 1$

$${v_\infty}^3(x) \sim \left(\tfrac{3}{4}x\right)^2;$$

hence

$$z'' + \frac{3}{x}z' + \frac{32}{9x^2}z \approx 0$$

near the origin. If the pressure load is analytic, then it is clear that the equation (2.3) has a regular singular point at the origin. The theory for these equations is well known; the asymptotic form of the solutions near the origin is obtained from the indicial equation. If we only assume that the pressure load is continuous, then the same techniques are applicable, but the asymptotic expansion is formal. Therefore, a solution z of (2.3) satisfies

$$z \sim A \cdot x^{-1} \sin\Big(\frac{\sqrt{23}}{3}\log x + \theta\Big) \qquad \text{as } x \to 0.$$

We define a set of linearly independent solutions based on their asymptotic behavior near the origin. Let

$$z_1 \sim x^{-1}\sin\Big(\frac{\sqrt{23}}{3}\log x\Big), \qquad z_2 \sim x^{-1}\cos\Big(\frac{\sqrt{23}}{3}\log x\Big)$$

as $x \to 0$. In the case of uniform pressure load the above formulas are exact. In general, a closed form cannot be found, but the solutions may be computed numerically.

The outer solution is of the form

$$v \sim v_\infty + \epsilon(\alpha)\Big(A(\alpha)z_1 + B(\alpha)z_2\Big)$$

where $\epsilon(\alpha) = o(1)$ as $\alpha \to 0$. The small x asymptotic expansion is

$$v(x) \sim (\tfrac{3}{4}x)^{\frac{2}{3}} + \epsilon(\alpha)\Big(A(\alpha)x^{-1}\sin\frac{\sqrt{23}}{3}\log x + B(\alpha)x^{-1}\cos\frac{\sqrt{23}}{3}\log x\Big).$$

The constants ϵ, A and B, depending on α, are determined by asymptotic matching for small x to a boundary layer solution.

Inner Solution. Locally about the origin, the boundary layer solution is just the membrane solution under uniform pressure load; i.e., $\hat{g}(x) \equiv 1$. As shown by CALLEGARI, REISS AND KELLER, the solution satisfying $\tilde{v}(0) = \alpha$ is

$$\tilde{v}(x) = \alpha\hat{v}\left(\frac{x}{\alpha^{\frac{3}{2}}}\right)$$

where $\hat{v}$ is the solution of

$$\hat{v}'' + \frac{3}{x}\hat{v}' = \frac{1}{\hat{v}^2},$$

with

$$\hat{v}(0) = 1 \qquad \text{and} \qquad \hat{v}'(0) = 0.$$

The asymptotic form of $\tilde{v}$ for $x \gg \alpha^{\frac{3}{2}}$ is

$$\tilde{v}(x) \sim (\tfrac{3}{4}x)^{\frac{2}{3}} + \frac{\alpha^{\frac{5}{2}}}{x}\kappa \cdot \sin\Big(\frac{\sqrt{23}}{3}\log\frac{x}{\alpha^{\frac{3}{2}}} + \phi\Big). \tag{2.4}$$

We have determined the constants ϕ and κ for the asymptotic behavior of the inner solution by numerical calculation using the *SANDIA-ODE* solver. The values are found to be $\kappa \approx 0.2571$, $\phi \approx 1.4191$.

Matching. The contributions of each of the solutions z_1, z_2 of the linearized outer equation (2.3) can be found by matching to the asymptotic behavior (2.4) of the inner solution in the limit as the boundary layer variable $x/\alpha^{\frac{3}{2}}$ becomes large. Thus we let

$$\epsilon = \alpha^{\frac{5}{2}}$$

and

$$A = \kappa \cdot \cos\Big(-\frac{\sqrt{23}}{2}\log\alpha + \phi\Big), \qquad B = \kappa \cdot \sin\Big(-\frac{\sqrt{23}}{2}\log\alpha + \phi\Big).$$

The uniform asymptotic expansion is therefore

$$\begin{aligned} v(x;\alpha) \sim & v_\infty(x) + \alpha^{\frac{5}{2}}\kappa\cos\Big(-\frac{\sqrt{23}}{2}\log\alpha + \phi\Big)\, z_1(x) + \\ & + \alpha^{\frac{5}{2}}\kappa\sin\Big(-\frac{\sqrt{23}}{2}\log\alpha + \phi\Big)\, z_2(x) + \\ & + \alpha\hat{v}\left(\frac{x}{\alpha^{\frac{3}{2}}}\right) - \left(\tfrac{3}{4}x\right)^{\frac{2}{3}} - \frac{\alpha^{\frac{5}{2}}\kappa}{x}\sin\Big(\frac{\sqrt{23}}{3}\log\frac{x}{\alpha^{\frac{3}{2}}} + \phi\Big). \end{aligned} \tag{2.5}$$

The folds of the solution branch are determined by the condition

$$\frac{dv(1;\alpha)}{d\alpha} = 0.$$

From the asymptotic expansion (2.5) we have

$$v(1;\alpha) \sim v_\infty(1) + \alpha^{\frac{5}{2}}\kappa\sqrt{z_1^2(1) + z_2^2(1)}\,\sin\Phi$$

where

$$\Phi = -\frac{\sqrt{23}}{2}\log\alpha + \phi + \tan^{-1}\frac{z_1(1)}{z_2(1)} \tag{2.6}$$

(the branch cut of the arctangent is chosen appropriately.) Differentiation with respect to α gives

$$\begin{aligned} \frac{dv(1;\alpha)}{d\alpha} & \sim \alpha^{\frac{3}{2}}\kappa\sqrt{z_1^2(1) + z_2^2(1)}\left(\frac{5}{2}\sin\Phi - \frac{\sqrt{23}}{2}\cos\Phi\right) \\ & \sim 2\sqrt{3}\alpha^{\frac{3}{2}}\kappa\sqrt{z_1^2(1) + z_2^2(1)}\,\sin\left(\Phi - \tan^{-1}\frac{\sqrt{23}}{5}\right). \end{aligned} \tag{2.7}$$

The right-hand side of equation (2.7) vanishes when

$$\Phi = n\pi + \tan^{-1}\frac{\sqrt{23}}{5}.$$

From the definition (2.6) of Φ, we have that the corresponding values of α are

$$\alpha_n = c \cdot \exp\left(-\frac{2n\pi}{\sqrt{23}}\right)$$

where

$$c = \exp\frac{2}{\sqrt{23}}\left(\phi + \tan^{-1}\frac{z_1(1)}{z_2(1)} - \tan^{-1}\frac{\sqrt{23}}{5}\right).$$

The values λ_n of the edge load corresponding to α_n, $n = 0, 1, \ldots$ are the asymptotic positions of the folds of the solution branch with respect to the edge load λ, valid for $n \to \infty$. The folds are labeled as in Figure (1.2) according to their position on the solution branch, λ_0 being the fold point occurring at the smallest value of the edge load. Fold points λ_n, λ_{n+2} are called successive because there are no other fold points between them. The above discussion implies that

$$\lambda_n \sim v_\infty(1) + C\exp\left(-\frac{5n\pi}{\sqrt{23}}\right)$$

for some constant C. Thus, the spacing of successive fold points decreases geometrically at leading order; i.e.,

$$\frac{\lambda_{n+2}-\lambda_n}{\lambda_n-\lambda_{n-2}} \sim b^2, \qquad \frac{\lambda_{n+2}-\lambda_n}{\lambda_{n+1}-\lambda_{n-1}} \sim -b, \tag{2.8}$$

as $n \to \infty$ where $b = \exp(-5\pi/\sqrt{23}) \approx 0.038$. This agrees with the result obtained by FIER[7] from a phase-plane analysis in the case of uniform pressure load.

---

[7] *Ph. D. Thesis, California Institute of Technology*, 1985

The annular membrane problem with $\eta = 0$ may be treated similarly. The small parameter is $v'(a)$, which is related to the circumferential stress at the inner edge. The ratio between successive fold spacings in the case of the annular membrane with $p(aR) \neq 0$ turns out to be identical to that of the circular membrane with $p(0) \neq 0$ as given by (2.8).

The advantage of the singular perturbation approach described here is that it doesn't depend on the knowledge of a transformation to put the equation into autonomous form. On the other hand, phase-plane analysis can be rigorously justified while the perturbation expansion is formal; a proof of the validity of the asymptotics would require careful analysis, which we have not attempted.

CHAPTER 3

Approximations from Compressive Membrane Solutions

For boundary conditions that are not too restrictive, it is possible to construct asymptotic approximations of solutions of the von Kármán equations (1.5) based on compressive membrane solutions. Boundary layer constructions for the plate problem based on tensile membrane solutions have been developed by SRUBSHCHIK AND YUDOVICH[1] for the case of tensile edge load, FRIEDRICHS AND STOKER[2] and BODNER[3] for the case of compressive edge load and BROMBERG[4] for the case of vanishing edge load.

In these constructions, a boundary layer appears at the edge of the plate and is necessary so that the approximation satisfies the boundary condition

$$u(1) = 0 \tag{3.1}$$

in the case of a clamped plate or

$$u'(1) + Qu(1) = 0 \tag{3.2}$$

in the case of a plate whose edge is elastically supported against rotation.

The boundary layer construction for tensile edge load, i.e., $v(1) = \lambda < 0$, is derived in Chapter 1. Recall that the outer solution for the stress v is taken to be a tensile (negative) solution v_0 of the Föppl membrane equation (2.1).

---

[1] *Dokl. Akad. Nauk SSSR* **139** (1961)

[2] *Amer. J. Math.* **64** (1941)

[3] *Q. Appl. Math.* **12** (1955)

[4] *Comm. Pure Appl. Math.* **9** (1956)

The uniform asymptotic expansion is given in (1.15). If the construction is attempted for a compressive outer solution, it is found that the boundary layer solution contains oscillatory terms that cannot be matched to the outer solution.

A multiscale type asymptotic construction is also carried out in Chapter 1 for fixed pressure load and vanishing thickness with $\lambda \to +\infty$. The expansion (1.16) then obtained is

$$v(x) \sim \lambda, \qquad u(x) \sim \frac{g(x)}{\lambda} - \frac{h}{\lambda^{\frac{1}{2}}} \cdot \kappa J_1(h^{-1}\lambda^{\frac{1}{2}}x)$$

with κ as defined in (1.17).

In the discussion that follows we generalize this asymptotic approximation to circular and annular plates with bounded edge load. We find that the stress varies "slowly" as compared to the $O(h^{-1})$ scale on which the oscillations occur. Hence, multiscale analysis can be employed. The approximations are carried out in detail for the case of a circular plate with the edge elastically supported against rotation. The simply-supported plate is contained in this class of problems as the special case where the support against rotation vanishes. The expansion is generalized to annular plates with the same support at the outer edge. The clamped plate may be considered as the limit where the support against rotation becomes unbounded—in the boundary condition (3.2), $Q \to +\infty$. Inspection of the asymptotic approximation in this limit shows that the expansion is not valid for the clamped plate unless the pressure load is self-equilibrating; i.e., $\hat{g}(1) = 0$. We also consider the asymptotic expansion (1.16) for large edge load as the support against rotation becomes unbounded and show that as $Q \to \infty$ we require $\lambda \gg h^{-\frac{5}{2}}$ for consistency of the expansion.

The approximation (1.16) breaks down when the condition (1.18) is met. In the approximation derived below a similar breakdown of the expansion is observed. For this case, we derive in Section (3.2) an asymptotic expansion having a boundary layer at the center of the plate.

3.1 Smooth Stress Solutions

Recall the radially symmetric von Kármán equations (1.5) for the bending of a thin circular plate under a pressure load

$$\begin{aligned} h^2\left(u'' + \frac{3}{x}u'\right) + vu &= g(x), \\ v'' + \frac{3}{x}v' - u^2 &= 0. \end{aligned} \tag{3.3}$$

The function g is assumed to be twice continuously differentiable for $x \in [0,1]$. We suppose a solution exists where the radial stress v is positive and has the asymptotic form

$$v(x;h) = v_0(x) + O(h^2) \qquad \text{as } h \to 0 \tag{3.4}$$

for $x > 0$. Then WKB analysis is applicable to the equilibrium equation (3.3a), which is linear in the displacement variable u. The approximation thus obtained can be used to develop formal small h asymptotics of solutions of the plate equations (3.3), which have compressive stress throughout. We do not attempt to justify rigorously the asymptotic expansions; however, numerical evidence is presented to support the conjecture that solutions of the plate equations (3.3) exist that have the asymptotic expansions derived below.

The Outer Solution. We first make the change of variable

$$w(x;h) = x^{\frac{3}{2}}(u(x;h) - u_0(x)) \tag{3.5}$$

where

$$u_0(x) = \frac{g(x)}{v_0(x)}. \tag{3.6}$$

Applied to the equilibrium equation (3.3a), this transformation eliminates the first derivative and the forcing terms—at least to leading order. Thus,

$$h^2 w'' + \left(v - \frac{3h^2}{4x^2}\right) w = -\frac{h^2}{x^{\frac{3}{2}}}(x^3 {u_0}')'. \tag{3.7}$$

If $w(x;h) = w_0(x)(1 + o(1))$, then the leading order equation, for $x \gg h$, is

$$h^2 w_0'' + v_0 w_0 = 0. \tag{3.8}$$

The WKB approximation is

$$w_0(x) = \frac{c}{{v_0}^{\frac{1}{4}}(x)} \cdot \cos(\tilde{x} + \phi) + O(ch) \qquad \text{as } h \to 0 \tag{3.9}$$

where

$$\tilde{x} = \frac{1}{h}\int_0^x {v_0}^{\frac{1}{2}}(s)\, ds. \tag{3.10}$$

Substituting the estimate (3.9) for w into the expression (3.5) and solving for the original variable u gives

$$u(x;h) = u_0(x) + \frac{c}{x^{\frac{3}{2}} {v_0}^{\frac{1}{4}}(x)} \cdot \cos(\tilde{x} + \phi) + O(ch) \qquad \text{as } h \to 0. \tag{3.11}$$

The error estimate for the solution is obtained from the formal expansion carried out to higher order. The region of validity is $x \gg h$. Provided the assumption (3.4) concerning the asymptotic form of the stress v holds, then the approximation (3.11) satisfies the equilibrium equation (3.3a) to $O(ch)$ in this region.

In the discussion pertaining to the clamped plate below we show it is necessary that $c = O(h)$ for consistency with the original assumption (3.4) of the asymptotic form of v.[5] The constant c is chosen to satisfy the boundary condition at the edge of the plate. We discuss the case of a plate where the edge is elastically supported against rotation; the corresponding boundary condition is given in equation (3.2). The smoothness conditions (1.6) are not satisfied by the outer solution, which is valid only for $x \gg h$. These conditions will come into play in the construction of the uniform asymptotic approximation, which follows the discussion of the outer solution. Using the approximation (3.11), the boundary condition (3.2) becomes

$$-\frac{c\lambda^{\frac{1}{4}}}{h} \cdot \sin\theta + u_0'(1) + Qu_0(1) + \frac{Qc}{\lambda^{\frac{1}{4}}} \cdot \cos\theta + O(c) = 0 \tag{3.12}$$

where

$$\lambda = v_0(1), \qquad \theta = \frac{K}{h} + \phi, \tag{3.13}$$

$$K = \int_0^1 v_0^{\frac{1}{2}}(s)\, ds. \tag{3.14}$$

The term containing the factor Qc is retained so that the formula will be uniformly valid as $Q \to \infty$. In general, we will have $\sin\theta \neq 0$; provided $Q = O(1)$, then $c = O(h)$ as desired. The case $\sin\theta = 0$ is treated in the subsequent Section (3.2), while the case $Q \to \infty$ is discussed in the latter part of this section.

To show explicitly the order of c, we let $c = h\kappa$. From (3.11) we obtain the asymptotic expansions for u and u'

$$u(x;h) = u_0(x) + h\frac{\kappa}{x^{\frac{3}{2}} v_0^{\frac{1}{4}}(x)} \cdot \cos(\tilde{x} + \phi) + O(h^2) \tag{3.15}$$

and

[5] See equation (3.54)

$$u'(x;h) = u_0'(x) - \frac{\kappa v_0^{\frac{1}{4}}(x)}{x^{\frac{3}{2}}} \cdot \sin(\tilde{x} + \phi) + O(h) \tag{3.16}$$

as $h \to 0$. The approximation (3.15) satisfies the equilibrium equation (3.3a) to $O(h^2)$. To satisfy the boundary condition (3.2) to $O(h)$, κ is taken to be

$$\kappa = \frac{u_0'(1) + Qu_0(1)}{\lambda^{\frac{1}{4}} \sin\theta - (hQ/\lambda^{\frac{1}{4}}) \cos\theta} \tag{3.17}$$

where θ is defined in (3.13). We are willing to settle for an error of $O(h)$ here because in the numerical formulation of the plate problem this boundary condition gets multiplied by h, and so an error of $O(h^2)$ is observed.

Another case in which the condition that $c = O(h)$ is satisfied is the clamped plate under self-equilibrating pressure load; that is, $g(1) = 0$. When $g(1) = 0$, the approximation $u_0 = g/v_0$ from membrane theory satisfies the boundary condition (3.1), and one finds $c = O(h^2)$ when the expansion is carried out to the next order. The formula (3.17) gives $\kappa = 0$ in this case. Clearly, the requirement that $c = O(h)$ is met and thus the expansion is consistent. However, if $g(1) \neq 0$, then in the limit $Q \to \infty$, we have

$$\kappa = -\frac{g(1)}{h\lambda^{\frac{3}{4}} \cos\theta}$$

and hence $c = O(1)$. Thus, for the clamped plate with nonself-equilibrating pressure load, the expansion is not consistent. Detailed discussion of this case is contained in the subsection entitled "The Clamped Plate." We will assume throughout the remaining derivation of the asymptotic expansion that $Q = O(1)$.

To obtain an asymptotic approximation for the stress, we substitute the approximation (3.15) for u into the compatibility equation (3.3b) and retain terms to $O(h)$. Thus, for $x \gg h$ we have

$$v'' + \frac{3}{x}v' = \frac{g^2(x)}{{v_0}^2} + 2\frac{h\kappa g(x)}{x^{\frac{3}{2}} v_0^{\frac{5}{4}}} \cos(\tilde{x} + \phi) + O(h^2). \tag{3.18}$$

Letting $v(x;h) = v_0(x) + v_1(x;h)$ where $v_1 = o(1)$ as $h \to 0$, we see that the leading order equation

$$v_0'' + \frac{3}{x} v_0' = \frac{g^2(x)}{{v_0}^2} \tag{3.19}$$

is simply the FÖPPL[6] membrane equation. The leading order boundary conditions are

$$v_0'(0) = 0, \qquad v_0(1) = \lambda \tag{3.20}$$

as in the Föppl membrane theory. As discussed in Chapter 2, this problem has both tensile and compressive solutions. We have assumed $\lambda > 0$, so the membrane solution v_0 will be compressive (positive) in the interval $x \in [0, 1]$.

The equation for v_1 is

$$v_1'' + \frac{3}{x} v_1' = 2h \frac{\kappa g(x)}{x^{\frac{3}{2}} {v_0}^{\frac{5}{4}}} \cos(\tilde{x} + \phi) + O(h^2) \tag{3.21}$$

with boundary conditions

$$v_1'(0;h) = 0, \qquad v_1(1;h) = 0. \tag{3.22}$$

Multiplying through by x^3 and integrating from 0 to x gives

$$x^3 v_1'(x;h) \sim 2h\kappa I_1(x;h) + h^2 \psi_1(x;h) \tag{3.23}$$

where

$$I_1(x;h) = \int_0^x \frac{\xi^{\frac{3}{2}} g(\xi)}{{v_0}^{\frac{5}{4}}(\xi)} \cos\Big(\frac{1}{h} \int_0^\xi {v_0}^{\frac{1}{2}}(\varsigma)\, d\varsigma + \phi\Big)\, d\xi.$$

The notation ψ_k is used to indicate an unknown function having derivatives up to order k that are $O(1)$ as $h \to 0$. The integral I_1 can be approximated

---

[6] *Vorlesungen über technische Mechanik*, Vol. 5, 1907

using integration by parts. Thus,

$$\begin{aligned} I_1(x;h) &= \int_0^x \frac{h\xi^{\frac{3}{2}}g(\xi)}{v_0^{\frac{7}{4}}(\xi)} \frac{d}{d\xi} \sin\left(\frac{1}{h}\int_0^\xi v_0^{\frac{1}{2}}(\varsigma)\,d\varsigma + \phi\right) d\xi \\ &= \frac{hx^{\frac{3}{2}}g(x)}{v_0^{\frac{7}{4}}(x)} \sin(\tilde{x}+\phi) - hI_2(x;h) \end{aligned}$$

where

$$I_2(x;h) = \int_0^x \frac{d}{d\xi}\left(\frac{\xi^{\frac{3}{2}}g(\xi)}{v_0^{\frac{7}{4}}(\xi)}\right) \sin\left(\frac{1}{h}\int_0^\xi v_0^{\frac{1}{2}}(\varsigma)\,d\varsigma + \phi\right) d\xi.$$

Using the assumption that g is twice continuously differentiable, we may integrate I_2 by parts. Then, by the Riemann-Lebesgue lemma, the integral I_2 is $O(h)$ and hence

$$I_1(x;h) = \frac{hx^{\frac{3}{2}}g(x)}{v_0^{\frac{7}{4}}} \sin(\tilde{x}+\phi) + O(h^2).$$

Substituting this estimate into the equation (3.23) and dividing through by x^3, we obtain

$$v_1{}'(x;h) = h^2 \frac{2\kappa g(x)}{x^{\frac{3}{2}} v_0^{\frac{7}{4}}} \sin(\tilde{x}+\phi) + h^2\psi_1(x;h). \tag{3.24}$$

In this asymptotic expansion for v_1, it appears that the error term is of the same order as the leading term, but the expression is still useful because it gives us the leading dependence of v_1 on $\tilde{x}$—because the error term is written as $h^2\psi_1$, we know that the $\tilde{x}$ dependence in the error occurs only at $O(h^3)$. Integrating from x to 1 in (3.24) and using the boundary condition $v_1(1;h) = 0$, we get

$$v_1(x;h) = -2h^2\kappa I_3(x;h) + h^2\psi_2(x;h)$$

where

$$I_3(x;h) = -\int_x^1 \frac{g(\xi)}{\xi^{\frac{3}{2}} v_0^{\frac{7}{4}}(\xi)} \sin\left(\frac{1}{h}\int_0^\xi v_0^{\frac{1}{2}}(\varsigma)\,d\varsigma + \phi\right) d\xi.$$

By a similar argument as that used above to obtain the asymptotics for I_1, integration by parts gives

$$I_3(x;h) \sim \frac{hg(x)}{x^{\frac{3}{2}} v_0^{\frac{9}{4}}(x)} \cos(\tilde{x} + \phi) + h\psi_1(x;h)$$

where we have included the $O(h)$ contribution from the endpoint $\xi = 1$ into the error term $h\psi_1$. Therefore,

$$v_1(x;h) = -h^3 \frac{2\kappa g(x)}{x^{\frac{3}{2}} v_0^{\frac{9}{4}}(x)} \cos(\tilde{x} + \phi) + h^2\psi_2(x;h).$$

Here again we have the somewhat strange combination of an error term that is asymptotically greater than the leading term of the expansion. Because the error term $h^2\psi_2$ has $O(h^2)$ derivatives up to the second order, we know that the dependence on $\tilde{x}$ occurs in the error term at $O(h^4)$.

The approximation for v obtained by combining v_0 and the asymptotic expansion for v_1 satisfies the equation (3.18) and the boundary condition (1.9) to $O(h^2)$. Thus,

$$v(x;h) = v_0(x) - h^3 \frac{2\kappa g(x)}{x^{\frac{3}{2}} v_0^{\frac{9}{4}}} \cos(\tilde{x} + \phi) + h^2\psi_2(x;h) \tag{3.25}$$

and

$$v'(x;h) = v_0{}'(x) + h^2 \frac{2\kappa g(x)}{x^{\frac{3}{2}} v_0^{\frac{7}{4}}} \sin(\tilde{x} + \phi) + h^2\psi_1(x;h) \tag{3.26}$$

as $h \to 0$, where v_0 is a positive Föppl membrane solution.

To recap, the approximations (3.15, 3.16, 3.25, 3.26) satisfy the plate equations (3.3) and the boundary condition (1.9) to $O(h^2)$ and the boundary condition (3.2) to $O(h)$, provided $x \gg h$. Estimates from the formal expansion indicate errors in the solution of $O(h^2)$ for x in this region.

The Uniform Asymptotic Approximation. The asymptotics obtained so far are not valid near the origin. Thus, for the circular plate there will be a region near the center of the plate that is not accurately described by the expansions (3.15, 3.16, 3.25, 3.26). We will construct a uniform asymptotic approximation, employing a multiscale analysis of the equilibrium equation (3.3a). This approximation is equivalent asymptotically in the region $x \gg h$ to that obtained above but will also be valid for $x = O(h)$. The error estimates become quite complicated since the same term may be of different order in the regions $x = O(1)$ and $x = O(h)$. However, a numerical calculation of the order to which the asymptotic expansion satisfies the equation and approximates the solution can be performed once the formula has been obtained. The numerics are done on the first-order system

$$\begin{aligned} hz_1' &= z_2, \qquad & h(x^3 z_2)' &= -x^3 z_1 z_3, \\ z_3' &= z_4, \qquad & (x^3 z_4)' &= x^3 z_1^2. \end{aligned} \tag{3.27}$$

This system is equivalent to the von Kármán equations (3.3) with

$$\begin{aligned} z_1 &= u, \qquad & z_2 &= hu', \\ z_3 &= v, \qquad & z_4 &= v'. \end{aligned}$$

Our aim is to obtain an asymptotic expansion $\mathbf{z}_A$ satisfying the system (3.27) to $O(h^{\frac{3}{2}})$ and approximating the solution $\mathbf{z} = [z_j]$, $j = 1, \ldots, 4$, with a relative error of $O(h)$. Consequently, terms in the equations or in the approximations whose effects are asymptotically small relative to the desired level of accuracy are generally neglected.

The following transformations are motivated by the discussions given in FRÖMAN AND FRÖMAN[7] concerning the WKB equation. We let

$$w = x^{\frac{3}{2}}(u - u_0)v_0^{\frac{1}{4}}, \tag{3.28}$$

[7] *JWKB Approximation; Contributions to the Theory*, 1965

where u_0 is defined in (3.6) and, taking $\tilde{x}$ as defined in (3.10), we suppose

$$w(x;h) \sim hw_1(\tilde{x},x) + h^2 w_2(\tilde{x},x),$$

$$v(x;h) \sim v_0(x) + h^2 v_2(x) + h^3 v_3(\tilde{x},x),$$

where v_0 satisfies the membrane problem (3.19, 3.20). It follows from the boundary condition (3.20a) that

$$\frac{h^2}{v_0(x)x^2} = \frac{1}{\tilde{x}^2} + O(h^2) \qquad \text{as } h \to 0 \tag{3.29}$$

uniformly for $x \in [0,1]$; thus, the factor $h^2 x^{-2}$ can be replaced as required by an $O(1)$ function of $\tilde{x}$.

Following the usual multiscale approach, we treat x and $\tilde{x}$ formally as independent variables. The differential terms in the equilibrium equation (3.3a) become

$$\begin{aligned} h^2 \frac{1}{x^3}\frac{d}{dx}\left(x^3 \frac{d}{dx} u\right) \sim & \frac{h v_0{}^{\frac{3}{4}}(x)}{x^{\frac{3}{2}}}\left(\frac{\partial^2}{\partial \tilde{x}^2} w_1 - \frac{3}{4\tilde{x}^2} w_1\right) + \\ & + \frac{h^2 v_0{}^{\frac{3}{4}}(x)}{x^{\frac{3}{2}}}\left(\frac{\partial^2}{\partial \tilde{x}^2} w_2 - \frac{3}{4\tilde{x}^2} w_2 + \frac{2}{v_0{}^{\frac{1}{2}}(x)}\frac{\partial^2}{\partial x \partial \tilde{x}} w_1\right) + \\ & + h^2\left(u_0''(x) + \frac{3}{x} u_0'(x)\right). \end{aligned} \tag{3.30}$$

The rest of the equation (3.3a) takes the form

$$uv - g(x) \sim \frac{h}{x^{\frac{3}{2}}} v_0 w_1 + \frac{h^2}{x^{\frac{3}{2}}} v_0 w_2 + h^2 F(x). \tag{3.31}$$

Substituting the expressions (3.30, 3.31) into the equilibrium equation (3.3a) and equating like terms, we obtain

$$\frac{\partial^2}{\partial \tilde{x}^2} w_1 + \left(1 - \frac{3}{4\tilde{x}^2}\right) w_1 = 0 \tag{3.32}$$

and

$$\frac{\partial^2}{\partial \tilde{x}^2} w_2 + \left(1 - \frac{3}{4\tilde{x}^2}\right) w_2 = -\frac{2}{v_0^{\frac{1}{2}}(x)} \frac{\partial^2}{\partial x \partial \tilde{x}} w_1 + F(x). \tag{3.33}$$

The benefits derived from making the transformations (3.10, 3.28) should now be apparent, as we have obtained an equation for the variable w_1 that is independent of x. The solution of the equation (3.32) that is bounded at the origin is

$$w_1 = A(x)\tilde{x}^{\frac{1}{2}} J_1(\tilde{x}) + B(x)\tilde{x}^{\frac{1}{2}} Y_1(\tilde{x}),$$

where $B(x) = O(x)$ as $x \to 0$. Solvability considerations in the higher-order equation (3.33) require A and B to be constants. Hence,

$$w_1 = \kappa \sqrt{\frac{\pi}{2}} \cdot \tilde{x}^{\frac{1}{2}} J_1(\tilde{x})$$

for some constant κ. We define

$$z_{A1}(x;h) \equiv u_0(x) + h \frac{\kappa}{x^{\frac{3}{2}} v_0^{\frac{1}{4}}(x)} \sqrt{\frac{\pi}{2}} \cdot \tilde{x}^{\frac{1}{2}} J_1(\tilde{x}),$$
$$z_{A2}(x;h) \equiv h\Big(u_0'(x) - \frac{\kappa v_0^{\frac{1}{4}}(x)}{x^{\frac{3}{2}}} \sqrt{\frac{\pi}{2}} \cdot \tilde{x}^{\frac{1}{2}} J_2(\tilde{x})\Big).$$

It may be verified from the recursion relations for the Bessel functions and formula (3.29) that for $x \in [0,1]$,

$$h z'_{A1}(x;h) = z_{A2} + O(h^{\frac{3}{2}}).$$

From the definitions of z_{A1}, z_{A2} above we obtain the uniform small thickness asymptotic approximations for u and u'

$$\begin{aligned} u(x;h) &= z_1 \sim u_0(x) + h \frac{\kappa}{x^{\frac{3}{2}} v_0^{\frac{1}{4}}(x)} \sqrt{\frac{\pi}{2}} \cdot \tilde{x}^{\frac{1}{2}} J_1(\tilde{x}), \\ u'(x;h) &= h^{-1} z_2 \sim u_0'(x) - \frac{\kappa v_0^{\frac{1}{4}}(x)}{x^{\frac{3}{2}}} \sqrt{\frac{\pi}{2}} \cdot \tilde{x}^{\frac{1}{2}} J_2(\tilde{x}). \end{aligned} \tag{3.34}$$

The constant κ is chosen such that the boundary condition (3.2) applied to the uniform asymptotic approximation is satisfied exactly. The formula

$$\kappa = \sqrt{\frac{2}{\pi}} \cdot \frac{u_0'(1) + Qu_0(1)}{\lambda^{\frac{1}{4}} \varsigma^{\frac{1}{2}} (J_2(\varsigma) - hQ\lambda^{-\frac{1}{2}} J_1(\varsigma))},$$

with $\varsigma = h^{-1}K$, can be derived from the approximations (3.34).

Large argument asymptotics of Bessel functions are given by

$$\begin{aligned} J_\nu(z) \sim & \sqrt{\frac{2}{\pi}} \cdot z^{-\frac{1}{2}} \cos\left(z - \frac{(1+2\nu)\pi}{4}\right) \; - \\ & - \sqrt{\frac{2}{\pi}} \cdot z^{-1} \frac{4\nu^2 - 1}{8} \sin\left(z - \frac{(1+2\nu)\pi}{4}\right). \end{aligned} \tag{3.35}$$

For $x \gg h$, we then obtain from (3.34a) that

$$u(x;h) \sim u_0(x) + \frac{\kappa h}{x^{\frac{3}{2}} v_0^{\frac{1}{4}}(x)} \cos(\tilde{x} + \phi),$$

where $\phi = -\frac{3}{4}\pi$; that is, the uniform asymptotic approximation z_{A1} is equivalent to the outer solution (3.15) in its region of validity. The expression (3.17) for the multiplying factor κ will hold asymptotically. Hence,

$$\kappa \sim \frac{u_0'(1) + Qu_0(1)}{\lambda^{\frac{1}{4}} \sin\theta - (hQ/\lambda^{\frac{1}{4}}) \cos\theta}, \quad \text{where} \quad \theta = \frac{K}{h} - \tfrac{3}{4}\pi \tag{3.36}$$

and K is defined in (3.14). As long as the denominator is bounded away from zero as $h \to 0$, i.e.,

$$h \neq \frac{K}{\left(n + \frac{3}{4}\right)\pi}, \tag{3.37}$$

then κ remains $O(1)$. The case where (3.37) does not hold is treated in Section (3.2).

We have now found the uniform approximations for u and u' in terms of the membrane solution v_0. To complete the analysis we must utilize the asymptotics derived so far to approximate the radial stress v and its derivative v' uniformly for $x \in [0,1]$. By substituting the asymptotics for u into the compatibility equation and integrating by parts, the asymptotic expansions for v and v' valid in the region $x = O(h)$ are obtained. Judicious use of the relation (3.29) then provides approximations that also match the outer expansion (3.25) for $x \gg h$. Maintaining the formalism of x and $\tilde{x}$ as independent variables creates as much confusion as it alleviates, so hereafter we treat everything—including $\tilde{x}$—as a function of the single independent variable x.

Substituting the asymptotic expansion (3.34) for u into (3.3b) gives

$$v'' + \frac{3}{x}v' \sim \frac{g^2}{{v_0}^2} + 2h\frac{g\kappa}{x^{\frac{3}{2}}{v_0}^{\frac{5}{4}}}\sqrt{\frac{\pi}{2}}\tilde{x}^{\frac{1}{2}}J_1(\tilde{x}) + h^2\frac{\kappa^2\pi}{2x^3{v_0}^{\frac{1}{2}}}\tilde{x}J_1^2(\tilde{x}).$$

Letting $v = v_0 + v_1$ and recalling that v_0 satisfies the membrane equation (3.19), we have

$$(x^3{v_1}')' \sim 2h\frac{g(x)\kappa x^{\frac{3}{2}}}{{v_0}^{\frac{5}{4}}(x)}\sqrt{\frac{\pi}{2}}\tilde{x}^{\frac{1}{2}}J_1(\tilde{x}) + h^2\frac{\kappa^2\pi}{2{v_0}^{\frac{1}{2}}(x)}\tilde{x}J_1^2(\tilde{x}).$$

For $x = O(h)$, this is by force of (3.29) equivalent to

$$(x^3{v_1}')' \sim 2h^{\frac{5}{2}}\frac{g(0)\kappa}{{v_0}^2(0)}\sqrt{\frac{\pi}{2}}\tilde{x}^2J_1(\tilde{x}) + h^2\frac{\kappa^2\pi}{2{v_0}^{\frac{1}{2}}(0)}\tilde{x}J_1^2(\tilde{x}).$$

The factor ${v_0}^{\frac{1}{2}}\tilde{x}^2J_1(\tilde{x})$ from the first term can be integrated exactly to yield $h\tilde{x}^2J_2(\tilde{x})$. In the second term, the factor ${v_0}^{\frac{1}{2}}\tilde{x}J_2(\tilde{x})$ may be treated similarly. Thus, integration from 0 to x gives

$$x^3{v_1}' \sim 2h^{\frac{7}{2}}\frac{g(0)\kappa}{{v_0}^{\frac{5}{2}}(0)}\sqrt{\frac{\pi}{2}}\tilde{x}^2J_2(\tilde{x}) + h^3\frac{\kappa^2\pi}{4v_0(0)}\tilde{x}^2\left(J_1^2(\tilde{x}) - J_0(\tilde{x})J_2(\tilde{x})\right).$$

Dividing through by x^3 and applying (3.29), we obtain

$${v_1}' \sim 2h^{\frac{1}{2}}\frac{g(0)\kappa}{v_0(0)}\sqrt{\frac{\pi}{2}}\tilde{x}^{-1}J_2(\tilde{x}) + \frac{\kappa^2\pi{v_0}^{\frac{1}{2}}(0)}{4}\tilde{x}^{-1}\left(J_1^2(\tilde{x}) - J_0(\tilde{x})J_2(\tilde{x})\right), \quad (3.38)$$

which is the asymptotic expansion for v_1' valid for $x = O(h)$. Another integration from 0 to x gives

$$
\begin{aligned}
v_1 \sim & - 2h^{\frac{3}{2}} \frac{g(0)\kappa}{v_0^{\frac{3}{2}}(0)} \sqrt{\frac{\pi}{2}} \tilde{x}^{-1} J_1(\tilde{x}) - \\
& - h\frac{\kappa^2 \pi}{8}\Big(J_0^2(\tilde{x}) + 2J_1^2(\tilde{x}) - J_0(\tilde{x})J_2(\tilde{x})\Big) + \text{constant},
\end{aligned}
\tag{3.39}
$$

which is the asymptotic expansion for v_1 valid for $x = O(h)$. In these manipulations we have made use of the following formulas for indefinite integrals of Bessel functions:

$$
\begin{aligned}
\int^z \varsigma^2 J_1(\varsigma)\, d\varsigma &= z^2 J_2(z), \\
\int^z \varsigma J_1^2(\varsigma)\, d\varsigma &= \frac{z^2}{2}\Big(J_1^2(z) - J_0(z)J_2(z)\Big), \\
\int^z \varsigma^{-1} J_2(\varsigma)\, d\varsigma &= -z^{-1} J_1(z), \\
\int^z \varsigma^{-1} J_1^2(\varsigma)\, d\varsigma &= -\frac{1}{2}\Big(J_0^2(z) + J_1^2(z)\Big), \\
\int^z \varsigma^{-1} J_0(\varsigma) J_2(\varsigma)\, d\varsigma &= -\frac{1}{2}\Big(J_0(z)J_2(z) - J_1^2(z)\Big).
\end{aligned}
$$

Matching with the outer solution shows that the constant in the formula (3.39) is $O(h^2)$ and hence is negligible for this approximation.

From (3.29) it can be shown that the estimates (3.38, 3.39) are asymptotically equivalent to

$$
\begin{aligned}
v_1 \sim & - 2h^3 \frac{g(x)\kappa}{x^{\frac{3}{2}} v_0^{\frac{9}{4}}(x)} \sqrt{\frac{\pi}{2}} \tilde{x}^{\frac{1}{2}} J_1(\tilde{x}) - \\
& - h^2 \frac{\kappa^2 \pi}{8 x v_0^{\frac{1}{2}}} \tilde{x}\Big(J_0^2(\tilde{x}) + 2J_1^2(\tilde{x}) - J_0(\tilde{x})J_2(\tilde{x})\Big), \\
v_1' \sim & 2h^2 \frac{g(x)\kappa}{x^{\frac{3}{2}} v_0^{\frac{7}{4}}(x)} \sqrt{\frac{\pi}{2}} \tilde{x}^{\frac{1}{2}} J_2(\tilde{x}) + \\
& + h^2 \frac{\kappa^2 \pi}{4x^2 v_0^{\frac{1}{2}}(x)} \tilde{x}\Big(J_1^2(\tilde{x}) - J_0(\tilde{x})J_2(\tilde{x})\Big)
\end{aligned}
\tag{3.40}
$$

in the region $x = O(h)$. Furthermore, these approximations match asymptotically the appropriate terms in the estimates (3.25, 3.26) valid for the region $x \gg h$. This can be verified using the large argument asymptotic expansions (3.35) of the Bessel functions. For if $x \gg h$, then the first term of the formula for v_1 becomes

$$-2h^3 \frac{g\kappa}{x^{\frac{3}{2}} v_0^{\frac{9}{4}}} \sqrt{\frac{\pi}{2}}\, \tilde{x}^{\frac{1}{2}} J_1(\tilde{x}) \sim -2h^3 \frac{g\kappa}{x^{\frac{3}{2}} v_0^{\frac{9}{4}}} \cos\chi,$$

where $\chi = \tilde{x} - \frac{3}{4}\pi$. The corresponding term for $v_1{}'$ becomes

$$2h^2 \frac{g\kappa}{x^{\frac{3}{2}} v_0^{\frac{7}{4}}} \sqrt{\frac{\pi}{2}}\, \tilde{x}^{\frac{1}{2}} J_2(\tilde{x}) \sim 2h^2 \frac{g\kappa}{x^{\frac{3}{2}} v_0^{\frac{7}{4}}} \sin\chi.$$

Also, using two terms from the expansion (3.35), we find

$$-h^2 \frac{\kappa^2 \pi}{8 x v_0^{\frac{1}{2}}} \tilde{x} \Big(J_0^2(\tilde{x}) + 2J_1^2(\tilde{x}) - J_0(\tilde{x}) J_2(\tilde{x}) \Big) \sim -h^2 \frac{\kappa^2}{2 x v_0^{\frac{1}{2}}} + O(h^4)$$

for the second term in the formula for v_1. Note that the $O(h^2)$ term does not depend on $\tilde{x}$. Similarly, the second term in the formula for $v_1{}'$ satisfies

$$h^2 \frac{\kappa^2 \pi}{4 x^2 v_0^{\frac{1}{2}}} \tilde{x} (J_1^2(\tilde{x}) - J_0(\tilde{x}) J_2(\tilde{x})) \sim h^2 \frac{\kappa^2}{2 x^2 v_0^{\frac{1}{2}}} + O(h^3).$$

Thus, the approximations (3.40) agree with the formulas (3.25, 3.26) valid for $x \gg h$, both in the terms that are retained and in the order of the error.

The uniform approximation is obtained by combining the membrane solution v_0, $v_0{}'$ with the asymptotics for v_1, $v_1{}'$. Thus, let

$$\begin{aligned} z_{A3}(x;h) \equiv & v_0 - 2h^3 \frac{g\kappa}{x^{\frac{3}{2}} v_0^{\frac{9}{4}}} \sqrt{\frac{\pi}{2}}\, \tilde{x}^{\frac{1}{2}} J_1(\tilde{x}) \; - \\ & - h^2 \frac{\kappa^2 \pi}{8 x v_0^{\frac{1}{2}}} \tilde{x} (J_0^2(\tilde{x}) + 2J_1^2(\tilde{x}) - J_0(\tilde{x}) J_2(\tilde{x})), \\ z_{A4}(x;h) \equiv & v_0{}' + 2h^2 \frac{g\kappa}{x^{\frac{3}{2}} v_0^{\frac{7}{4}}} \sqrt{\frac{\pi}{2}}\, \tilde{x}^{\frac{1}{2}} J_2(\tilde{x}) \; + \\ & + h^2 \frac{\kappa^2 \pi}{4 x^2 v_0^{\frac{1}{2}}} \tilde{x} (J_1^2(\tilde{x}) - J_0(\tilde{x}) J_2(\tilde{x})). \end{aligned}$$

The uniform asymptotic approximations of the radial stress and its derivative are

$$v(x;h) \sim z_{A3}(x;h), \qquad v'(x;h) \sim z_{A4}(x;h) \qquad \text{as } h \to 0. \tag{3.41}$$

Observe that v and v' are $O(1)$ throughout the domain $x \in [0,1]$; that is, the radial stress is smooth to order 1. This will not be the case for the asymptotic approximation derived in Section (3.2), which has a boundary layer in the stress near $x = 0$.

The Annular Plate. A multiscale asymptotic expansion for the annular plate solution may be obtained similarly. We fix $a > 0$; thus, a region about the center of the plate is excluded, and the difficulties encountered in the circular plate approximation for $x = O(h)$ are avoided in this case. If we take $v(a) = \eta > 0$ and suppose that $v(x;h) \sim v_0(x;A) > 0$ as $h \to 0$ for $x \in [a,1]$, then the expansions (3.15, 3.25) are uniformly valid. Hence, we have

$$\begin{aligned} v(x;h) &= v_0(x;A) + O(h^2), \\ u(x;h) &= u_0(x;A) + \frac{h\kappa}{x^{\frac{3}{2}} {v_0}^{\frac{1}{4}}(x)} \cos(\tilde{x} + \phi) + O(h^2) \end{aligned} \tag{3.42}$$

where

$$\tilde{x} = \frac{1}{h} \int_a^x {v_0}^{\frac{1}{2}}(s;A)\, ds,$$

$$u_0(x;A) = \frac{g(x) + x^{-2}A}{v_0(x;A)},$$

and $v_0(x;A)$ is a positive solution of

$${v_0}'' + \frac{3}{x} {v_0}' = \frac{(g(x) + x^{-2}A)^2}{{v_0}^2} \tag{3.43}$$

with

$$v_0(a;A) = \eta, \qquad v_0(1;A) = \lambda,$$

provided such a solution exists. Although the regions of parameter space where solutions exist have not been quantitatively investigated by us, the equation (3.43) reveals that the quantity $v_0''(x) + (3/x)v_0'(x)$ will be large if $v_0(x)$ is small; thus, it is reasonable to suppose that solutions may not exist if η and λ are too small.

To satisfy the boundary condition

$$a^2 u(a)\eta = A, \tag{3.44}$$

we require

$$u(a) = u_0(a; A);$$

thus, we must have either $\kappa = 0$ or $\cos\phi = 0$. We must also have

$$a u_0'(a; A) + (1+\nu)u_0(a; A) - \kappa\left(\frac{\eta^{\frac{1}{4}}}{a^{\frac{3}{2}}}\sin\phi - \frac{h(1+\nu)}{a^{\frac{3}{2}}\eta^{\frac{1}{4}}}\cos\phi\right) = 0 \tag{3.45}$$

and

$$u_0'(1; A) + Q u_0(1; A) - \kappa\left(\lambda^{\frac{1}{4}}\sin(\theta(A)+\phi) - \frac{hQ}{\lambda^{\frac{1}{4}}}\cos(\theta(A)+\phi)\right) = 0 \tag{3.46}$$

where

$$\theta(A) = h^{-1}\int_a^1 v_0^{\frac{1}{2}}(s; A)\,ds.$$

Letting

$$\begin{aligned}\alpha(A) &= a u_0'(a; A) + (1+\nu)u_0(a; A)\\ &= \frac{2}{\eta} - A\left(\frac{1-\nu}{\eta a^2} + \frac{v_0'(a; A)}{a\eta^2}\right)\end{aligned}$$

and

$$\begin{aligned}\beta(A) &= u_0'(1; A) + Q u_0(1; A)\\ &= \frac{g'(1) + Qg(1)}{\lambda} - \frac{g(1)v_0'(1; A)}{\lambda^2} - A\left(\frac{2-Q}{\lambda} + \frac{v_0'(1; A)}{\lambda^2}\right),\end{aligned}$$

then if $\kappa = 0$, we must have from (3.45, 3.46) that

$$\alpha(A) = \beta(A) = 0.$$

In general, we cannot choose a value of A such that both of these conditions are satisfied; thus, to satisfy (3.44) we must have $\cos\phi = 0$ and so we take $\phi = \pi/2$.

The conditions (3.45, 3.46) become

$$\alpha(A) = \kappa\,\frac{\eta^{\frac{1}{4}}}{a^{\frac{3}{2}}},$$

$$\beta(A) = \kappa\left(\lambda^{\frac{1}{4}}\cos\theta(A) + \frac{hQ}{\lambda^{\frac{1}{4}}}\sin\theta(A)\right).$$

Eliminating κ between these equations yields

$$\alpha(A)\left(\lambda^{\frac{1}{4}}\cos\theta(A) + \frac{hQ}{\lambda^{\frac{1}{4}}}\sin\theta(A)\right) = \beta(A)\,\frac{\eta^{\frac{1}{4}}}{a^{\frac{3}{2}}}. \tag{3.47}$$

This condition implicitly defines A provided some solution of (3.47) exists. Although we expect that for some values of η and λ a solution of (3.47) may not exist, we show that for $Q = O(1)$ and $\eta = \lambda$ large as $h \to 0$, a value of A can be found that asymptotically satisfies this condition.

Thus, let $\eta = \lambda \to +\infty$ and suppose $A = O(1)$. Then

$$v_0(x; A) \sim \lambda;$$

that is, to leading order, v_0 is independent of A. Thus, in the first approximation,

$$\theta = h^{-1}\lambda^{\frac{1}{2}}(1-a)$$

and the condition (3.47) is then linear in A at leading order. Thus, as $h \to 0$ we have

$$((1-\nu)\cos\theta + (Q-2)\sqrt{a})A \sim 2a^2\cos\theta - (g'(1) + Qg(1))\sqrt{a}\,.$$

The coefficient of A will in general be nonzero and the solution for A will be $O(1)$. Thus, we conjecture that for λ and η sufficiently large, there exists at least one solution of (3.47).

Once A is known, κ is then found to be

$$\kappa = \alpha(A)\,\frac{a^{\frac{3}{2}}}{\eta^{\frac{1}{4}}}.$$

This expansion is *not* uniformly valid as $a \to 0$; the asymptotics must be carried out with more care to be applicable in this limit.

In the limit $Q \to +\infty$, condition (3.47) becomes

$$\alpha(A)\frac{h}{\lambda^{\frac{1}{4}}}\sin\theta(A) = \frac{(g(1)+A)\eta^{\frac{1}{4}}}{\lambda a^{\frac{3}{2}}}. \tag{3.48}$$

Thus, $A = -g(1) + O(h)$; that is, in the case of the annular plate clamped at its outer edge with $v(a) = \eta > 0$, we choose A such that the function $\hat{g}(x) = g(x) + x^{-2}A$ satisfies $\hat{g}(1) = 0$.

If we specify the radial stress to vanish at the inner edge, i.e., $\eta = 0$, then $v(a) = 0$ and the expansion (3.15) is not uniformly valid as $x \to a$. To obtain a uniformly valid expansion we use a formula related to Langer's uniform expansion for the WKB problem with one turning point. Thus,

$$\begin{aligned} v(x;h) &= v_0(x) + O(h^{\frac{5}{3}}),\\ u(x;h) &= u_0(x) + h^{\frac{5}{6}}\,\frac{\varsigma^{\frac{1}{4}}}{{v_0}^{\frac{1}{4}}(x)}\left(\alpha Ai(-\varsigma) + \beta Bi(-\varsigma)\right) + O(h^{\frac{5}{3}}) \end{aligned} \tag{3.49}$$

where

$$\tilde{x} = \frac{1}{h}\int_a^x {v_0}^{\frac{1}{2}}(s)\,ds, \qquad \varsigma = \left(\tfrac{3}{2}\tilde{x}\right)^{\frac{2}{3}}.$$

We let ${v_0}'(a) = \gamma$. At $x = a$ we have

$$u(a) \sim \frac{2}{a\gamma} + O(h^{\frac{2}{3}}),$$

$$u'(a) \sim \frac{-4}{a^3\gamma^4} - \gamma^{\frac{1}{6}}\left(\alpha Ai'(0) + \beta Bi'(0)\right).$$

Using

$$Ai'(0) = -\frac{1}{3^{\frac{1}{3}}\Gamma(\frac{2}{3})}, \qquad Bi'(0) = \frac{1}{3^{\frac{2}{3}}\Gamma(\frac{2}{3})},$$

then we must have

$$3^{\frac{1}{3}}\alpha - \beta = -\frac{3^{\frac{2}{3}}\Gamma(\frac{2}{3})}{\gamma^{\frac{1}{6}}}\left(\frac{-4}{a^3\gamma^4} + (1+\nu)\frac{2}{a^2\gamma}\right) \tag{3.50}$$

to satisfy the boundary condition $au'(a) + (1+\nu)u(a) = 0$.

At the outer edge we have

$$\begin{aligned} u'(1) + Qu(1) \sim \text{constant} \cdot h^{-\frac{1}{6}}\Big(&\alpha\cos\theta - \beta\sin\theta + h^{\frac{5}{6}}Qg(1) + \\ &+ \frac{hQ}{\lambda^{\frac{1}{2}}}(\alpha\sin\theta + \beta\cos\theta)\Big) \end{aligned} \tag{3.51}$$

where

$$\theta = \frac{1}{h}\int_a^1 v_0^{\frac{1}{2}}(s)\,ds + \tfrac{1}{4}\pi.$$

Hence, to satisfy $u'(1) + Qu(1) = 0$ for $Q = O(1)$, we take

$$\alpha \sim \kappa\sin\theta, \qquad \beta \sim \kappa\cos\theta.$$

We may solve in equation (3.50) for κ provided

$$\frac{1}{h}\int_a^1 v_0^{\frac{1}{2}}(s)\,ds \neq (n - \tfrac{1}{4})\pi - \tan^{-1}3^{-\frac{1}{3}}.$$

For $Q \to +\infty$ we find from (3.51) that $\kappa = O(h^{-\frac{5}{6}})$ unless $g(1) = 0$. We cannot recover the Föppl membrane equation unless $\kappa = o(h^{-\frac{5}{6}})$, so the expansion is not valid for the clamped annular plate unless the load is self-equilibrating.

The Clamped Circular Plate. The case of a plate with clamped edge may be considered as the limit of the plate, with the edge elastically supported against rotation, where the strength of support against rotation becomes infinitely large; i.e., $Q \to +\infty$. Taking this limit in the expansion (3.11) for the circular plate yields

$$u(x;h) \sim u_0(x) + \frac{c}{x^{\frac{3}{2}} v_0^{\frac{1}{4}}(x)} \cos(\tilde{x} + \phi) \tag{3.52}$$

for $x \gg h$, where

$$c = \frac{-u_0(1)\lambda^{\frac{1}{4}}}{\cos(\tilde{x} + \phi)} = \frac{-g(1)}{\lambda^{\frac{3}{4}} \cos(\tilde{x} + \phi)}. \tag{3.53}$$

Thus, if $g(1) \neq 0$ and $\lambda = O(1)$ then $c = O(1)$. Substitution of the expansion (3.52) for u into the compatibility equation (3.3b) gives the leading-order equation

$$v_0'' + \frac{3}{x} v_0' = \frac{g^2}{v_0^2} + \frac{c^2}{2x^3 v_0^{\frac{1}{2}}}, \tag{3.54}$$

where we have dropped the oscillatory cross-term, which does not contribute to v at $O(1)$. Note that (3.54) illustrates the necessity of requiring $c = O(h)$ to obtain $v \sim v_0 + O(h^2)$, where v_0 is a Föppl membrane solution. Thus when $c = O(1)$ the Föppl membrane equation is no longer the leading order equation for the stress. On the other hand, no solutions of this "membrane" equation (3.54) that are positive on $x \in (0, 1]$ remain bounded at the origin. Solutions of these equations that are positive on $x \in (x_0, 1]$ may be obtained if $g(x_0) = 0$. However, the expansion thus obtained will not satisfy $hu' \to 0$ as $h \to 0$. In Appendix I it is noted that this condition is required for validity of the von Kármán equations.

One way to get around these difficulties is to remove the restriction that v remain $O(1)$ as $h \to 0$. In Chapter 1 the asymptotic expansion (1.16) was derived for the plate elastically supported against rotation. In the limit $Q \to \infty$ this expansion becomes

$$u(x) \sim \frac{g(x)}{\lambda} - \frac{1}{x^{\frac{3}{2}}} \cdot \kappa \sqrt{\frac{\pi \tilde{x}}{2}}\, J_1(\tilde{x}),$$

where $\tilde{x} = h^{-1}\lambda^{\frac{1}{2}}x$ and

$$\kappa = \frac{g(1)}{\lambda\cos(h^{-1}\lambda^{\frac{1}{2}} - \frac{3}{4}\pi)}.$$

For $x \gg h/\sqrt{\lambda}$ this is equivalent to

$$u(x) \sim \frac{g(x)}{\lambda} - \frac{1}{x^{\frac{3}{2}}} \cdot \kappa\cos\left(h^{-1}\lambda^{\frac{1}{2}}x - \tfrac{3}{4}\pi\right).$$

The equation for the next term of $v = \lambda + v_1$ is then

$$v_1'' + \frac{3}{x}v_1' = \frac{\kappa^2}{2x^3},$$

which has the solution

$$v_1 = -\tfrac{1}{4}\kappa^2\log x. \tag{3.55}$$

For the validity of the expansion for u, WKB theory requires

$$h^{-1}\int_x^1 v^{\frac{1}{2}}(s)\,ds \sim h^{-1}\sqrt{\lambda}(1-x) + o(1).$$

Now, expanding the integrand and inserting the formula (3.55) for v_1 we have

$$\begin{aligned} h^{-1}\int_x^1 v^{\frac{1}{2}}(s)\,ds &\sim h^{-1}\sqrt{\lambda}(1-x) + \frac{1}{2h\lambda^{\frac{1}{2}}}\int_x^1 v_1(s)\,ds \\ &\sim h^{-1}\sqrt{\lambda}(1-x) + O(h^{-1}\lambda^{-\frac{5}{2}}). \end{aligned}$$

Thus, it is necessary that $\lambda \gg h^{-\frac{2}{5}}$ for the consistency of this asymptotic expansion.

We are forced to conclude that the assumption of smooth $O(1)$ compressive radial stress is not valid in the case of the clamped circular plate. In Chapter 4 it is proved that solutions for the clamped circular plate with $O(1)$ stress cannot asymptotically approach the compressive Föppl membrane solutions as the thickness tends to 0.

Numerical Calculations. We wish to evaluate the uniform asymptotic approximations (3.34, 3.41) derived in the previous section. These formulas include the compressive membrane solution v_0, which is not known analytically and thus must be calculated numerically. We use the finite difference method described in Appendix II, a variation of the box scheme with a uniform grid. Oscillations occur in the asymptotic approximation with a frequency of $O(h^{-1})$; therefore, a mesh interval of $O(h)$ is chosen to resolve this structure uniformly. The iteration method described in Appendix II is employed to obtain the solution of the finite difference equations.

The calculations were carried out with a uniform pressure load, i.e., $g \equiv 1$, for the α values 0.50, 0.35, 0.25 and thicknesses h chosen to satisfy

$$\frac{1}{h_n} K(\alpha) = (n + \tfrac{1}{4})\pi$$

for $n = 1, \ldots, 6$. The index n will be referred to as the branch number.

The approximations in the case of $\alpha = 0.50$ appear in Figures (3.1–3.4) as solid curves. The dashed lines represent the membrane solution. Figure (3.3) illustrates the convergence of the radial stress v to the membrane solution v_0. That u' is *not* asymptotic to u_0' is clearly seen from Figure (3.2). Also observe in Figures (3.1) and (3.2) the peaks at or near the center of the plate of order $O(h^{-\frac{1}{2}})$ and $O(h^{-\frac{3}{2}})$, respectively.

We estimate the order to which the asymptotic approximation satisfies the plate equations by inserting the calculated values into the finite difference approximation of the first-order system (3.27) derived in Appendix II. In Figure (3.5), we present a log-log plot of the maximum norm of the residual versus the thickness. Lines are drawn between points corresponding to the same membrane solution and same parity of the branch number n. The slopes

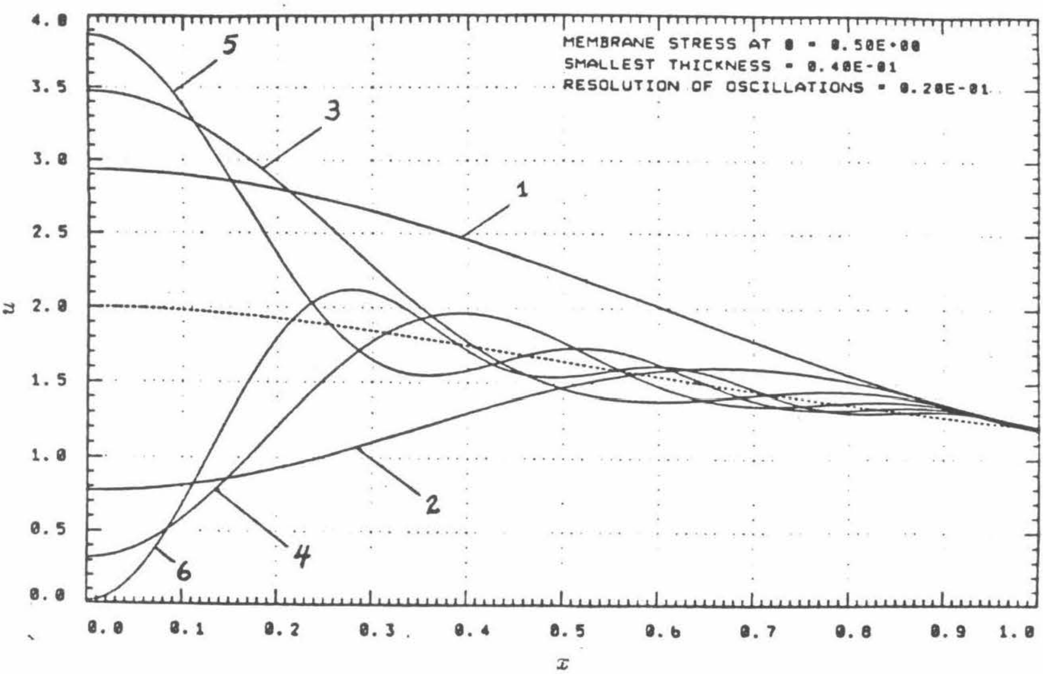

FIGURE 3.1. Asymptotic approximation of $u = z_1$ with $\alpha = 0.50$
The solid lines represent the uniform asymptotic approximation for the plate solution based on the membrane solution with $v_0(0) = \alpha = 0.50$; in this figure we plot $u(x)$. The thickness h is chosen such that $h_n^{-1}K(0.50) = (n + \frac{1}{4})\pi$. The curves are labeled by the index n with $1 \leq n \leq 6$. The dashed line represents the membrane solution $u_0(x)$ from which the asymptotic expansion was constructed.

of these lines provide estimates of the order. The slopes in Figure (3.5) are at least 1.5, supporting the conjecture that the residual is $O(h^{\frac{3}{2}})$.

The order of the error in taking the uniform asymptotic expansions (3.34, 3.41) as an approximation to a solution of the plate equations is estimated similarly. For each choice of $v_0(0) = \alpha$ and thickness h we must obtain a nearby plate solution. This is done by taking the asymptotic approximation as an initial guess and then applying an iterative method of constrained Newton type to the discretized plate equations as described in Appendix II. There is no guarantee that this method will converge for all values of α and h, but convergence is obtained most of the time. Divergence is observed only near

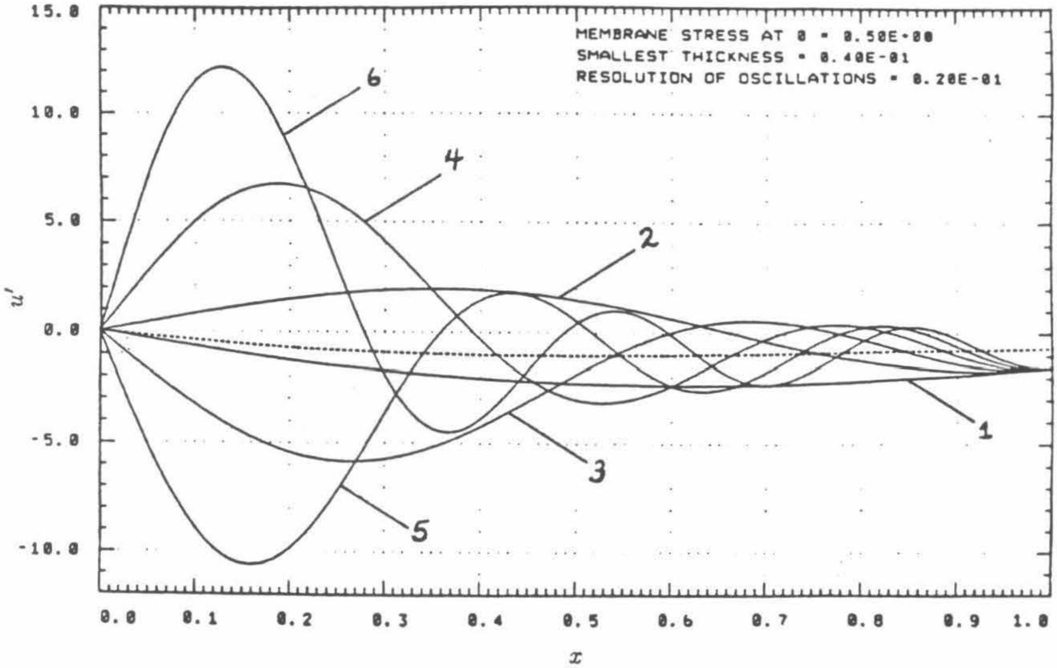

FIGURE 3.2. Asymptotic approximation of $u' = h^{-1}z_2$ with $\alpha = 0.50$
Similar to Figure (3.1) except that we plot $u'(x)$ with solid lines and $u_0'(x)$ with the dashed line.

the points where the uniform asymptotic approximation breaks down. The results are presented in Figure (3.6). The conjecture of an $O(h)$ remainder in the asymptotic approximation is borne out by these calculations.

Breakdown of the Asymptotics. It has been observed that

$$K = \int_0^1 v_0^{\frac{1}{2}}(s)\ ds \tag{3.56}$$

is a most critical quantity in determining the nature of plate solutions that are asymptotic to the membrane solution v_0. It is thus worthwhile to study how this quantity varies with the solution considered. Recall from the discussion of the compressive membrane solution in Chapter 2 that specification of the radial stress at the center of the membrane $v(0) = \alpha \geq 0$ uniquely determines

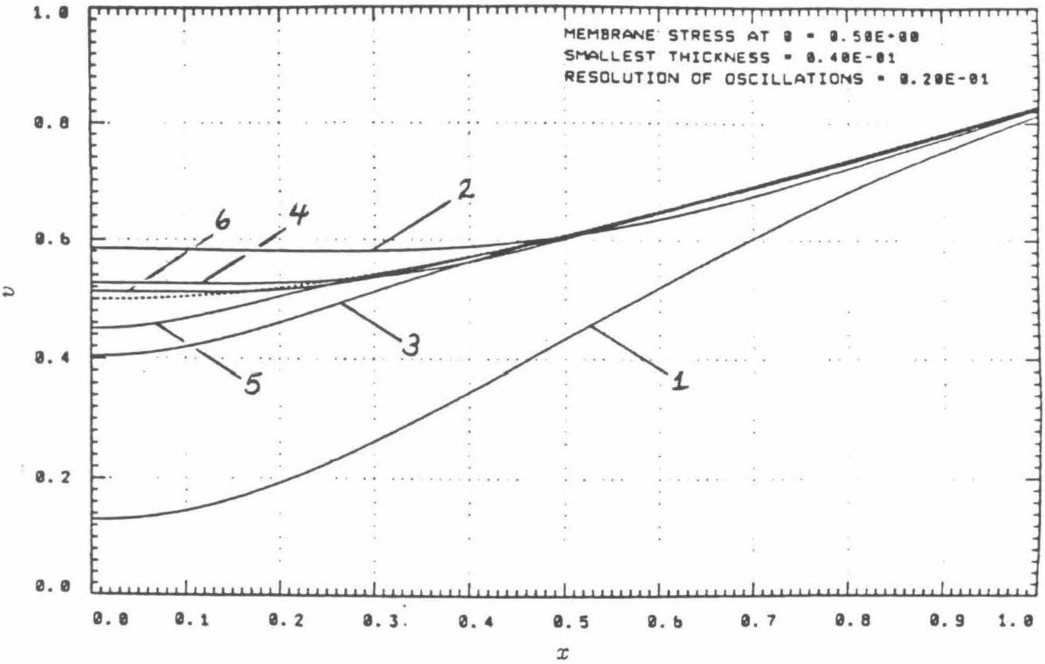

FIGURE 3.3. Asymptotic approximation of $v = z_3$ with $\alpha = 0.50$
Similar to Figure (3.1) except that we plot $v(x)$ with solid lines and $v_0(x)$ with the dashed line.

the membrane solution. Hence, if we let $v_0(x; \alpha)$ be the membrane solution with $v_0(0; \alpha) = \alpha \geq 0$, then

$$K(\alpha) \equiv \int_0^1 v_0^{\frac{1}{2}}(s; \alpha)\, ds \tag{3.57}$$

is well-defined.

Numerical estimates of $K(\alpha)$ are obtained by calculation of the membrane solution on a nonuniform grid as described in Appendix II and integration of the resulting discrete solution by the trapezoidal rule. Plots of α versus $K(\alpha)/\pi$ appear in Figure (3.7). A variety of loads were used in the calculations. It appears from these plots that K is a single-valued function of $\alpha \geq 0$. We take this as sufficient evidence that this property holds regardless of the load.

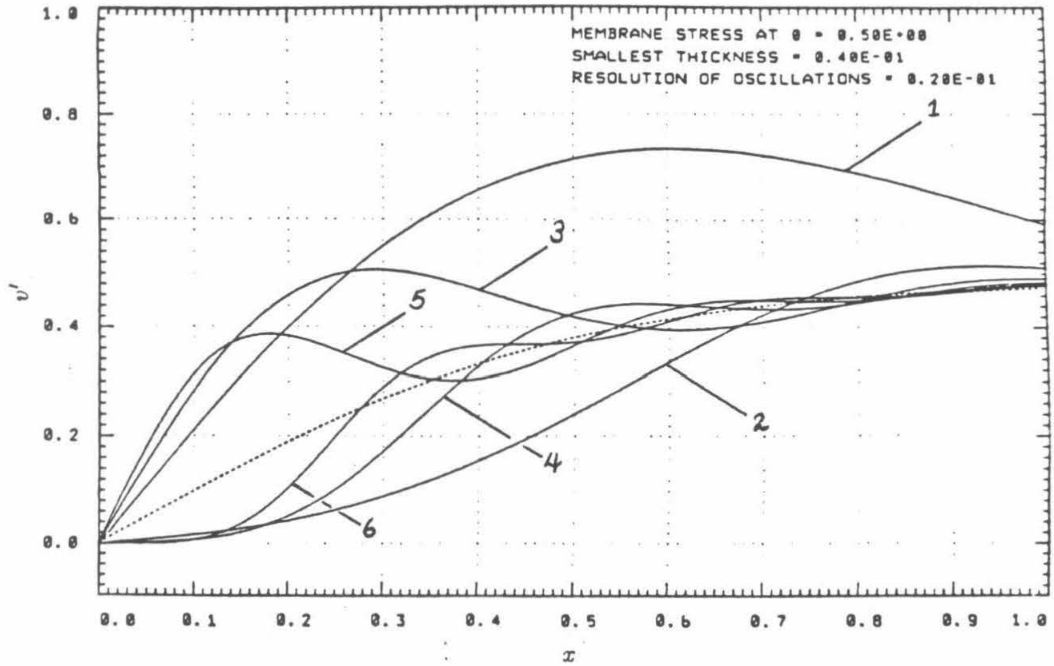

FIGURE 3.4. Asymptotic approximation of $v' = z_4$ with $\alpha = 0.50$
Similar to Figure (3.1) except that we plot $v'(x)$ with solid lines and $v_0'(x)$ with a dashed line.

Recall from (3.37) that the values of α and h at which the uniform asymptotic analysis breaks down are given by

$$\frac{1}{h} K(\alpha) = \left(n + \tfrac{3}{4}\right) \pi. \tag{3.58}$$

For fixed h, unique values α_n can be found that satisfy (3.58) provided

$$n \geq \frac{1}{h\pi} K(0) - \tfrac{3}{4}.$$

The uniqueness of these values is a consequence of the monotonicity of K. On the other hand, if α is fixed, then unique values h_n can be found that satisfy (3.58) for $n \geq 0$. These are given by

$$h_n = \frac{K(\alpha)}{\left(n + \frac{3}{4}\right) \pi}. \tag{3.59}$$

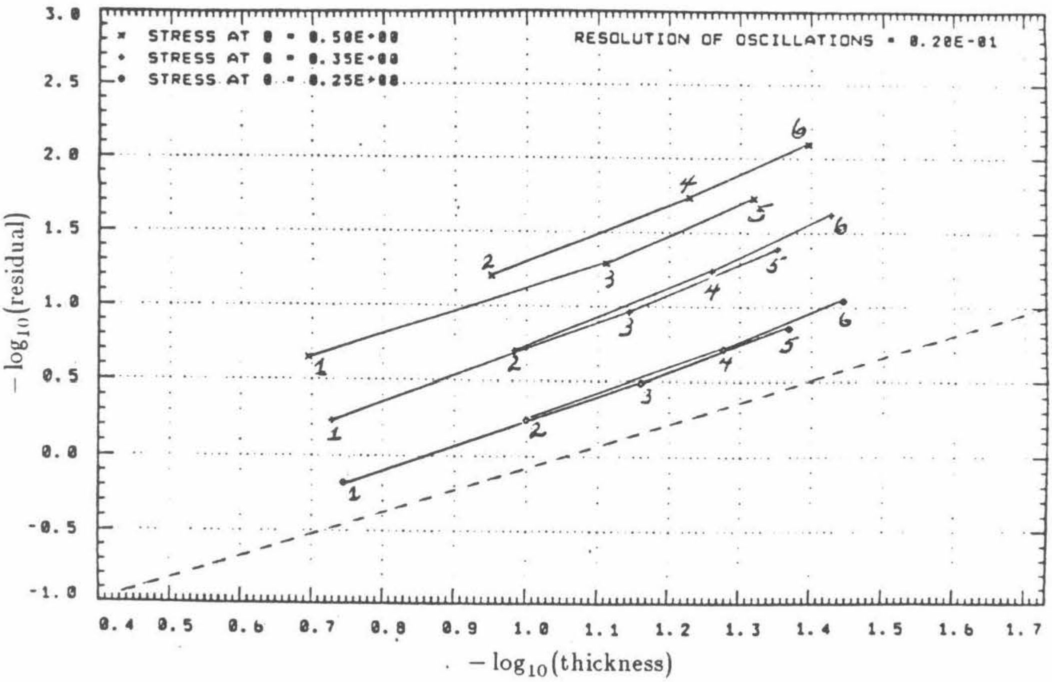

FIGURE 3.5. Estimation of the order of the residual

The marks represent the points $(-\log_{10} h,\ -\log_{10} R)$, where R is the maximum norm of the residual obtained by substituting the uniform asymptotic approximation into the discretized plate problem. Different symbols are used depending on the value of $\alpha = v_0(0)$ of the membrane solution from which the approximation is constructed. Each point is labelled according to the index n, where $h_n^{-1} K(\alpha) = (n + \frac{1}{4})\pi$. The slope m of the lines connecting these points provides an estimate of the order of the residual; $R = O(h^m)$. We estimate $R = O(h^{1.5})$; a dashed line of slope $m = 1.5$ is given for comparison.

Clearly, h_n tends to zero as n tends to ∞. Thus, for a particular membrane solution, plate solutions may be found that asymptotically approach this membrane solution as $h \to 0$ while excluding a countably infinite set of values h_n with $h_n \to 0$ as $n \to +\infty$.

The significance of the breakdown of the approximation is that it indicates a change in the dominant balance. In the discussion below, it is observed that a boundary layer develops near $x = 0$, while the compressive membrane solution with a correction of $O(h)$ is a valid approximation of the radial

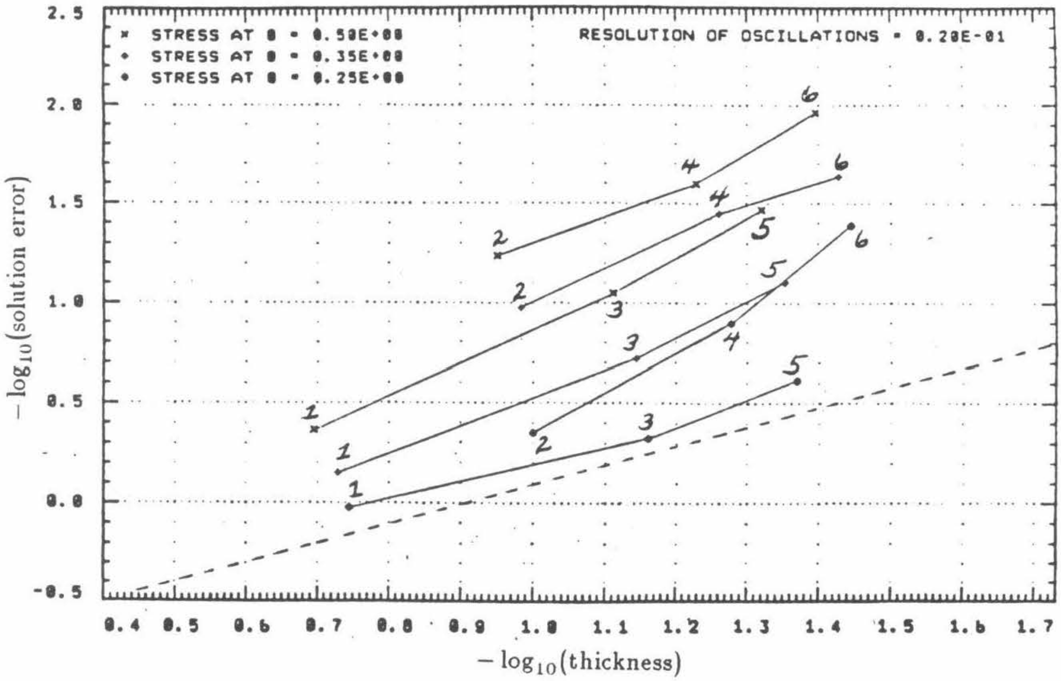

FIGURE 3.6. Estimation of the order of the remainder
Similar to the last figure except that the points $(-\log_{10} h, -\log_{10} \|\Delta\mathbf{Z}\|)$ are plotted, where $\Delta\mathbf{Z}$ is the difference between the uniform asymptotic approximation and a related plate solution calculated numerically. The maximum norm is used. We estimate $\|\Delta\mathbf{Z}\| = O(h)$; a dashed line of slope $m = 1$ is given for comparison.

stress v away from $x = 0$.

3.2 Solutions with a Boundary Layer in the Stress

With some modifications, the preceding analysis can be extended to the case where the oscillatory contribution to u is of $O(h^{\frac{1}{2}})$ for $x \gg h$ and the radial stress v has the form

$$v(x;h) \sim v_0(x) + hv_1(x) + O(h^2) \qquad \text{for } x \gg h,$$

where v_0 is a positive membrane solution that satisfies

$$\frac{1}{h}\int_0^1 v_0^{\frac{1}{2}}(s)\,ds = (n + \tfrac{3}{4})\,\pi. \tag{3.60}$$

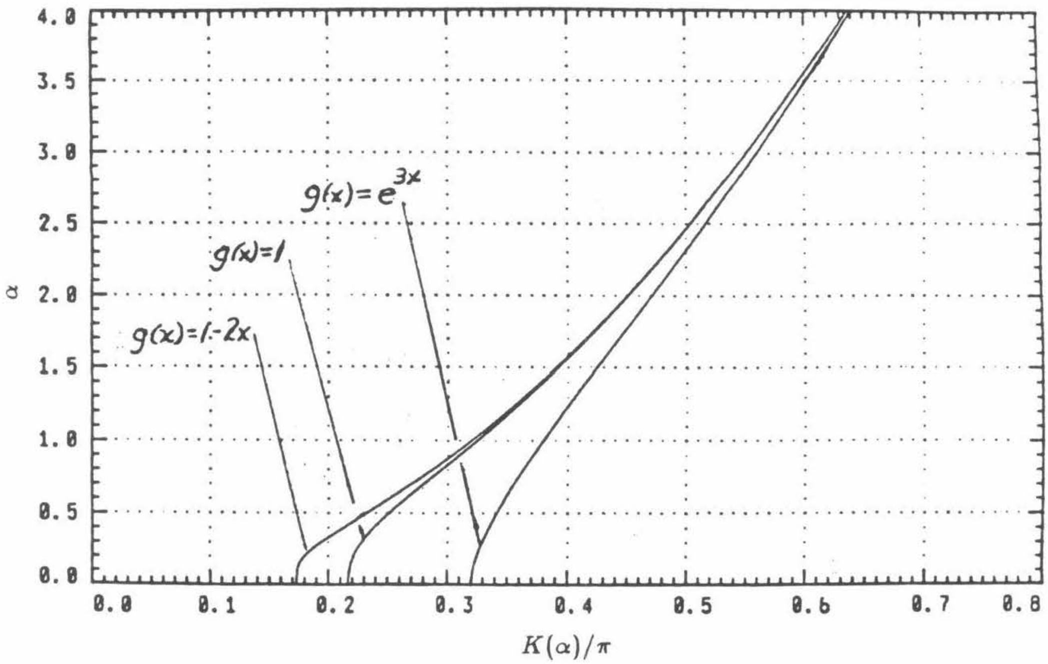

FIGURE 3.7. Study of $K(\alpha)$

Curves of α(ordinate) and $K(\alpha)/\pi$(abscissa) are labelled according to the function g used in the membrane equation.

Denote by λ_0 the value $v_0(0)$. Recalling the definition (3.57) of K, we see that (3.60) implies

$$\frac{1}{h}K(\lambda_0) = \left(n + \tfrac{3}{4}\right)\pi.$$

This is the case for which the asymptotics (3.34, 3.41) do not apply.

The Outer Solution. WKB analysis applied to the equilibrium equation (3.3a) gives

$$u(x) \sim u_0(x) - h\frac{g(x)}{v_0{}^2(x)}v_1(x) + h^{\frac{1}{2}}\frac{\kappa\lambda_0{}^{\frac{1}{2}}}{x^{\frac{3}{2}}v_0{}^{\frac{1}{4}}(x)} \cdot \cos(\tilde{x} + \phi) + O(h^{\frac{3}{2}}) \qquad (3.61)$$

as $h \to 0$, where the scale on which the oscillations occur is

$$\tilde{x} = \frac{1}{h}\int_0^x v_0{}^{\frac{1}{2}}(s)\,ds + \int_{h\lambda_0{}^{-\frac{1}{2}}}^{x} \frac{v_1(s)}{2v_0{}^{\frac{1}{2}}(s)}\,ds. \qquad (3.62)$$

The integrands in the definition (3.62) of $\tilde{x}$ consist of the first two terms of the expansion

$$\begin{aligned} h^{-1}v^{\frac{1}{2}}(x) &= h^{-1}(v_0(x) + hv_1(x) + O(h^2))^{\frac{1}{2}} \\ &= h^{-1}v_0{}^{\frac{1}{2}}(x) + \frac{v_1(x)}{2v_0{}^{\frac{1}{2}}(x)} + O(h). \end{aligned}$$

The second integral ranges over the interval $(h\lambda_0{}^{-\frac{1}{2}}, x)$, rather than $(0, x)$, because it turns out that v_1 has a singularity at the origin. The parameters ϕ and κ are as yet undetermined constants.

Substitution of the asymptotics (3.61) for u into the compatibility equation (3.3*b*) yields the outer equation

$$\begin{aligned} \left(v_0{}'' + \frac{3}{x}v_0{}'\right) + h\left(\cdot v_1'' + \frac{3}{x}v_1'\right) \sim \frac{g^2(x)}{v_0{}^2} &+ \\ + h\left(-2\frac{g^2(x)}{v_0{}^3}v_1 + \frac{\kappa^2\lambda_0}{2v_0{}^{\frac{1}{2}}x^3}\right)&. \quad (3.63) \end{aligned}$$

The neglected portion of this equation contains either smooth terms of $O(h^2)$ or oscillatory terms of $O(h^{\frac{1}{2}})$. Multiscale analysis can be used to justify ignoring the $O(h^{\frac{1}{2}})$ oscillatory terms even though they appear in the equation (3.63) to be asymptotically greater than some terms that are retained. For if we have the linear equation

$$y'' + \frac{3}{x}y' + \frac{2g^2(x)}{v_0{}^3(x)}y = f\cos(h^{-1}\theta(x)),$$

then let the solution y be of the form

$$y = y_0(\tilde{x}, x) + hy_1(\tilde{x}, x) + \ldots$$

where

$$\tilde{x} = h^{-1}\theta(x).$$

We find that y_0 and y_1 are functions of x only and

$$\frac{\partial^2}{\partial x^2}y_0 + \frac{3}{x}\frac{\partial}{\partial x}y_0 + \frac{2g^2(x)}{v_0{}^3(x)}y_0 = 0,$$
$$\frac{\partial^2}{\partial x^2}y_1 + \frac{3}{x}\frac{\partial}{\partial x}y_1 + \frac{2g^2(x)}{v_0{}^3(x)}y_1 = 0,$$
$$\theta'^2\frac{\partial^2}{\partial \tilde{x}^2}y_2 - f\cos\tilde{x} = 0.$$

The solutions y_0 and y_1 could be taken to be arbitrary solutions of the homogeneous equation; however, that contribution can be absorbed into v_0 and v_1. Thus, we take $y_0 = y_1 = 0$. The leading contribution is from y_2 and is $O(f \cdot h^2)$. Thus, the oscillatory terms in the outer equation (3.63) contribute to v at $O(h^{\frac{5}{2}})$ and are neglected for this approximation.

Equating terms of $O(h)$ in the outer equation (3.63), we obtain

$$v_1'' + \frac{3}{x}v_1' + 2\frac{g^2(x)}{v_0{}^3}v_1 = \frac{\kappa^2\lambda_0}{2v_0{}^{\frac{1}{2}}x^3}. \tag{3.64}$$

The homogeneous equation

$$v_1'' + \frac{3}{x}v_1' + 2\frac{g^2(x)}{v_0{}^3}v_1 = 0$$

has two linearly independent solutions, one of which is bounded at the origin. The multiple of this solution with value 1 at $x = 0$ is denoted by y_1. Recalling from the preceding section $v_0(0;\alpha) = \alpha$, we see that

$$\frac{d}{d\alpha}v_0(x;\alpha) = y_1(x). \tag{3.65}$$

The other solution of the homogeneous equation has a singularity at the origin of the form x^{-2} and thus will have no contribution at this order. There is a particular solution of the equation (3.64) that has the form

$$v_{1p} = -\frac{\kappa^2\lambda_0{}^{\frac{1}{2}}}{2x} + \kappa^2\Phi(x)$$

where $\Phi(0) = 0$. Letting

$$b(x) = -\frac{\lambda_0^{\frac{1}{2}}}{2x} + \Phi(x),$$

then $v_{1p}(x) = \kappa^2 b(x)$ and hence, v_1 may be expressed as

$$v_1(x) = \gamma y_1 + \kappa^2 b(x).$$

The constant γ is determined so that the boundary condition (3.2) is satisfied to $O(h)$. We must have $\tilde{x} + \phi = n\pi$ when $x = 1$. Thus, the condition for γ in terms of ϕ and κ is

$$\frac{1}{h}K(\lambda_0) + \gamma K'(\lambda_0) + \kappa^2 B + \phi = n\pi \tag{3.66}$$

where the constant B is given by

$$B = \int_{h\lambda_0^{-\frac{1}{2}}}^{x} \frac{b(s)}{2v_0^{\frac{1}{2}}(s)}\, ds.$$

We have used the relation

$$K'(\alpha) = \int_0^1 \frac{y_1(s)}{2v_0^{\frac{1}{2}}(s;\alpha)}\, ds,$$

which follows from the definition (3.57) of K and the formula (3.65) for the derivative of $v_0(x;\alpha)$ with respect to α.

The asymptotics of the outer solution for $x \to 0$ are

$$\begin{aligned} v(x) &\sim \lambda_0 + h\gamma - h\frac{\kappa^2 \lambda_0^{\frac{1}{2}}}{2x}, \\ u(x) &\sim h^{\frac{1}{2}} \frac{\kappa \lambda_0^{\frac{1}{4}}}{x^{\frac{3}{2}}} \cos\left(\left(\frac{\lambda_0^{\frac{1}{2}}}{h} + \frac{\gamma}{2\lambda_0^{\frac{1}{2}}} \right) x - \frac{\kappa^2}{4} \log \frac{\lambda_0^{\frac{1}{2}}}{h} x + \phi \right). \end{aligned} \tag{3.67}$$

The parameters κ and ϕ will be determined by asymptotic matching with a boundary layer solution about $x = 0$.

The Boundary Layer. The asymptotics (3.67) for the outer solution become invalid when $x = O(h)$. In this region, the approximation for v is still $O(1)$, but the approximation for u is $O(h^{-1})$. This suggests the following scaling; let

$$\begin{gathered} \hat{x} = \frac{x}{h}, \\ \hat{u}(\hat{x}) = hu(x) + O(h), \qquad \hat{v}(\hat{x}) = v(x) + O(h). \end{gathered} \tag{3.68}$$

Then the leading order boundary layer equations are

$$\begin{aligned} \hat{u}'' + \frac{3}{\hat{x}}\hat{u}' + \hat{v}\hat{u} &= 0, \\ \hat{v}'' + \frac{3}{\hat{x}}\hat{v}' &= \hat{u}^2. \end{aligned} \tag{3.69}$$

Note that these equations are equivalent to the plate equations in the case of no normal pressure.

The solutions of these equations that are bounded at the origin are described by a 2-parameter family. A solution is characterized uniquely by specifying

$$\hat{v}(0) = \alpha, \qquad \hat{u}(0) = \beta.$$

Observe that the transformations

$$\hat{u} \to -\hat{u}$$

and

$$\begin{gathered} \hat{x} \to \frac{\hat{x}}{c}, \\ \hat{v} \to c^2\hat{v}, \qquad \hat{u} \to c^2\hat{u} \end{gathered}$$

take one solution into another. Thus, from the 1-parameter family of solutions $\hat{v}^*$, $\hat{u}^*$, defined by specifying

$$\hat{v}^*(0; r) = r, \qquad \hat{u}^*(0; r) = 1,$$

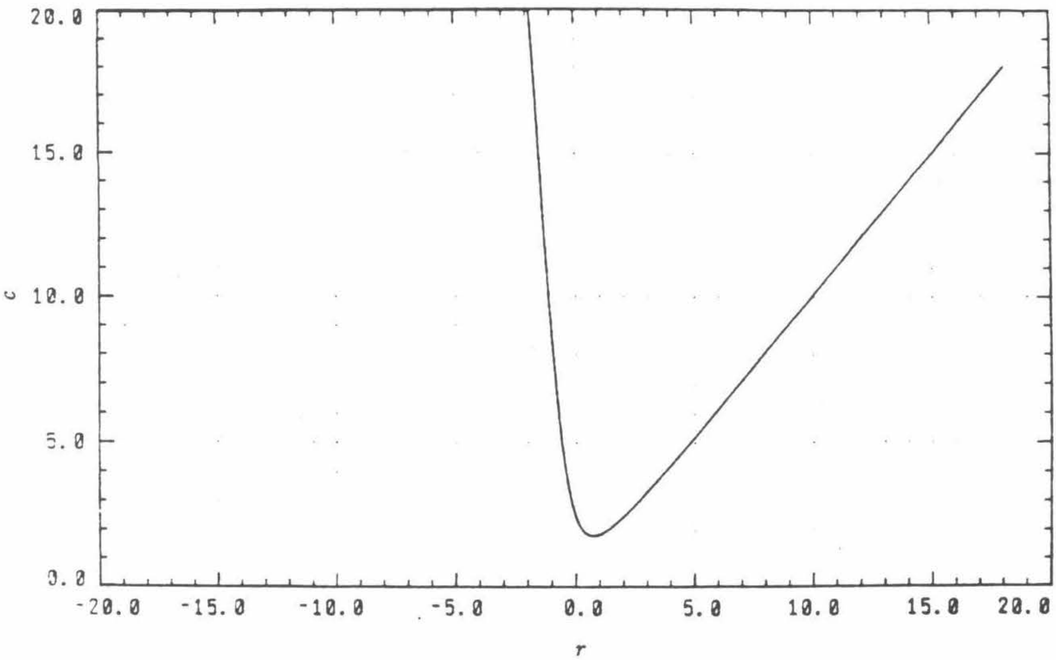

FIGURE 3.8. The limit of $\hat{v}'$ as $\hat{x} \to +\infty$
The function $c(r) = (\lim_{x \to \infty} \hat{v}'(x; r))^{\frac{1}{2}}$ is plotted.

we may obtain all the solutions—except the trivial solutions $\hat{v} \equiv r$, $\hat{u} \equiv 0$—by an appropriate scaling of independent and dependent variables.

The asymptotic behavior for large $\hat{x}$ is that $\hat{v}'$ tends to a constant value and $\hat{u}'$ vanishes as $\hat{x} \to +\infty$. More precisely,

$$\hat{v}'(\hat{x}; r) \sim c^2(r) - \frac{\hat{\kappa}^2(r)c(r)}{2\hat{x}},$$
$$\hat{u}'(\hat{x}; r) \sim \frac{c^{\frac{1}{2}}(r)\hat{\kappa}(r)}{\hat{x}^{\frac{3}{2}}} \cos\left(c(r)\hat{x} - \frac{\hat{\kappa}^2(r)}{4} \log c(r)\hat{x} + \hat{\phi}(r)\right)$$

where for specificity we take $\hat{\kappa} \geq 0$.

The constant $c(r)$ is defined by

$$c(r) = \sqrt{\lim_{x \to \infty} \hat{v}'(x; r)}.$$

The numerical calculations to obtain the values of $c(r)$ as well as $\hat{\phi}(r)$ and

$\hat{\kappa}(r)$ are described below. In Figure (3.8), we have plotted $c(r)$ versus r. For $\hat{\lambda}_0 > 0$, let

$$d = \frac{\hat{\lambda}_0^{\frac{1}{2}}}{c(r)},$$

$$\alpha(r, \hat{\lambda}_0) = rd^2, \qquad \beta(r, \hat{\lambda}_0) = d^2.$$

Then the boundary layer solutions $\hat{u}(\hat{x}; r, \hat{\lambda}_0)$, $\hat{v}(\hat{x}; r, \hat{\lambda}_0)$, obtained by specifying

$$\hat{v}(0; r, \hat{\lambda}_0) = \alpha(r, \hat{\lambda}_0), \qquad \hat{u}(0; r, \hat{\lambda}_0) = \pm\beta(r, \hat{\lambda}_0),$$

satisfy

$$\lim_{x\to\infty} \hat{v}(x; r) = \hat{\lambda}_0.$$

Note that

$$\hat{v}(\hat{x}; r, \hat{\lambda}_0) = d^2 \hat{v}^{\cdot} (\hat{x}d; r), \qquad \hat{u}(\hat{x}; r, \hat{\lambda}_0) = \pm d^2 \hat{u}^{\cdot} (\hat{x}d; r).$$

The explicit dependence on r and $\hat{\lambda}_0$ will hereafter be suppressed when the notation is unambiguous. The large $\hat{x}$ asymptotics of these solutions are

$$\begin{aligned} \hat{v}(\hat{x}) &\sim \hat{\lambda}_0 - \frac{\hat{\lambda}_0^{\frac{1}{2}} \hat{\kappa}^2}{2\hat{x}}, \\ \hat{u}(\hat{x}) &\sim \pm \frac{\hat{\lambda}_0^{\frac{1}{4}} \hat{\kappa}}{\hat{x}^{\frac{3}{2}}} \cos\left(\hat{\lambda}_0^{\frac{1}{2}} \hat{x} - \frac{\hat{\kappa}^2}{4} \log \hat{\lambda}_0^{\frac{1}{2}} \hat{x} + \hat{\phi} \right). \end{aligned} \tag{3.70}$$

Asymptotic Matching. Comparing (3.70) with (3.67) and recalling the definitions (3.68) of the boundary layer variables, then to match with the outer solution in the overlap region, $h \ll x \ll 1$, we must have

$$\hat{\lambda}_0 = \lambda_0 + h\gamma,$$

$$\hat{\kappa} = |\kappa|, \qquad \hat{\phi} = \phi.$$

Recalling the condition (3.66) for γ, we see that

$$\gamma = \frac{\frac{3}{4}\pi - \hat{\phi} - B\hat{\kappa}^2}{K'(\lambda_0)}. \tag{3.71}$$

The uniform asymptotic approximation for the plate solution is obtained in the usual way by adding the outer and inner expansions and subtracting the matching terms. Thus, as $h \to 0$,

$$\begin{aligned}
v(x) \sim & v_0(x) + h(\gamma y_1(x) + \kappa^2 b(x)) + \hat{v}\left(\frac{x}{h}; r, \lambda_0 + h\gamma\right) - \\
& - \left(\lambda_0 + h\gamma - h\frac{\lambda_0^{\frac{1}{2}}\kappa^2}{2x}\right), \\
u(x) \sim & u_0(x) - h\frac{g}{v_0^2}v_1 + h^{\frac{1}{2}}\frac{\kappa\lambda_0^{\frac{1}{2}}}{x^{\frac{3}{2}}v_0^{\frac{1}{4}}(x)} \cdot \cos(\tilde{x} + \phi) + \\
& + h^{-1}\hat{u}\left(\frac{x}{h}; r, \lambda_0 + h\gamma\right) - \\
& - h^{\frac{1}{2}}\frac{\kappa\lambda_0^{\frac{1}{4}}}{x^{\frac{3}{2}}}\cos\left(\left(\frac{\lambda_0^{\frac{1}{2}}}{h} + \frac{\gamma}{2\lambda_0^{\frac{1}{2}}}\right)x - \frac{\kappa^2}{4}\log\lambda_0^{\frac{1}{2}}\frac{x}{h} + \phi\right),
\end{aligned} \tag{3.72}$$

where

$$\tilde{x} = \frac{1}{h}\int_0^x v_0^{\frac{1}{2}}(s)\,ds + \int_{h\lambda_0^{-\frac{1}{2}}}^x \frac{\gamma y_1(s) + \kappa^2 b(s)}{2v_0^{\frac{1}{2}}(s)}\,ds. \tag{3.73}$$

The constants satisfy $\lambda_0 = v_0(0)$ with $h^{-1}K(\lambda_0) = (n + \frac{3}{4})\pi$ and

$$\kappa = \pm\hat{\kappa}(r), \qquad \phi = \hat{\phi}(r),$$

with γ defined as in (3.71).

Numerics of Boundary Layer Solutions. Numerical calculations of the boundary layer solutions are performed using the *SANDIA-ODE* software package. This canned routine uses a predictor-corrector method with automatic step control for solving initial-value problems for first-order systems of ordinary differential equations. Given initial values $\hat{v}(0) = \nu$, $\hat{u}(0) = \eta > 0$, the solution is estimated at a small value of $\hat{x}$ using the series expansion about the singular point $x = 0$. The initial-value problem is then solved using the packaged routine up to a value of $\hat{x}$ where the quantity $\hat{v}'$ is found to be sufficiently small. The estimates of the constants $\alpha(r,s)$, $\beta(r,s) > 0$, $\hat{\kappa}(r)$ and $\hat{\phi}(r)$ are obtained from the formulas

$$r = \frac{\nu}{\eta},$$

$$w = \hat{x}^{\frac{3}{2}}\hat{u}, \qquad w' = \hat{x}^{\frac{3}{2}}\hat{u}' + \frac{3}{2\hat{x}}w,$$

$$S \approx \sqrt{\hat{v} + \frac{\hat{v}w^2 + w'^2}{2\hat{x}\hat{v}}},$$

$$\alpha(r,S) = \nu, \qquad \alpha(r,s) = \frac{|s|}{S}\alpha(r,S),$$

$$\beta(r,S) = \eta, \qquad \beta(r,s) = \frac{s}{S}\beta(r,S),$$

$$\hat{\kappa}(r) \approx \sqrt{\frac{\hat{v}w^2 + w'^2}{S\hat{v}}},$$

$$\hat{\phi}(r) \approx \tan^{-1}\frac{-w'}{\sqrt{\hat{v}}w} - S\hat{x} + \frac{\hat{\kappa}^2(r)}{4}\log S\hat{x} + n\pi.$$

The integer n is chosen such that $\hat{\phi}(r) \to \frac{3}{4}\pi$ as $r \to +\infty$ and $\hat{\phi}$ is a continuous function of r.

In Figure (3.9), $\beta(r,s)$ is plotted versus $\alpha(r,s)$ for $s = \pm 0.5$, ± 1 and ± 2. Recall that α gives the value of the radial stress at the center of the plate, $v(0) \sim \alpha(r, \lambda_0 + h\gamma)$, and β is related to the value of the displacement variable at the center of the plate, $u(0) \sim h^{-1}\beta(r, \lambda_0 + h\gamma)$. The points $(s,0)$ and $(0,0)$ in the plane (α,β) correspond to $r = +\infty$ and $r = -\infty$, respectively. Figure (3.10) is the plot of $\hat{\kappa}$ versus α and Figure (3.11) is the plot of $\hat{\phi}$ versus α.

The Limiting Case $r \to -\infty$. The numerical calculations described above

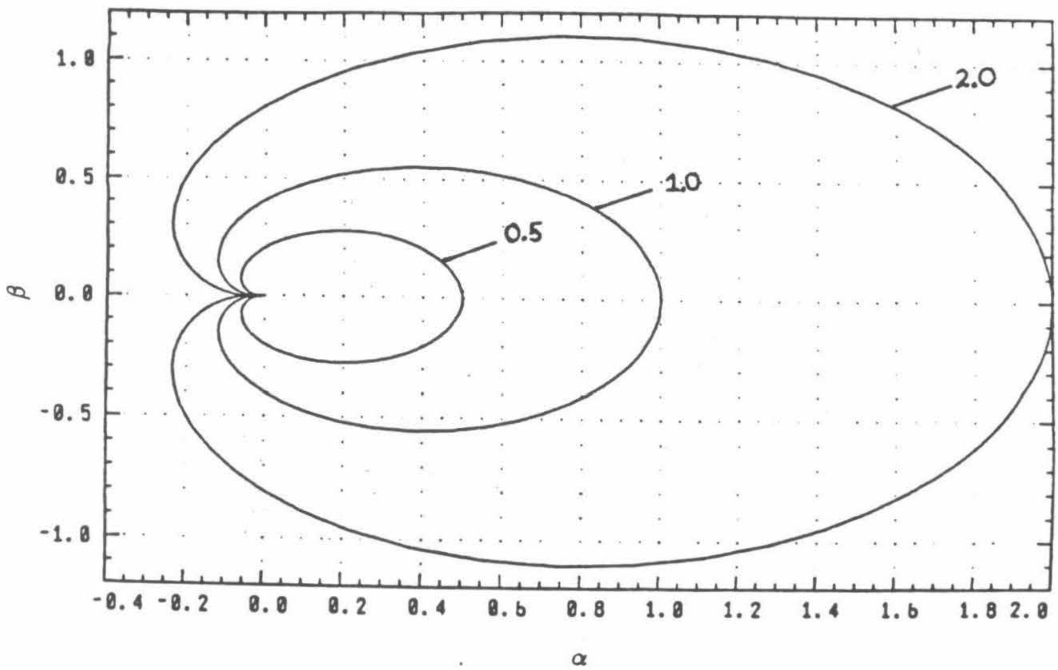

FIGURE 3.9. Boundary layer solutions—values at $x = 0$

The curve of points $(\alpha(r,s), \beta(r,s))$ parameterized by r is plotted for s values of 0.5, 1.0, and 2.0.

reveal as $r \to -\infty$, the constants α and β vanish, while the constants $\hat{\phi}$ and $\hat{\kappa}$ become unbounded.

α	$\log\hat{\phi}/\log\|\alpha\|$	$\log\hat{\kappa}/\log\|\alpha\|$	$\log\beta/\log\|\alpha\|$
-0.097	-2.113	-0.632	1.200
-0.050	-2.014	-0.636	1.526
-0.036	-1.576	-0.629	1.750
-0.020	-1.355	-0.620	2.117
-0.015	-1.292	-0.617	2.322
-0.000	-1.103	-0.608	

TABLE 3.1. Estimates of Exponents

The first 5 lines were obtained from numerical calculations; the last line is the extrapolation to the singular case $\alpha = 0$.

In Table (3.1) estimates are presented of the exponents of $\hat{\phi}$, $\hat{\kappa}$ and β with

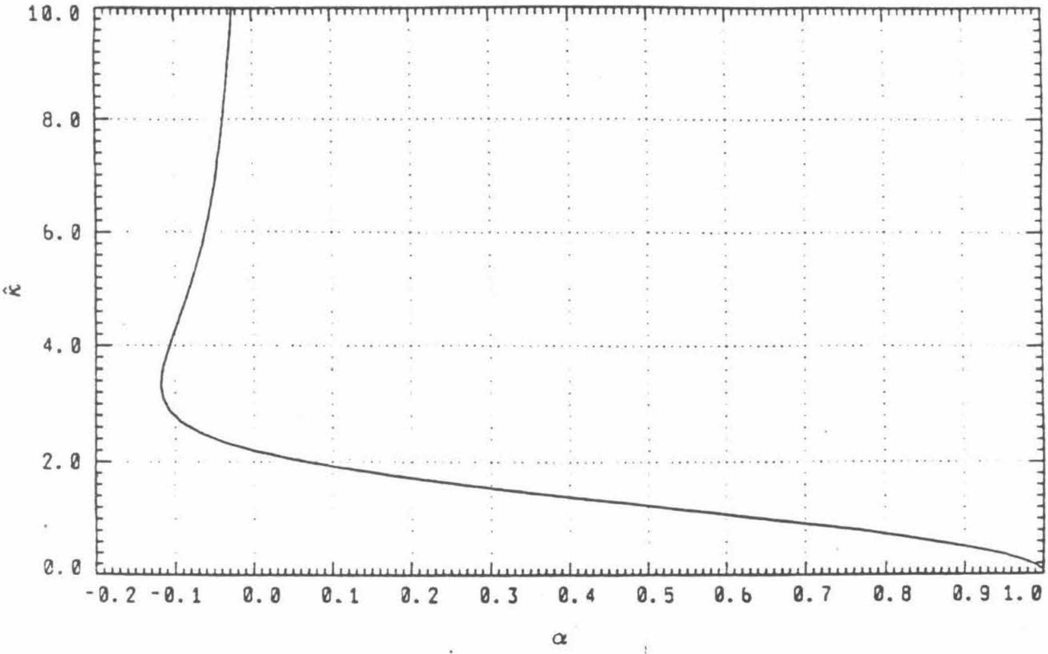

FIGURE 3.10. Boundary layer solutions—the parameter $\hat{\kappa}$
The curve of points $(\alpha(r, S), \hat{\kappa}(r))$ parameterized by r is plotted.

respect to α. In the last line are the linear extrapolations to $\alpha = 0$ for the exponents of $\hat{\phi}$ and $\hat{\kappa}$—the exponent of β does not appear to converge. These calculations indicate

$$\hat{\phi}(r) = O\left(|\alpha(r)|^{-1.1}\right)$$

and

$$\hat{\kappa}(r) = O\left(|\alpha(r)|^{-0.6}\right)$$

as $r \to -\infty$. The accuracy of these estimates is not high, but there is sufficient evidence to claim $\hat{\phi} \ll \hat{\kappa}^2$ as $r \to -\infty$. Hence, the term in $\hat{\kappa}^2$ dominates in the formula (3.71) for γ. Furthermore, $B \to -\infty$ as $h \to 0$ and thus $\gamma \to +\infty$ as $r \to -\infty$ for sufficiently small h. Clearly, the tendency is for $\hat{\lambda}_0 = \lambda_0 + h\gamma$ to increase in the limit $r \to -\infty$ and, in fact, the estimates

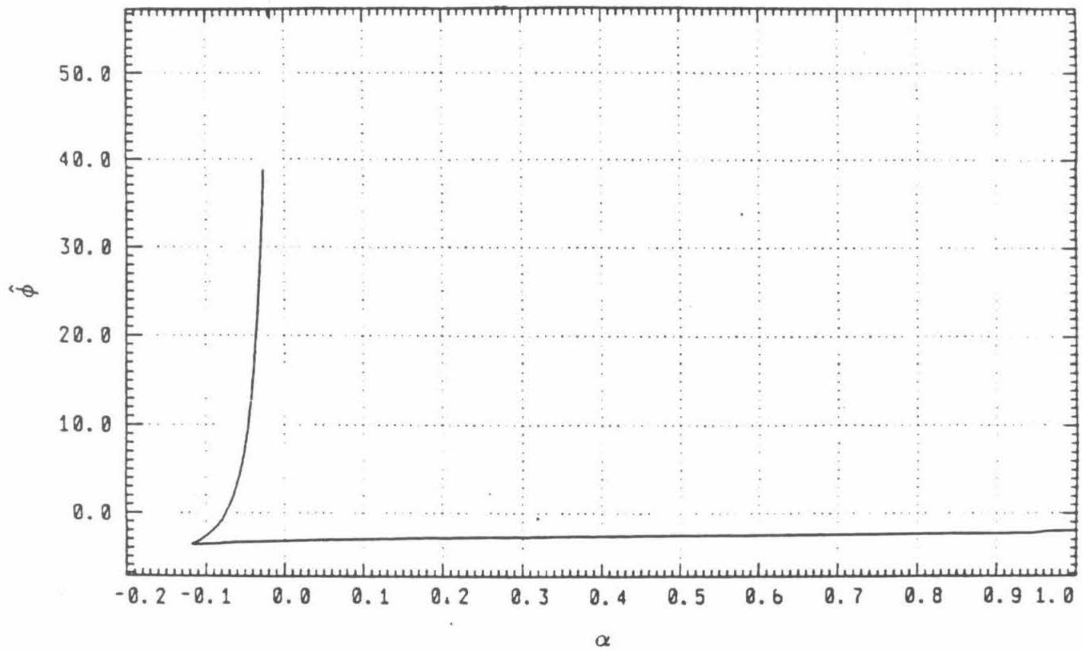

FIGURE 3.11. Boundary layer solutions—the parameter $\hat{\phi}$
The curve of points $(\alpha(r,S),\ \hat{\phi}(r))$ parameterized by r is plotted.

indicate $v(0) \sim \alpha(r,1)\hat{\lambda}_0 = O(|\alpha|^{-0.2})$. Furthermore, in the neighborhood of the point $\alpha = 0$, $\beta = 0$ the numerical estimates indicate that β becomes *transcendentally* small; that is, $\beta \ll \alpha^M$ as $r \to -\infty$ for any $M > 0$. Clearly, the assumptions that $v = O(1)$ and $u = O(h^{-1})$ near $x = 0$ break down in this limit. There may be yet another dominant balance in the equations. Nonetheless, we will limit our discussion of the plate solution asymptotics to those cases already introduced and leave any additional cases to future investigators.

CHAPTER 4

Nonexistence Result for the Clamped Circular Plate

In the previous chapter, we constructed asymptotic expansions of plate solutions based on compressive membrane solutions. There we saw that it was possible to satisfy the boundary condition for the plate whose edge is elastically supported against rotation; in the case of an annular plate, we could in some cases satisfy the clamped edge condition. For the circular plate however, the asymptotic expansion failed when the clamped edge condition was imposed. In this chapter, the cause of the failure of the expansion in the case of the clamped circular plate is investigated. We find that—taking a quite general interpretation of what is meant by asymptotic approach—it is not possible to find solutions of the circular clamped plate problem that asymptotically approach a given Föppl membrane solution as the thickness vanishes. The main result is stated and proved in Section 4; preliminary transformations and lemmas to be used in the proof of the main result appear in Sections 1–3. We now give an outline of the discussions contained in the following sections.

Outline. The chapter is divided into four sections. We give here a brief outline of the contents of each section.

Section 1. We make a set of transformations to convert the von Kármán plate equations (3.3) into a first-order system. First, we subtract out a positive solution v_0 of the Föppl membrane equation; solutions that are unbounded at the origin are allowed in addition to the bounded Föppl membrane solutions. The new dependent variables measure the deviation from the proposed "asymptotic limit" that is of interest—that is, v_0 and the corresponding function $u_0 = g/v_0$. Several changes of variable are performed to obtain a system that has the form

$$\begin{aligned} h\mathbf{z}_I' &= B\mathbf{z}_I + \dots, \\ \mathbf{z}_{II}' &= A(t;h)\mathbf{z}_{II} + \dots, \end{aligned} \tag{4.1}$$

where

$$B = \begin{pmatrix} 0 & 1 \\ -1 & 0 \end{pmatrix}$$

and $A(t;h)$ is bounded uniformly for h sufficiently small. The remaining terms are either $o(1)$ as $h \to 0$ or vanish quadratically as the dependent variables vanish. Thus, we have partitioned the variables into two sets according to their leading behavior in the linearized equations; the variables in $\mathbf{z}_I$ have simple oscillations of constant amplitude and frequency $O(h^{-1})$; the variables in $\mathbf{z}_{II}$ are smooth. The independent variable we choose is

$$t = \int_{x_0}^{x} v_0^{\frac{1}{2}}(\xi)\, d\xi,$$

where $0 < \tilde{x}_0 < x_0 < 1$ and $v_0(x) > 0$ for $x \in (\tilde{x}_0, 1]$. Note that the domain corresponding to $x \in (\tilde{x}_0, 1]$ is $t \in (T_0, T_1]$, where

$$T_0 = -\int_{\tilde{x}_0}^{x_0} v_0^{\frac{1}{2}}(s)\, ds \geq -\infty, \qquad T_1 = \int_{x_0}^{1} v_0^{\frac{1}{2}}(s)\, ds < +\infty.$$

Section 2. We next define a comparison function $\mathcal{A}$ for the solution $\mathbf{z}_I$, $\mathbf{z}_{II}$ by

$$\mathcal{A}(t) = \left(\|\mathbf{z}_I(t)\|^2 + \|X^{-1}(t;h)\mathbf{z}_{II}(t)\|^2\right)^{\frac{1}{2}},$$

where the norm is the Euclidean norm and the matrix X satisfies

$$X'(t;h) = A(t;h)X(t;h), \qquad X(T_1;h) = I.$$

The motivation for this definition is that a solution of the linearized equations gives a constant value of $\mathcal{A}$ to leading order. We can study the growth of the solution of the first-order system (4.1) through the behavior of this scalar comparison function. An integral inequality is then derived for $\mathcal{A}(t)$, valid for $t \in [\tau_0, T_1]$, where $\tau_0 > T_0$.

Section 3. We prove two lemmas for the growth of $\mathcal{A}$ based on the integral inequality obtained in the previous step. Basically, the result is that if $\mathcal{A}$ is small at some point, it will be small everywhere. The boundary conditions for the differential equation (4.1) gives us that

$$\mathcal{A}(T_1) \geq a_1 > 0.$$

Hence we conclude that $\mathcal{A}$ is bounded away from zero uniformly for $t \in [\tau_0, T_1]$ in the limit $h \to 0$.

Section 4. We show that assuming that the plate solution asymptotically approaches the membrane solution leads to a contradiction, for if we suppose that solutions u_n, v_n exist for corresponding values of the thickness h_n with $h_n \to 0$ as $n \to \infty$ such that $v_n(x_n)$, $v_n{}'(x_n)$ are $O(1)$ and $u_n(x_n)v_n(x_n) - g(x_n)$, $h_n u_n{}'(x_n)$, are $o(1)$ as $n \to \infty$ for $0 < x_0 \leq x_n \leq x_1$, then there is a subsequence for which the comparison function $\mathcal{A}_n$ is small at the corresponding points $t_n \in [0, T_1]$. It was shown in the previous step that $\mathcal{A}_n$ is bounded away from zero on the interval $[0, T_1]$, and hence we have arrived at a contradiction. Therefore, the plate solutions cannot asymptotically approach the membrane solutions.

4.1 Transformation to a First-Order System

Recall the von Kármán equations (3.3)

$$\begin{aligned} h^2\left(u'' + \frac{3}{x}u'\right) + uv &= g(x), \\ v'' + \frac{3}{x}v' &= u^2. \end{aligned} \tag{4.2}$$

The boundary conditions in the case of a clamped circular plate are

$$\begin{aligned} u'(0) &= 0, \qquad & u(1) &= 0, \\ v'(0) &= 0, \qquad & v(1) &= \lambda. \end{aligned} \tag{4.3}$$

We make a sequence of tranformations to put these equations into a form that is most useful for the theoretical study which follows.

Deviation from the Membrane Solution. We are interested in the deviation of the plate solutions from a given solution of the Föppl equation. Thus let $v_0(x)$ satisfy the Föppl membrane equation (2.1) on $(0,1]$ and be positive for $x \in (\tilde{x}_0, 1]$. It is possible for $v_0(\tilde{x}_0)$ to vanish for $\tilde{x}_0 > 0$ if $g(\tilde{x}_0) = 0$; the following analysis is valid only for $x > \tilde{x}_0$. It is not assumed that this solution is bounded at the origin. As before, let

$$u_0(x) = \frac{g(x)}{v_0(x)}.$$

We define

$$u_1 = u - u_0, \qquad v_1 = v - v_0.$$

Substitution into the plate equations (4.2) gives

$$\begin{aligned} h^2\left({u_1}'' + \frac{3}{x}{u_1}'\right) + u_1 v_0 + u_0 v_1 + u_1 v_1 &= -h^2\left({u_0}'' + \frac{3}{x}{u_0}'\right), \\ {v_1}'' + \frac{3}{x}{v_1}' &= 2u_1 u_0 + {u_1}^2. \end{aligned} \tag{4.4}$$

The boundary conditions at the point $x = 1$ become

$$u_1(1) = -u_0(1) = -\frac{g(1)}{\lambda_0}, \qquad v_1(1) = \lambda - \lambda_0$$

where $\lambda_0 = v_0(1)$. Assuming $g(1) \neq 0$, we have that $u_1(1)$ must equal a nonzero constant.

Scaling. We now scale the dependent variables as follows:

$$u_2 = {v_0}^{\frac{1}{4}} x^{\frac{3}{2}} u_1, \qquad v_2 = {v_0}^{\frac{1}{4}} x^{\frac{3}{2}} v_1.$$

Also, we define a new independent variable

$$t = \int_{x_0}^{x} {v_0}^{\frac{1}{2}}(s)\, ds$$

where $\tilde{x}_0 < x_0 < 1$. These transformations eliminate the first derivative terms and also give us a factor of 1 on the leading order linear term of u_2 in the first equation. We set

$$T_0 = -\int_{\tilde{x}_0}^{x_0} {v_0}^{\frac{1}{2}}(s)\, ds \geq -\infty, \qquad T_1 = \int_{x_0}^{1} {v_0}^{\frac{1}{2}}(s)\, ds < +\infty.$$

Thus, after substitution into (4.4), we have

$$\begin{aligned} &h^2 {u_2}'' + u_2 + \beta v_2 = -\gamma u_2 v_2 + h^2 q - h^2 \alpha u_2, \\ &{v_2}'' - 2\beta u_2 + \alpha v_2 = \gamma {u_2}^2, \end{aligned} \tag{4.5}$$

for $t \in (T_0, T_1]$ where

$$\mathcal{L} = \frac{d^2}{dx^2} + \frac{3}{x}\frac{d}{dx},$$

$$\alpha(t) = \frac{x^{\frac{3}{2}}}{{v_0}^{\frac{3}{4}}(x)} \mathcal{L}(x^{-\frac{3}{2}} {v_0}^{-\frac{1}{4}}(x)), \qquad q(t) = -\frac{x^{\frac{3}{2}}}{{v_0}^{\frac{3}{4}}(x)} \mathcal{L} u_0(x), \tag{4.6}$$

$$\beta(t) = \frac{g(x)}{{v_0}^2(x)}, \qquad \gamma(t) = x^{-\frac{3}{2}} {v_0}^{-\frac{5}{4}}(x).$$

The boundary conditions at the point $t = T_1$ are

$$u_2(T_1) = -\frac{g(1)}{{\lambda_0}^{\frac{3}{4}}}, \qquad v_2(T_1) = {\lambda_0}^{\frac{1}{4}}(\lambda - \lambda_0).$$

Observe that $u_2(T_1)$ is a nonzero constant.

Conversion to a First-Order System. To convert these two second-order equations (4.5) into a first-order system, we let

$$\mathbf{y}_I = \begin{pmatrix} u_2 \\ h{u_2}' \end{pmatrix}, \qquad \mathbf{y}_{II} = \begin{pmatrix} v_2 \\ {v_2}' \end{pmatrix}.$$

Substitution into the equations (4.5) yields

$$\begin{aligned} h{\mathbf{y}_I}' &= B\mathbf{y}_I - \beta L\mathbf{y}_{II} + (h^2 q - \gamma \langle D_1\mathbf{y}_I, \mathbf{y}_{II}\rangle)\mathbf{e}_2 - h^2\alpha L\mathbf{y}_I, \\ {\mathbf{y}_{II}}' &= 2\beta L\mathbf{y}_I + (-\alpha L + U)\mathbf{y}_{II} + \gamma \langle D_1\mathbf{y}_I, \mathbf{y}_I\rangle \mathbf{e}_2, \end{aligned} \tag{4.7}$$

where

$$B = \begin{pmatrix} 0 & 1 \\ -1 & 0 \end{pmatrix}, \qquad L = \begin{pmatrix} 0 & 0 \\ 1 & 0 \end{pmatrix}, \qquad U = \begin{pmatrix} 0 & 1 \\ 0 & 0 \end{pmatrix},$$

$$D_1 = \begin{pmatrix} 1 & 0 \\ 0 & 0 \end{pmatrix}, \qquad D_2 = \begin{pmatrix} 0 & 0 \\ 0 & 1 \end{pmatrix},$$

$$\mathbf{e}_1 = \begin{pmatrix} 1 \\ 0 \end{pmatrix}, \qquad \mathbf{e}_2 = \begin{pmatrix} 0 \\ 1 \end{pmatrix}.$$

The boundary conditions at $t = T_1$ are

$$\langle \mathbf{e}_1, \mathbf{y}_I\rangle = -\frac{g(1)}{{\lambda_0}^{\frac{3}{4}}}, \qquad \langle \mathbf{e}_1, \mathbf{y}_{II}\rangle = {\lambda_0}^{\frac{1}{4}}(\lambda - \lambda_0).$$

The inner product $\langle \cdot, \cdot \rangle$ is the usual vector dot product.

Decoupling. We form linear combinations of the vectors $\mathbf{y}_I$, $\mathbf{y}_{II}$ to eliminate the coupling in the leading order linear terms of the system (4.7). Thus, let

$$\mathbf{z}_I = \mathbf{y}_I + \beta D_1\mathbf{y}_{II}, \qquad \mathbf{z}_{II} = \mathbf{y}_{II} + 2h\beta D_2\mathbf{y}_I.$$

Substitution in the system (4.7) yields

$$\begin{aligned} h{\mathbf{z}_I}' &= (B + h^2 S_I)\mathbf{z}_I + hR_I\mathbf{z}_{II} + h^2 q_I\mathbf{e}_2 + Q_I(\mathbf{z}_I, \mathbf{z}_{II}), \\ {\mathbf{z}_{II}}' &= (C + h^2 S_{II})\mathbf{z}_{II} + hR_{II}\mathbf{z}_I + h^2 q_{II}\mathbf{e}_2 + Q_{II}(\mathbf{z}_I, \mathbf{z}_{II}), \end{aligned} \tag{4.8}$$

where

$$C = \begin{pmatrix} 0 & 1 \\ -(\alpha + 2\beta^2) & 0 \end{pmatrix},$$

$$R_I = \begin{pmatrix} \beta' & \beta \\ h\alpha\beta & 0 \end{pmatrix}, \qquad R_{II} = \begin{pmatrix} 0 & -2\beta \\ -h\alpha\beta & 2\beta' \end{pmatrix},$$

$$S_I = \begin{pmatrix} 0 & -2\beta^2 \\ -\alpha & 0 \end{pmatrix}, \qquad S_{II} = \begin{pmatrix} 0 & 0 \\ 2\alpha\beta^2 & 0 \end{pmatrix},$$

$$q_I = q, \qquad q_{II} = 2\beta q,$$

$$Q_I(\mathbf{x}, \mathbf{y}) = -\gamma(x_1 - \beta y_1) y_1 \mathbf{e}_2, \qquad Q_{II}(\mathbf{x}, \mathbf{y}) = -\gamma(x_1 - \beta y_1)(x_1 - 3\beta y_1)\mathbf{e}_2,$$

with $\mathbf{x} = [x_j]$ and $\mathbf{y} = [y_j]$. The boundary conditions at $t = T_1$ are

$$\langle \mathbf{e}_1, \mathbf{z}_I \rangle = -\frac{g(1)}{\lambda_0^{\frac{7}{4}}}(\lambda - 2\lambda_0), \qquad \langle \mathbf{e}_1, \mathbf{z}_{II} \rangle = \lambda_0^{\frac{1}{4}}(\lambda - \lambda_0).$$

Note that with these boundary conditions we have

$$\|\mathbf{z}_I\|^2 + \|\mathbf{z}_{II}\|^2 \geq a_0^2 \tag{4.9}$$

where

$$a_0^2 = \min_{\lambda \in (-\infty, +\infty)} \left(\frac{g^2(1)}{\lambda_0^{\frac{7}{2}}}(\lambda - 2\lambda_0)^2 + \lambda_0^{\frac{1}{2}}(\lambda - \lambda_0)^2 \right).$$

Solving for a_0, we find

$$a_0 = \sqrt{\frac{g^2(1)\lambda_0^{\frac{5}{2}}}{g^2(1) + \lambda_0^4}}.$$

Clearly, $a_0 > 0$ and so the quantity $\|\mathbf{z}_I(T_1)\|^2 + \|\mathbf{z}_{II}(T_1)\|^2$ is uniformly bounded away from zero as $h \to 0$.

Summary of the Transformations. The new variables t, $\mathbf{z}_I$ and $\mathbf{z}_{II}$ are related to the original variables x, u and v as follows:

$$t = \int_{x_0}^{x} v_0^{\frac{1}{2}}(s)\, ds,$$

$$\mathbf{z}_I = \begin{pmatrix} x^{\frac{3}{2}} v_0{}^{\frac{1}{4}} \Delta u + x^{\frac{3}{2}} g(x) v_0{}^{-\frac{7}{4}}(x) \Delta v \\ h(x^{\frac{3}{2}} v_0{}^{\frac{1}{4}} \Delta u)' \end{pmatrix}, \tag{4.10}$$

$$\mathbf{z}_{II} = \begin{pmatrix} x^{\frac{3}{2}} v_0{}^{\frac{1}{4}} \Delta v \\ (x^{\frac{3}{2}} v_0{}^{\frac{1}{4}} \Delta v)' + 2h^2 g(x) v_0{}^{-2}(x)(x^{\frac{3}{2}} v_0{}^{\frac{1}{4}} \Delta u)' \end{pmatrix}$$

where $\Delta u = u - u_0$, $\Delta v = v - v_0$, and the prime denotes differentiation with respect to x. Furthermore, the following functions of the original variables u and v may be obtained from the components of $\mathbf{z}_I = [\mathbf{z}_{Ij}]$ and $\mathbf{z}_{II} = [\mathbf{z}_{IIj}]$, $j = 1, 2$:

$$\begin{aligned}
v(x) &= v_0(x) + x^{-\frac{3}{2}} v_0{}^{-\frac{1}{4}}(x) \mathbf{z}_{II1}, \\
u(x) &= u_0(x) + x^{-\frac{3}{2}} v_0{}^{-\frac{1}{4}}(x) \mathbf{z}_{I1} - x^{-\frac{3}{2}} v_0{}^{-\frac{9}{4}}(x) g(x) \mathbf{z}_{II1}, \\
v'(x) &= v_0'(x) + 2h^2 x^{-\frac{3}{2}} v_0{}^{-\frac{9}{4}}(x) g(x) \left(\frac{3}{2x} + \frac{v_0'(x)}{4v_0(x)} \right) \mathbf{z}_{I1} - \\
&\quad - x^{-\frac{3}{2}} v_0{}^{-\frac{1}{4}}(x) \left(\frac{3}{2x} + \frac{v_0'(x)}{4v_0(x)} \right) \left(1 + 2h^2 \frac{g^2(x)}{v_0{}^4(x)} \right) \mathbf{z}_{II1} - \\
&\quad - 2h x^{-\frac{3}{2}} v_0{}^{-\frac{9}{4}}(x) g(x) \mathbf{z}_{I2} + x^{-\frac{3}{2}} v_0{}^{-\frac{1}{4}}(x) \mathbf{z}_{II2}, \\
hu'(x) &= hu_0'(x) - h x^{-\frac{3}{2}} v_0{}^{-\frac{1}{4}}(x) \left(\frac{3}{2x} + \frac{v_0'(x)}{4v_0(x)} \right) \mathbf{z}_{I1} + \\
&\quad + h x^{-\frac{3}{2}} v_0{}^{-\frac{9}{4}}(x) g(x) \left(\frac{3}{2x} + \frac{v_0'(x)}{4v_0(x)} \right) \mathbf{z}_{II1} + x^{-\frac{3}{2}} v_0{}^{-\frac{1}{4}}(x) \mathbf{z}_{I2}.
\end{aligned} \tag{4.11}$$

Note that the coefficients in (4.10, 4.11) are uniformly bounded for x and h suitably restricted. Thus, we have

$$\begin{pmatrix} v(x) \\ u(x) \\ v'(x) \\ hu'(x) \end{pmatrix} = \begin{pmatrix} v_0(x) \\ u_0(x) \\ v_0'(x) \\ hu_0'(x) \end{pmatrix} + M(x;h) \begin{pmatrix} \mathbf{z}_I(t(x)) \\ \mathbf{z}_{II}(t(x)) \end{pmatrix}$$

where $M(x)$ is a matrix satisfying

$$\|M(x;h)\| \leq K, \qquad \|M^{-1}(x;h)\| \leq K$$

for $x \in [x_0, 1]$, $h \in [0,1]$ with K independent of x and h. Also, note that

$$u(x)v(x) - g(x) = x^{-\frac{3}{2}} v_0{}^{\frac{3}{4}}(x)\mathbf{z}_{I1} + x^{-3} v_0{}^{-\frac{5}{2}}(x)\mathbf{z}_{II1}\left(v_0{}^2(x)\mathbf{z}_{I1} - g(x)\mathbf{z}_{II1}\right).$$

Thus, for $\|\mathbf{z}_I\| + \|\mathbf{z}_{II}\| \to 0$, $u(x)v(x) - g(x) \to 0$ uniformly for $x \in [x_0, 1]$, $h \in [0,1]$.

4.2 Derivation of an Integral Inequality

In this section we discuss solutions of a system of differential equations, defined on the domain $t \in (T_0, T_1]$, of form

$$\begin{aligned} h\mathbf{z}_I{}' &= B(\mathbf{z}_I + \nabla_I \phi(t, \mathbf{z}_I, \mathbf{z}_{II}; h)) + hF_I(t, \mathbf{z}_I, \mathbf{z}_{II}, h), \\ \mathbf{z}_{II}{}' &= A\mathbf{z}_{II} + F_{II}(t, \mathbf{z}_I, \mathbf{z}_{II}, h) \end{aligned} \tag{4.12}$$

where

$$\nabla_I \phi = \frac{\partial}{\partial \varsigma} \phi(\cdot, \varsigma, \cdot; h), \qquad \nabla_{II} \phi = \frac{\partial}{\partial \varsigma} \phi(\cdot, \cdot, \varsigma; h).$$

The matrix B is assumed to be independent of t, nonsingular and antisymmetric. The vectors $\mathbf{z}_I$ and $\mathbf{z}_{II}$ are of dimension m and n, respectively; the results that follow are essentially independent of the dimensions. However, the $m \times m$ matrix B cannot be both nonsingular and antisymmetric unless m is even. For the plate problem, of course, m and n are two.

The discussion is motivated in part by the results of KREISS.[1] The results of this paper imply that for the system (4.12), if $\mathbf{z}_I$ and $\mathbf{z}_{II}$ are $O(h)$ at some point $t \in [\tau_0, T_1]$, then the solution is $O(h)$ for all $t \in [\tau_0, T_1]$. In the next

[1] *SIAM J. Numer. Anal.* **16** (1979)

two sections, we show that if $\mathbf{z}_I$ and $\mathbf{z}_{I\!I}$ are bounded by some constant δ sufficiently small, then the solution is bounded by 4δ for all $t \in [\tau_0, T_1]$.

We now state some hypotheses concerning ϕ, F_I, $F_{I\!I}$ and the matrix A. The scalar function ϕ is assumed to vanish like the cube of $\mathbf{z}_I$ and $\mathbf{z}_{I\!I}$ at leading order in h. It may also have an $o(1)$ contribution of arbitrary form. More precisely, a region Ω in the space with elements $(t, (\mathbf{z}_I, \mathbf{z}_{I\!I}), h)$ is defined to be $[\tau_0, T_1] \times D \times [0, h_0]$, with D being the ball of radius Z given by

$$D = \{(\mathbf{x}, \mathbf{y}) : x \in \mathbb{R}^m, y \in \mathbb{R}^n, \|\mathbf{x}\|^2 + \|\mathbf{y}\|^2 \leq Z^2\}.$$

The norms used in this definition and subsequently are the Euclidean norms for the appropriate spaces, $\mathbb{R}^m$ and $\mathbb{R}^n$. The constants $\tau_0 > T_0$, $Z > 0$ and $h_0 > 0$ are considered fixed for the remainder of the discussion. We assume that

$$|\phi(t, \mathbf{x}, \mathbf{y}; h)| \leq C_0(\|\mathbf{x}\|^2 + \|\mathbf{y}\|^2)^{\frac{3}{2}} + \psi_0(h) \tag{4.13}$$

for $(t, (\mathbf{x}, \mathbf{y}), h) \in \Omega$. The notation C_j will be used hereafter to denote positive constants independent of t, $\mathbf{x}$, $\mathbf{y}$ and h; C_j may depend only on the choice of τ_0, Z and h_0. The notation $\psi_j(h)$ is used to denote positive functions of h that are independent of t, $\mathbf{x}$ and $\mathbf{y}$, and satisfy $\psi_j(h) = o(1)$ as $h \to 0$; ψ_j may depend on the choice of τ_0, Z and h_0. We further suppose that

$$\left|\frac{\partial}{\partial t}\phi(t, \mathbf{x}, \mathbf{y}; h)\right| \leq C_0(\|\mathbf{x}\|^2 + \|\mathbf{y}\|^2)^{\frac{3}{2}} + \psi_0(h), \tag{4.14}$$

$$\|\nabla_I \phi(t, \mathbf{x}, \mathbf{y}; h)\| \leq C_0(\|\mathbf{x}\|^2 + \|\mathbf{y}\|^2) + \psi_0(h) \tag{4.15}$$

and

$$\|\nabla_{I\!I} \phi(t, \mathbf{x}, \mathbf{y}; h)\| \leq C_0(\|\mathbf{x}\|^2 + \|\mathbf{y}\|^2) + \psi_0(h) \tag{4.16}$$

for $(t, (\mathbf{x}, \mathbf{y}), h) \in \Omega$. The vector function F_I is assumed to be $o(1)$ as $h \to 0$; that is,

$$\|F_I(t, \mathbf{x}, \mathbf{y}; h)\| \leq \psi_0(h) \tag{4.17}$$

for $(t,(\mathbf{x},\mathbf{y}),h) \in \Omega$. We suppose that the vector function F_{II} vanishes quadratically in $\mathbf{z}_I$ and $\mathbf{z}_{II}$ to leading order in h. It may also have a contribution that is $o(1)$ as $h \to 0$. Thus, let

$$\|F_{II}(t,\mathbf{x},\mathbf{y};h)\| \le C_0(\|\mathbf{x}\|^2 + \|\mathbf{y}\|^2) + \psi_0(h) \tag{4.18}$$

for $(t,(\mathbf{x},\mathbf{y}),h) \in \Omega$. The matrix $A(t;h)$ is required to be uniformly bounded for $t \in [\tau_0, T_1]$, $h \in [0, h_0]$. Thus, we assume

$$\|A(t;h)\| \le C_0 \tag{4.19}$$

for $t \in [\tau_0, T_1]$, $h \in [0, h_0]$.

In the case of the von Kármán equations, we have shown that the two second-order plate equations can be transformed into a system of first-order equations that have the form (4.8). These equations can be put into the form (4.12) and the hypotheses (4.13–4.19) verified if A, ϕ, F_I and F_{II} are appropriately chosen. Recall that

$$B = \begin{pmatrix} 0 & 1 \\ -1 & 0 \end{pmatrix}.$$

Clearly, B is antisymmetric and nonsingular. We let

$$\begin{aligned}\phi(t,\mathbf{x},\mathbf{y};h) =& \frac{h^2}{2}(\alpha(t)x_1^2 - 2\beta^2(t)x_2^2) - \\ & - h^2\alpha(t)\beta(t)x_1y_1 + h\beta'(t)x_2y_1 + h\beta(t)x_2y_2 - \\ & - h^2 q(t)x_1 + \tfrac{1}{2}\gamma(t)x_1y_1(x_1 - 2\beta(t)y_1)\end{aligned}$$

and

$$F_I(t,\mathbf{x},\mathbf{y};h) = \begin{pmatrix} 0 \\ 0 \end{pmatrix}.$$

Taking the gradient of ϕ with respect to $\mathbf{x}$, we have

$$\nabla_I\, \phi(t, \mathbf{x}, \mathbf{y}; h) = \begin{pmatrix} h^2\alpha(x_1 - \beta y_1) - h^2 q + \gamma(x_1 - \beta y_1)y_1 \\ \\ -2h^2\beta^2 x_2 + h\beta' y_1 + h\beta y_2 \end{pmatrix}.$$

Multiplying this expression by B gives

$$B\nabla_I\, \phi(t, \mathbf{x}, \mathbf{y}; h) = \begin{pmatrix} -2h^2\beta^2 x_2 + h\beta' y_1 + h\beta y_2 \\ \\ -h^2\alpha(x_1 - \beta y_1) + h^2 q - \gamma(x_1 - \beta y_1)y_1 \end{pmatrix}.$$

It may be easily verified that the equations (4.8a) are of the form (4.12a), with B, ϕ and F_I as defined.

To satisfy the assumptions (4.13–4.17) we must have $\alpha(t)$ be continuously differentiable and $\beta(t)$ be twice continuously differentiable for $\tau_0 \le t \le T_1$; thus, we suppose that g is twice continuously differentiable on $[0, 1]$. Recalling the definitions (4.6) of α and β, we see that under this assumption α and β will have the necessary smoothness.

We now define

$$A(t; h) = \begin{pmatrix} 0 & 1 \\ A_{21} & 0 \end{pmatrix}$$

where

$$A_{21} = -\alpha(t) - 2\beta^2(t) + 2h^2\alpha(t)\beta^2(t).$$

The matrix $A(t; h)$ is uniformly bounded for $\tau_0 \le t \le T_1$; this follows from the assumption that $g(x)$ is continuous. Hence, the assumption (4.19) is satisfied. Note that ϕ and A are *not* uniformly bounded on $[T_0, T_1]$ because of the possible singularity at T_0 of the function $\alpha(t)$; this is the motivation for the restriction $\tau_0 > T_0$.

Furthermore, we let

$$F_{II}(t, \mathbf{x}, \mathbf{y}; h) = \begin{pmatrix} -2h\beta(t)x_2 \\ \\ F_{II\,2} \end{pmatrix}$$

where

$$F_{II2} = -\, h^2\alpha(t)\beta(t)x_1 + 2h\beta'(t)x_2 + 2h\beta(t)q(t) \; +$$

$$+\, \gamma(t)(x_1 - 3\beta(t)x_2)(x_1 - \beta(t)x_2).$$

Clearly the equations (4.8b) are of the form (4.12b), with A and F_{II} as defined. The assumptions (4.18, 4.19) are easily verified.

The Comparison Function. We may get some idea of the behavior of the solutions of the nonlinear system (4.12) in the limit of small h, $\mathbf{z}_I$ and $\mathbf{z}_{II}$ by studying the leading order linearized equations

$$h\mathbf{z}_I{}' = B\mathbf{z}_I, \qquad \mathbf{z}_{II}{}' = A(t;0)\mathbf{z}_{II}. \tag{4.20}$$

We define a scalar function $\mathcal{A} \geq 0$ by

$$\mathcal{A}^2(t) = \|\mathbf{z}_I(t)\|^2 + \|X^{-1}(t)\mathbf{z}_{II}(t)\|^2 \tag{4.21}$$

where X is a fundamental matrix solution of the leading order linearization of (4.12a); that is,

$$X'(t) = A(t;0)X(t), \qquad X(T_1) = I. \tag{4.22}$$

Because A is bounded for $t \in [\tau_0, T_1]$, then $X(t)$ is invertible for all t in this interval. As discussed earlier, $\mathcal{A}$ is a comparison function for the solution $\mathbf{z}_I$, $\mathbf{z}_{II}$. A solution of the leading order linearized system (4.20) will give a constant value of $\mathcal{A}$. To show this, we take the derivative of $\mathcal{A}^2$ with respect to t. Thus,

$$(\mathcal{A}^2)' = 2\mathbf{z}_I{}^T\mathbf{z}_I{}' + 2(X^{-1}\mathbf{z}_{II})^T(X^{-1}\mathbf{z}_{II}{}' + (X^{-1})'\mathbf{z}_{II}). \tag{4.23}$$

From the identity

$$X^{-1}X = I,$$

differentiation with respect to t gives

$$(X^{-1})'X + X^{-1}X' = 0.$$

From (4.22) we have

$$(X^{-1})'X + X^{-1}A(t;0)X = 0.$$

Multiplying on the right by X^{-1} and solving for $(X^{-1})'$, we obtain

$$(X^{-1})' = -X^{-1}A(t;0).$$

Substitution into the equation (4.23) gives

$$(\mathcal{A}^2)' = 2\mathbf{z}_I{}^T\mathbf{z}_I{}' + 2(X^{-1}\mathbf{z}_{II})^T X^{-1}(\mathbf{z}_{II}{}' - A(t;0)\mathbf{z}_{II}).$$

Using the differential equations (4.20b), the second term in the right-hand side vanishes. Hence,

$$(\mathcal{A}^2)' = 2\mathbf{z}_I{}^T\mathbf{z}_I{}'.$$

This is equivalent to

$$(\mathcal{A}^2)' = -2(B\mathbf{z}_I)^T B^{-1}\mathbf{z}_I{}'$$

where we have made use of the fact that B is antisymmetric and nonsingular, and hence B^{-1} exists and is also antisymmetric. Substituting from the differential equations (4.20a) for $B\mathbf{z}_I$, we find

$$(\mathcal{A}^2)' = -2(\mathbf{z}_I{}')^T B^{-1}\mathbf{z}_I{}'$$

and because B^{-1} is antisymmetric, this term also vanishes. Thus, we have shown that in the case of the linearized equations (4.20) $\mathcal{A}$ is a constant independent of t; the value of $\mathcal{A}$ depends only on the choice of the solution $(\mathbf{z}_I, \mathbf{z}_{II})$.

Motivated by the above discussion for the linearized equations, we form, from a solution $(\mathbf{z}_I, \mathbf{z}_{II})$ of the nonlinear equations (4.12), the scalar function

$$\mathcal{A}^2(t) = \|\mathbf{z}_I(t)\|^2 + \|X^{-1}(t;h)\mathbf{z}_{II}(t)\|^2 \tag{4.24}$$

where

$$X'(t;h) = A(t;h)X(t;h), \qquad X(T;h) = I.$$

We next derive estimates on the growth of $\mathcal{A}$, which hold for h, $\mathbf{z}_I$ and $\mathbf{z}_{II}$ sufficiently small.

Taking the derivative of $\mathcal{A}^2$ with respect to t, we find

$$(\mathcal{A}^2)' = 2{\mathbf{z}_I}^T{\mathbf{z}_I}' + 2(X^{-1}\mathbf{z}_{II})^T(X^{-1}{\mathbf{z}_{II}}' + (X^{-1})'\mathbf{z}_{II}). \tag{4.25}$$

As noted before, the matrix X^{-1} satisfies the differential equation

$$(X^{-1})' = -X^{-1}A(t;h).$$

Substituting into the equation (4.25), we obtain

$$(\mathcal{A}^2)' = 2{\mathbf{z}_I}^T{\mathbf{z}_I}' + 2(X^{-1}\mathbf{z}_{II})^T X^{-1}({\mathbf{z}_{II}}' - A(t;h)\mathbf{z}_{II}). \tag{4.26}$$

Using the differential equations (4.12), then for the first term we have

$${\mathbf{z}_I}^T{\mathbf{z}_I}' = -(B\mathbf{z}_I)^T B^{-1}{\mathbf{z}_I}' = -(h{\mathbf{z}_I}' - B\nabla_I\phi - F_I)^T B^{-1}{\mathbf{z}_I}'.$$

Recall that $\mathbf{x}^T B^{-1}\mathbf{x} = 0$ for arbitrary $\mathbf{x}$ and in particular, this holds for $\mathbf{x} = {\mathbf{z}_I}'$. Therefore,

$$\begin{aligned} {\mathbf{z}_I}^T{\mathbf{z}_I}' &= (B\nabla_I\phi + hF_I)^T B^{-1}{\mathbf{z}_I}' \\ &= -\nabla_I\phi^T{\mathbf{z}_I}' - (B^{-1}F_I)^T h{\mathbf{z}_I}'. \end{aligned} \tag{4.27}$$

We may substitute from the differential equations $(4.12a)$ for $h\mathbf{z}_I'$ to obtain

$$\begin{aligned} {\mathbf{z}_I}^T \mathbf{z}_I' &= -\nabla_I \phi^T \mathbf{z}_I' - (B^{-1}F_I)^T (B\mathbf{z}_I + B\nabla_I \phi + F_I) \\ &= -\nabla_I \phi^T \mathbf{z}_I' + {F_I}^T(\mathbf{z}_I + \nabla_I \phi). \end{aligned} \tag{4.28}$$

Furthermore, from the equations $(4.12b)$ we have

$$(X^{-1}\mathbf{z}_{II})^T X^{-1}(\mathbf{z}_{II}' - A\mathbf{z}_{II}) = (X^{-1}\mathbf{z}_{II})^T X^{-1} F_{II} \tag{4.29}$$

for the second term in the expression (4.26).

Integrating both sides of the equation (4.26) from $\tau > \tau_0$ to $t \le T_1$ and employing the expressions (4.28, 4.29) gives

$$\mathcal{A}^2(t) - \mathcal{A}^2(\dot{\tau}) = 2\int_\tau^t (m_1(s) + f_2(s) + f_3(s))\, ds \tag{4.30}$$

where

$$\begin{aligned} m(t) &= -\nabla_I \phi^T(t, \mathbf{z}_I(t), \mathbf{z}_{II}(t); h)\, \mathbf{z}_I'(t), \\ f_2(t) &= {F_I}^T(t, \mathbf{z}_I(t), \mathbf{z}_{II}(t); h)\, (\mathbf{z}_I(t) + \nabla_I \phi(t, \mathbf{z}_I(t), \mathbf{z}_{II}(t); h)), \\ f_3(t) &= (X^{-1}(t;h)\mathbf{z}_{II}(t))^T\, X^{-1}(t;h) F_{II}(t, \mathbf{z}_I(t), \mathbf{z}_{II}(t); h). \end{aligned} \tag{4.31}$$

We define

$$I_0(t) = 2\int_\tau^t m(s)\, ds. \tag{4.32}$$

Observe that

$$\begin{aligned} \frac{d}{dt}\phi(t, \mathbf{z}_I(t), \mathbf{z}_{II}(t); h) = &\frac{\partial}{\partial t}\phi(t, \mathbf{z}_I(t), \mathbf{z}_{II}(t); h) + \\ &+ \nabla_I \phi^T(t, \mathbf{z}_I(t), \mathbf{z}_{II}(t); h)\mathbf{z}_I'(t) + \\ &+ \nabla_{II} \phi^T(t, \mathbf{z}_I(t), \mathbf{z}_{II}(t); h)\mathbf{z}_{II}'(t). \end{aligned}$$

Hence, from the definitions (4.31, 4.32) of m and I_0, we find

$$I_0(t) = -2(\phi(t, \mathbf{z}_I(t), \mathbf{z}_{II}(t); h) - \phi(\tau, \mathbf{z}_I(\tau), \mathbf{z}_{II}(\tau); h)) +$$
$$+ 2\int_\tau^t \frac{\partial}{\partial t}\phi(s, \mathbf{z}_I(s), \mathbf{z}_{II}(s); h)\, ds +$$
$$+ 2\int_\tau^t \nabla_{II}\,\phi^T(s, \mathbf{z}_I(s), \mathbf{z}_{II}(s); h)\mathbf{z}_{II}'(s), ds.$$

Substitution from the differential equations (4.12*b*) for $\mathbf{z}_{II}'$ yields

$$I_0(t) = f_0(t) + 2\int_\tau^t f_1(s)\, ds$$

where

$$f_0(t) = -2(\phi(t, \mathbf{z}_I(t), \mathbf{z}_{II}(t); h) - \phi(\tau, \mathbf{z}_I(\tau), \mathbf{z}_{II}(\tau); h)),$$
$$f_1(t) = \frac{\partial}{\partial t}\phi(t, \mathbf{z}_I(t), \mathbf{z}_{II}(t); h) +$$
$$+ \nabla_{II}\,\phi^T(t, \mathbf{z}_I(t), \mathbf{z}_{II}(t); h)(A(t; h)\mathbf{z}_{II} + F_{II}(t, \mathbf{z}_I(t), \mathbf{z}_{II}(t); h)).$$

The expression (4.30) now becomes

$$\mathcal{A}^2(t) - \mathcal{A}^2(\tau) = f_0(t) + I_1(t) + I_2(t) + I_3(t) \tag{4.33}$$

where

$$I_j(t) = 2\int_\tau^t f_j(s)\, ds \qquad \text{for } j = 1,\ 2,\ 3.$$

We may now employ the assumptions (4.13–4.19) to obtain an integral inequality for $\mathcal{A}$.

The Inequality. We will derive bounds for each of the terms in the right-hand side of (4.33) separately. The assumptions (4.13–4.19) provide bounds in terms of the norms of $\mathbf{z}_I$ and $\mathbf{z}_{II}$. From the definition (4.24) of $\mathcal{A}$ and the

Cauchy-Schwartz inequality, we obtain

$$\mathcal{A}^2(t) \geq \|\mathbf{z}_I(t)\|^2 + \frac{\|\mathbf{z}_{II}(t)\|^2}{\|X(t;h)\|^2}.$$

From the differential equation (4.22), which determines X and the assumption (4.19) that A is uniformly bounded, it is clear that X is also uniformly bounded for $t \in [\tau_0, T_1]$, $h \in [0, h_0]$. For if

$$a = \max_{\substack{t\in[\tau_0,T_1] \\ h\in[0,\, h_0]}} \|A(t;h)\|, \tag{4.34}$$

then

$$\|X(t;h)\| \leq e^{a(T_1-t)}.$$

We let

$$C_1 = \max\left\{C_0,\ e^{a(T_1-t)},\ \max_{h\in[0,h_0]} \psi_0(h)\right\}.$$

Hence,

$$\|\mathbf{z}_I(t)\|^2 + \|\mathbf{z}_{II}(t)\|^2 \leq {C_1}^2 \mathcal{A}^2(t) \tag{4.35}$$

for $t \in [\tau_0, T_1]$, $h \in [0, h_0]$. We define $\tilde{\Omega} = [\tau_0, T_1] \times [0, \tilde{Z}] \times [0, h_0]$, where we choose $\tilde{Z}$ sufficiently small that if

$$\left(t, \left(\|\mathbf{x}\|^2 + \|X^{-1}(t;h)\mathbf{y}\|^2\right)^{\frac{1}{2}}, h\right) \in \tilde{\Omega},$$

then

$$(t, (\mathbf{x}, \mathbf{y}), h) \in \Omega.$$

To accomplish this, we let

$$\tilde{Z} = \frac{Z}{C_1}$$

where a is defined as in (4.34).

We now use the upper bound (4.13) for the absolute value of ϕ and the lower bound (4.35) for $\mathcal{A}$ to obtain

$$\begin{aligned} |f_0| \leq & C_1(\|\mathbf{z}_I(t)\|^2 + \|\mathbf{z}_{II}(t)\|^2)^{\frac{3}{2}} + C_1(\|\mathbf{z}_I(\tau)\|^2 + \|\mathbf{z}_{II}(\tau)\|^2)^{\frac{3}{2}} + 2\psi_0(h) \\ \leq & {C_1}^4(\mathcal{A}^3(t) + \mathcal{A}^3(\tau)) + 2\psi_0(h), \end{aligned} \tag{4.36}$$

provided $(s, \mathcal{A}(s), h) \in \tilde{\Omega}$ for $s \in [\tau, t]$. Similarly, we use the bounds (4.13–4.16) for ϕ and its derivatives as well as the bounds (4.17–4.19) for F_I, F_{II} and A to obtain

$$\begin{aligned} |I_1| \leq & \int_\tau^t 2(C_1 + {C_1}^2(1+Z))(\|\mathbf{z}_I(s)\|^2 + \|\mathbf{z}_{II}(s)\|^2)^{\frac{3}{2}}\, ds \; + \\ & + 2(T_1 - \tau_0)(1 + C_1(1 + Z + 2Z^2))\psi_0(h) \\ \leq & \int_\tau^t 2({C_1}^4 + {C_1}^5(1+Z))\mathcal{A}^3(s)\, ds \; + \\ & + 2(T_1 - \tau_0)(1 + C_1(1 + Z + 2Z^2))\psi_0(h), \end{aligned} \tag{4.37}$$

$$|I_2| \leq 2(T_1 - \tau_0)(Z + C_1(1 + Z^2))\psi_0(h), \tag{4.38}$$

and

$$\begin{aligned} |I_3| \leq & \int_\tau^t 2{C_1}^3(\|\mathbf{z}_I(s)\|^2 + \|\mathbf{z}_{II}(s)\|^2)^{\frac{3}{2}}\, ds + {C_1}^2 Z\psi_0(h) \\ \leq & \int_\tau^t 2{C_1}^6\mathcal{A}^3(s)\, ds + 2(T_1 - \tau_0){C_1}^2 Z\psi_0(h), \end{aligned} \tag{4.39}$$

provided $(s, \mathcal{A}(s), h) \in \tilde{\Omega}$ for $s \in [\tau, t]$. We let

$$C_2 = \max\{{C_1}^4, 2({C_1}^4 + {C_1}^5(1+Z)) + 2{C_1}^6\}$$

and

$$\psi_2(h) = (2 + 2(T_1 - \tau_0)(1 + Z + C_1(1 + Z + 3Z^2) + {C_1}^2 Z))\psi_0(h).$$

Therefore, from the expression (4.33) and the estimates (4.36–4.39), we have the integral inequality

$$\mathcal{A}^2(t) - \mathcal{A}^2(\tau) \leq C_2(\mathcal{A}^3(t) + \mathcal{A}^3(\tau)) + \int_\tau^t C_2\mathcal{A}^3(s)\,ds + \psi_2(h), \tag{4.40}$$

provided $(s, \mathcal{A}(s), h) \in \tilde{\Omega}$ for $s \in [\tau, t]$.

4.3 **Two Lemmas**

We showed in the previous section that the scalar function $\mathcal{A}$ satisfies

$$\mathcal{A}^2(t) - \mathcal{A}^2(\tau) \leq C_2(\mathcal{A}^3(t) + \mathcal{A}^3(\tau)) + C_2\int_\tau^t \mathcal{A}^3(s)\,ds + \psi(h) \tag{4.41}$$

for $\tau_0 \leq \tau \leq t \leq T_1$, provided $(s, \mathcal{A}(s), h) \in \tilde{\Omega}$ for $s \in [\tau, t]$. We now prove a lemma that enables us to claim that $\mathcal{A}(t)$ is small for $t \in [\tau, T_1]$, provided $\mathcal{A}(\tau)$ is small.

Lemma 1. *Let $z(s) \geq 0$ be a continuous function defined on $s \in [0,1]$ satisfying*

$$z^2(s) - z^2(0) \leq z^3(s) + z^3(0) + \int_0^s z^3(r)\,dr + \epsilon \tag{4.42}$$

where $\epsilon \geq 0$. Then there exist a positive constant δ_0 and a function $\epsilon_0(\delta)$ positive for $\delta \leq \delta_0$ such that if $z(0) \leq \delta \leq \delta_0$ and $\epsilon \leq \epsilon_0(\delta)$, then $z(s) \leq 4\delta$ for $s \in [0,1]$.

Proof. We show that $z(s)$ is bounded above by a continuous function $\bar{z}(s)$ that satisfies an integral equation related to the inequality (4.42) and also satisfies $\bar{z}(s) \leq 4\delta$ for $s \in [0,1]$. Thus, let

$$\bar{z}^2(s) - \delta^2 = \bar{z}^3(s) + \delta^3 + \int_0^s \bar{z}^3(r)\,dr + \epsilon. \tag{4.43}$$

At the initial point $s = 0$ we have

$$\bar{z}^3(0) - \bar{z}^2(0) + \delta^2 + \delta^3 + \epsilon = 0.$$

We must have δ and ϵ sufficiently small so that there is a solution to this equation for $\bar{z}(0)$ in the interval $[\delta, \infty)$. Let

$$P(\varsigma) = \varsigma^3 - \varsigma^2 + \delta^2 + \delta^3 + \epsilon.$$

Clearly, $P(\delta) > 0$. If we specify $\delta \leq \delta_0 < 1/3$ and ϵ sufficiently small, we may obtain $P(2\delta) < 0$. This, then, assures us the existence of a zero of P between δ and 2δ. We let $\delta_0 \leq 1/8$ and $\epsilon_0(\delta) = 2\delta^2(1 - 3\delta)$. We then have

$$P(2\delta) \leq -3\delta^2(1 - 3\delta) + \epsilon_0(\delta) < 0$$

as desired. Let $\varsigma^* \in (\delta, 2\delta)$ satisfy $P(\varsigma^*) = 0$. We specify $\bar{z}(0) = \varsigma^*$. Clearly, $\bar{z}(0) > z(0)$.

Next, we show that a continuous solution of the integral equation (4.43) exists for $s \in [0, 1]$. This is accomplished by solving for $\bar{z}$ implicitly from the integral equation. Differentiating (4.43) gives

$$2\bar{z}\bar{z}' = 3\bar{z}^2\bar{z}' + \bar{z}^3.$$

This is equivalent to

$$ds = \frac{2 - 3\bar{z}}{\bar{z}^2} d\bar{z}.$$

Integrating, we find

$$s = c - \frac{2}{\bar{z}} - 3 \log \bar{z} \tag{4.44}$$

where

$$c = \frac{2}{\varsigma^*} - 3 \log \varsigma^*.$$

To show that the expression (4.44) implicitly defines a continuous function $\bar{z}(s)$ on the interval $s \in [0, 1]$, it is sufficient to show that $ds/d\bar{z}$ is positive for $\bar{z} \in [\delta, 4\delta]$ and $s(4\delta) \geq 1$. The implicit function theorem then implies that

$\bar{z}(s)$ exists for $s \in [0,1]$. In addition, this gives us the desired estimate; that is, $\bar{z}(s) \leq 4\delta$ for $s \in [0,1]$. The derivative of $s(\bar{z})$ is

$$\frac{ds}{d\bar{z}} = \frac{2 - 3\bar{z}}{\bar{z}^2}.$$

For $0 < \bar{z} < 2/3$, $ds/d\bar{z} > 0$. Because we have chosen $\delta \leq \delta_0 \leq 1/8$, then

$$\frac{ds}{d\bar{z}} > 0 \qquad \text{for } \delta \leq \bar{z} \leq 4\delta.$$

Furthermore, because $\varsigma^* < 2\delta$, we have from (4.44) that

$$s(4\delta) \geq \frac{1}{2\delta} - 3\log 2.$$

We now specify that

$$\delta_0 = \min\left\{\frac{1}{8}, \frac{1}{2 + 6\log 2}\right\}.$$

Hence,

$$s(4\delta) \geq 1$$

as desired. To recap, we have shown that a continuous solution $\bar{z}(s)$ of the integral equation (4.43) exists for $s \in [0,1]$, satisfying $\bar{z}(0) > \delta$ and $\bar{z}(1) \leq 4\delta$.

We now show that $\bar{z}(s) > z(s)$ for $s \in [0,1]$. Suppose this is not true. We have assumed that z is continuous and have shown that $\bar{z}$ is continuous by the implicit function theorem. Also recall that $z(0) < \bar{z}(0)$. Hence, there is a smallest value of $s = s^* > 0$ for which $z(s^*) = \bar{z}(s^*)$. Thus, we have

$$\bar{z}(s) > z(s) \qquad \text{for } 0 \leq s < s^*$$

and therefore,

$$\bar{z}^3(s^*) + \delta^2 + \delta^3 + \int_0^{s^*} \bar{z}^3(r)\,dr > z^3(s^*) + z(0)^2 + z(0)^3 + \int_0^{s^*} z^3(r)\,dr.$$

From the inequality (4.42) satisfied by z and the integral equation (4.43) satisfied by $\bar{z}$, we then obtain

$$\begin{aligned}\bar{z}^2(s^*) &= \bar{z}^3(s^*) + \delta^2 + \delta^3 + \int_0^{s^*} \bar{z}^3(r)\,dr + \epsilon \\ &> z^3(s^*) + z(0)^2 + z(0)^3 + \int_0^{s^*} z^3(r)\,dr + \epsilon \geq z^2(s^*).\end{aligned}$$

But this implies that $\bar{z}(s^*) > z(s^*)$, which contradicts the assumption that $\bar{z}(s^*) = z(s^*)$. Hence, $\bar{z}(s) > z(s)$ for $s \in [0,1]$. Recalling that $\bar{z}(1) \leq 4\delta$, then we have obtained the desired estimate for $z(1)$. The constant δ_0 and function ϵ_0 were chosen to be

$$\delta_0 = \min\left\{\frac{1}{8}, \frac{1}{2 + 6\log 2}\right\}$$

and

$$\epsilon_0(\delta) = 2\delta^2(1 - 3\delta).$$

Because $\delta_0 < 1/3$, then the function $\epsilon_0(\delta)$ will be positive for $\delta \leq \delta_0$ as desired. ∎

We will now apply Lemma 1 to obtain estimates for $\mathcal{A}$. We let $0 < h \leq h_0$ be fixed and set

$$\begin{aligned}C_3 = C_2 \max(1, T_1 - \tau_0), &\qquad \epsilon = {C_3}^2 \psi_2(h), \\ s = \frac{t - \tau}{T_1 - \tau}, &\qquad z(s) = C_3 \mathcal{A}(t).\end{aligned}$$

The integral inequality (4.42) is then obtained by multiplying (4.41) by ${C_3}^2$ and substituting for $\mathcal{A}$, t and ψ_2. From the definition of $\mathcal{A}$ in terms of the continuous functions $\mathbf{z}_I$, $\mathbf{z}_{II}$ and X, it follows that $\mathcal{A}$ is continuous and consequently, z is continuous. Because $\psi_2 = o(1)$ as $h \to 0$, we may find

$h_1(\delta) \in (0, h_0]$ such that for $h \in [0, h_1(\delta)]$ we have

$$C_3{}^2 \psi_2(h) \leq \epsilon_0(\delta)$$

for $\delta > 0$ arbitrarily small.

We now prove a lemma that gives an upper bound for the comparison function evaluated at the endpoint, $\mathcal{A}(T_1)$, based on the value of $\mathcal{A}$ at some interior point.

Lemma 2. *Let $\delta \leq \min\{\frac{1}{8}C_3\tilde{Z}, \delta_0\}$ and $h \leq h_1(\delta)$. If*

$$\mathcal{A}(t) \leq \frac{1}{C_3}\delta \qquad \text{for some } t \in [\tau_0, T_1],$$

then

$$\mathcal{A}(T_1) \leq \frac{4}{C_3}\delta.$$

Proof. The integral inequality (4.41) holds, provided $\mathcal{A}(s) \leq \tilde{Z}$ for $s \in [\tau, t]$. We let $\tilde{T} \in (\tau_0, T]$ be the greatest value such that

$$\mathcal{A}(t) \leq \tilde{Z} \qquad \text{for } t \in (\tau_0, \tilde{T}].$$

Note from the continuity of $\mathcal{A}$ that if $\mathcal{A}(\tilde{T}) < \tilde{Z}$, then $\tilde{T} = T$. From Lemma 1 it follows immediately that

$$\mathcal{A}(\tilde{T}) \leq \frac{4}{C_3}\delta \leq \tfrac{1}{2}\tilde{Z}.$$

Hence, $\tilde{T} = T$ and the proof is complete. ∎

Letting $a_1 = a_0/C_3$, we know from (4.9) and (4.35) that

$$\mathcal{A}(T) \geq a_1 > 0.$$

Hence, we let

$$\delta = \min\left\{\tfrac{1}{8}C_3 a_1, \tfrac{1}{8}C_3\tilde{Z}, \delta_0\right\}.$$

The Lemma 2 implies that for $h \in (0, h_1(\delta)]$ we have

$$\mathcal{A}(t) \geq \frac{1}{C_3}\delta \qquad \text{for } t \in [\tau_0, T].$$

For if this does not hold for some $t \in [\tau_0, T]$ and $h \in (0, h_1(\delta)]$, we obtain from Lemma 2 that $\mathcal{A}(T) < a_1$, which contradicts that $\mathcal{A}(T) \geq a_1$.

4.4 The Main Result

We have shown that the comparison function $\mathcal{A}$ is bounded away from zero uniformly as $h \to 0$ on any interval $[\tau_0, \tau_1]$, with $\tau_0 > T_0$, $\tau_1 \leq T_1$. We now obtain the main result.

Theorem. *The following statement is* **false**: there exist sequences $\{h_n\}$, $\{u_n\}$, $\{v_n\}$, $n = 1, 2, \ldots$, satisfying

i) $h_n \to 0$ as $n \to \infty$;

ii) u_n, v_n are continuous solutions of the clamped circular plate problem, that is, the equations (4.2) with boundary conditions 4.3), with thickness h_n and fixed g, where g is twice continuously differentiable and $g(1) \neq 0$;

iii) for some $C > 0$ and points $\{x_n\}$, $0 < x_0 < x_n \leq 1$,

$$|v_n(x_n)| + |v_n{}'(x_n)| \leq C,$$

$$|u_n(x_n)v_n(x_n) - g(x_n)| + |h_n u_n{}'(x_n)| \to 0$$

as $n \to \infty$;

iv) for some $m > 0$, $v_n(x_n) \geq m$ for all n.

Proof. We assume the statement to be true and show that this assumption leads to a contradiction. We may extract a subsequence such that for some constants $\alpha > 0$, $\beta \geq 0$, and for some $\hat{x} \in [x_0, 1]$,

$$x_n \to \hat{x}, \qquad v_n(x_n) \to \alpha, \quad \text{and} \quad v_n{}'(x_n) \to \beta \quad \text{as } n \to \infty. \tag{4.45}$$

We know that $\beta \geq 0$ because of

$$v'(x) = x^{-3} \int_0^x \xi^3 u^2(\xi)\, d\xi \geq 0.$$

Also, $\alpha \geq m > 0$. Let v_0 be the solution of the Föppl membrane equation (2.1) satisfying $v_0(\hat{x}) = \alpha$, $v_0{}'(\hat{x}) = \beta$. Clearly, $v_0(x) \geq \alpha > 0$ for $x \geq \hat{x}$. Let $u_0 = g/v_0$.

Recall that we must choose x_0 such that $v_0(x_0) > 0$; because $v_0(\hat{x}) > 0$, we may choose $x_0 < \hat{x}$. For some integer N, if $n \geq N$, then $x_n > x_0$.

We form the sequences $\{\mathbf{z}_I^n\}$, $\{\mathbf{z}_{II}^n\}$ and $\{\mathcal{A}_n\}$ from the formulas (4.10), (4.24). Recall from the definition (4.24) of $\mathcal{A}_n$ that if $h_n \to 0$ and

$$\begin{aligned} &|v_n(x_n) - v_0(x_n)| + |v_n{}'(x_n) - v_0{}'(x_n)| \; + \\ &\qquad + |u_n(x_n)v_n(x_n) - g(x_n)| + |h_n u_n{}'(x_n)| \to 0 \end{aligned}$$

for $x_n \geq x_0 > 0$ as $n \to \infty$, then for points $\{t_n\}$ corresponding to the points $\{x_n\}$,

$$\mathcal{A}_n(t_n) \to 0 \qquad \text{as } n \to \infty.$$

Because v_0 and $v_0{}'$ are continuous, the formulas (4.45) and assumption (iii) imply that

$$\mathcal{A}_n(t_n) \to 0$$

where

$$T_1 \leq t_n = \int_{x_0}^{x_n} v_0{}^{\frac{1}{2}}(s)\, ds \geq 0 \qquad \text{for } n \geq N.$$

But we have the implication from Lemma 2 that $\mathcal{A}_n(t)$ is bounded uniformly away from zero for $t \in [0, T_1]$, and hence we have arrived at a contradiction; thus the proof is complete. ∎

Discussion. In Chapter 1 we saw that for the elastica with clamped edges, a similar result holds. It was shown that if the assumption $hu' \to 0$ as $h \to 0$ is relaxed to allow $hu' = O(1)$, then the asymptotic expansion (1.22) is obtained. In Chapter 3, we attempted to find a similar expansion under the assumption that $hu' = O(1)$. The leading order equation (3.54) for the stress is not the Föppl membrane equation in this case. In **Appendix I**, we show that the assumption $hu' \to 0$ as $h \to 0$ can be motivated physically from the assumption that the shear strains are negligible.

APPENDIX I

The von Kármán Plate Theory

As discussed in Chapter 1, we consider circular and annular plates undergoing radially symmetric deformation; a schematic of the deformation is shown in Figure (1.1). We denote by ϵ_r, ϵ_c, ϵ_z the normal strains in the radial, circumferential and vertical directions; σ_r, σ_c, σ_z are the corresponding stresses. In the von Kármán plate theory, shear strains are considered negligible. Following STOKER,[1] we adopt the nonlinear strains

$$\epsilon_r = \frac{d\rho}{dr} + \frac{1}{2}\left(\frac{dw}{dr}\right)^2, \qquad \epsilon_c = \frac{1}{r}\rho, \tag{I.1}$$

based on the assumptions that the displacements are small compared to the large dimension R of the plate and that the derivative of the horizontal displacement ρ is of the order of the square of the derivative of the vertical displacement w. The compatibility condition is obtained by eliminating ρ between the equations (I.1). Hence,

$$\epsilon_c + r\frac{d}{dr}\epsilon_c = \epsilon_r - \frac{1}{2}\left(\frac{dw}{dr}\right)^2. \tag{I.2}$$

We also make the assumption that at the middle surface $z = 0$, the shear strains ϵ_{rz} and ϵ_{cz} vanish with z to a power higher than the first; that is,

$$\epsilon_{rz} = O(z^2), \qquad \epsilon_{cz} = O(z^2).$$

This is somewhat more general than the standard assumption that the normals to the undeformed middle surface remain the normals to the deformed middle surface.

---

[1] *Nonlinear Elasticity*, 1968

In Cartesian coordinates, the equilibrium conditions from the resolution of forces at the middle surface, $z = 0$, that are parallel to the tangent plane are

$$\frac{d}{dx}\sigma_x + \frac{d}{dy}\tau_{xy} = 0, \qquad \frac{d}{dy}\sigma_y + \frac{d}{dx}\tau_{xy} = 0 \tag{I.3}$$

where σ_x and σ_y are the normal stresses in the horizontal directions x and y, respectively; τ_{xy} is the horizontal shear stress. Using

$$\sigma_x = \frac{x^2}{x^2+y^2}\sigma_r + \frac{y^2}{x^2+y^2}\sigma_c, \qquad \sigma_y = \frac{y^2}{x^2+y^2}\sigma_r + \frac{x^2}{x^2+y^2}\sigma_c,$$
$$\tau_{xy} = \frac{xy}{x^2+y^2}(\sigma_r - \sigma_c),$$

the conditions (I.3) reduce to

$$\sigma_r - \sigma_c + r\frac{d}{dr}\sigma_r = 0. \tag{I.4}$$

To satisfy this condition we let

$$\sigma_r = -\tilde{v}, \qquad \sigma_c = -\tilde{v} - r\frac{d\tilde{v}}{dr}.$$

According to standard notation, the Airy stress function ϕ is related to $\tilde{v}$ by

$$\tilde{v} = -\frac{1}{r}\frac{d\phi}{dr}. \tag{I.5}$$

Note that positive $\tilde{v}$ corresponds to compressive radial stress.

We assume the linear stress-strain relations

$$\begin{aligned}
\sigma_r &= \frac{E}{(1+\nu)(1-2\nu)}\Big((1-\nu)\epsilon_r + \nu\epsilon_c + \nu\epsilon_z\Big),\\
\sigma_c &= \frac{E}{(1+\nu)(1-2\nu)}\Big((1-\nu)\epsilon_c + \nu\epsilon_r + \nu\epsilon_z\Big),\\
\sigma_z &= \frac{E}{(1+\nu)(1-2\nu)}\Big((1-\nu)\epsilon_z + \nu\epsilon_r + \nu\epsilon_c\Big)
\end{aligned} \tag{I.6}$$

where E is Young's modulus and ν is Poisson's ratio. The normal stress in the vertical direction σ_z is

$$\sigma_z = (z + \tfrac{1}{2}H)\frac{p(r)}{H} + O(H^2)$$

where p is the pressure load. We assume $p = O(H/R)$, and so $\sigma_z = O(H/R)$. Thus, to leading order in H/R we have

$$\epsilon_z = -\frac{\nu}{1-\nu}(\epsilon_r + \epsilon_c). \tag{I.7}$$

Using (I.7) to eliminate ϵ_z from (I.6), the expressions for σ_r, σ_c now become

$$\sigma_r = \frac{E}{1-\nu^2}(\epsilon_r + \nu\epsilon_c), \qquad \sigma_c = \frac{E}{1-\nu^2}(\epsilon_c + \nu\epsilon_r).$$

Solving for the strains in terms of the stresses, we find

$$\begin{aligned} \epsilon_r &= \frac{1}{E}(\sigma_r - \nu\sigma_c) = \frac{-1}{E}\Big(\tilde{v} - \nu\frac{d}{dr}(r\tilde{v})\Big), \\ \epsilon_c &= \frac{1}{E}(\sigma_c - \nu\sigma_r) = \frac{-1}{E}\Big(\frac{d}{dr}(r\tilde{v}) - \nu\tilde{v}\Big). \end{aligned} \tag{I.8}$$

Substitution of (I.8) into the compatibility equation (I.2) gives

$$\frac{2}{E}\Big(r^2\frac{d^2\tilde{v}}{dr^2} + 3r\frac{d\tilde{v}}{dr}\Big) = \Big(\frac{dw}{dr}\Big)^2. \tag{I.9}$$

Letting

$$\tilde{u} = \frac{1}{r}\frac{dw}{dr}, \tag{I.10}$$

we have

$$\frac{2}{E}\Big(\frac{d^2\tilde{v}}{dr^2} + \frac{3}{r}\frac{d\tilde{v}}{dr}\Big) = \tilde{u}^2. \tag{I.11}$$

The relations (I.8) for the strains in terms of $\tilde{v}$ also give

$$\rho = \frac{-1}{E}(r^2\tilde{v}' + r(1-\nu)\tilde{v})$$

where we have utilized $\epsilon_c = r^{-1}\rho$.

We may obtain from (I.11) the compatibility condition in the form in which it is more commonly seen in the von Kármán plate theory. The equation (I.9) may be written in terms of the Airy stress function as

$$\frac{2}{E}\frac{d}{dr}\frac{1}{r}\frac{d}{dr}r\frac{d\phi}{dr}+\frac{1}{r}\left(\frac{dw}{dr}\right)^2=0. \tag{I.12}$$

The Laplacian for radially symmetric functions is

$$\nabla^2=\frac{1}{r}\frac{d}{dr}r\frac{d}{dr};$$

thus

$$\frac{2}{E}r\frac{d}{dr}\nabla^2\phi+\left(\frac{dw}{dr}\right)^2=0.$$

Differentiating once and dividing by $2r$, we obtain

$$\frac{1}{E}\nabla^4\phi+\frac{1}{r}\frac{d^2w}{dr^2}\frac{dw}{dr}=0, \tag{I.13}$$

which is the compatibility condition from the von Kármán plate theory when radial symmetry is assumed.

The compatibility condition (I.12) implies the equation (I.13), but the converse is not necessarily true. For if equation (I.13) is satisfied, then, multiplying by r and integrating once, we have

$$\frac{1}{E}r\frac{d}{dr}\frac{1}{r}\frac{d}{dr}r\frac{d\phi}{dr}+\frac{1}{2}\left(\frac{dw}{dr}\right)^2=C,$$

and this is equivalent to the equation (I.12) only if $C=0$.

The equilibrium equation obtained by resolving forces normal to the tangent plane is exactly the same as in the von Kármán plate theory derived without assuming radial symmetry. Thus,

$$\frac{E}{2}(\gamma H)^2\nabla^4w-\frac{1}{r}\frac{d}{dr}\left(\frac{d\phi}{dr}\frac{dw}{dr}\right)=\frac{p}{hR} \tag{I.14}$$

where $\gamma^2 = (6(1-\nu^2))^{-1}$. From the definitions (I.5, I.10) of $\tilde{v}$ and $\tilde{u}$, (I.14) is equivalent to

$$\frac{E}{2}(\gamma H)^2 \frac{1}{r}\frac{d}{dr} r \frac{d}{dr} \frac{1}{r}\frac{d}{dr} r^2 \tilde{u} + \frac{1}{r}\frac{d}{dr}(r^2 \tilde{u}\tilde{v}) = \frac{p}{hR}. \tag{I.15}$$

The equations (I.15, I.11) are further manipulated to reduce the order and to nondimensionalize the problem to obtain the equations (4.2) as described in Chapter 1.

In terms of the dimensionless variables x, u and v, the original variables evaluated at the midplane $z = 0$ are

$$\begin{gathered} r = xR, \\ w(r) = -R\tau \int_x^1 su(s)\,ds, \\ \rho(r) = \frac{-R\tau^2}{2}(x^2 v'(x) + x(1-\nu)v(x)), \\ \epsilon_r(r) = \frac{\tau^2}{2}(\nu x v'(x) - (1-\nu)v(x)), \\ \epsilon_c(r) = \frac{-\tau^2}{2}(xv'(x) + (1-\nu)v(x)), \\ \sigma_r(r) = \frac{-E\tau^2}{2}v(x), \qquad \sigma_c(r) = \frac{-E\tau^2}{2}(xv'(x) + v(x)), \end{gathered}$$

where

$$\tau^3 = \frac{\gamma^3 R}{HE} \cdot p(aR).$$

We will use the formulas above to discuss the validity of the assumptions used to derive the von Kármán plate theory for the asymptotic expansions that are derived in this dissertation. The first assumption we address is that the strains are small. It is easy to verify that the asymptotic expansions (3.34, 3.41) and (3.72) for circular plates and (3.42), (3.49) for annular plates yield, at $z = 0$,

$$\epsilon_r = O(\tau^2), \qquad \epsilon_c = O(\tau^2) \qquad \text{as } h,\ \tau \to 0;$$

that is, it is sufficient to require $\tau = o(1)$ as $h \to 0$ to obtain small strains at the midplane. The expansion (1.16) for large compressive edge load λ yields

$$\epsilon_r = O(\lambda\tau^2), \quad \epsilon_c = O(\lambda\tau^2) \quad \text{as } h,\, \tau \to 0.$$

Thus, we must have $\tau \ll \lambda^{-\frac{1}{2}}$ for the strains to be small. We must also check the validity of the assumption that the strains remain approximately constant throughout the thickness. From the assumption that the shear strains are negligible we have

$$\frac{\partial \rho}{\partial z} = -\frac{\partial w}{\partial r}.$$

Thus

$$\rho(r,z) \sim \rho(r,0) - z\,\frac{\partial w}{\partial r}.$$

From the formula (I.1) for the strains we have

$$\epsilon_r(r,z) \sim \epsilon_r(r,0) - z\,\frac{\partial^2 w}{\partial r^2},$$
$$\epsilon_c(r,z) \sim \epsilon_c(r,z) - z\,\frac{1}{r}\frac{\partial w}{\partial r}.$$

Thus, we must have

$$\frac{\partial^2 w}{\partial r^2} \ll \frac{1}{H}, \qquad \frac{1}{r}\frac{\partial w}{\partial r} \ll \frac{1}{H}$$

as $h,\, \tau \to 0$. This condition will be satisfied if

$$hxu'(x) \to 0 \quad \text{and} \qquad hu(x) \to 0 \quad \text{uniformly as } h \to 0.$$

If these conditions are not satisfied, we must question the validity of the assumption that the shear strains are negligible.

Thus, we see that the condition $|hu'| \to 0$ for $x > 0$, that appeared in the result presented in Chapter 4, is physically motivated by the assumption that the shear strains are negligible. We must also remark that the assumption $hu \to 0$ is violated for $x = O(h)$ in the construction (3.72), where the boundary layer appeared at the center of the plate. It may be possible to deal with these cases within the framework of a plate theory that accounts for shear strains.

APPENDIX II

Numerical Calculations for the Plate and Membrane Equations

For the numerical calculations, the plate and membrane equations are replaced by finite difference equations. In some applications, we need to approximate a particular membrane solution for which we specify either $v(0) = \alpha > 0$ or $v(1) = \lambda < 0$. As discussed in Chapter 2, these conditions specify unique membrane solutions. An iterative method is used to obtain these solutions. For some applications it was found to be helpful to use a nonuniform mesh. We generally calculate the solutions of the plate equations by the HOC continuation procedure; the exception is in Chapter 3 where the asymptotic expansion for the plate solution is used as an initial guess for the iteration procedure. The von Kármán plate equations are found to be particularly suitable for high-order continuation because of the simple structure of the nonlinearities. The asymptotic expansion for large stress is used to obtain a starting point for the continuation procedure and to enable us to calculate more than one solution branch. We also discuss the implementation of this method for the membrane equations in which we use numerical differentiation to obtain expansion coefficients. The methods described here are equally applicable to the annular membrane and plate problems.

Discretization. We will discuss the discretization for the circular plate elastically supported against rotation; the problem may be formulated similarly for circular plates with other boundary conditions, for annular plates with zero applied stress at the inner edge and circular or annular membranes.

The annular plate with nonzero stress at the inner edge has the additional complication that the constant A must be determined; we will not discuss numerical calculations for this case. The von Kármán plate equations (4.2) are equivalent to the first-order system

$$hz_1' = f_1(x, \mathbf{z}) \equiv z_2, \tag{II.1a}$$

$$h(x^3 z_2)' = f_2(x, \mathbf{z}) \equiv x^3(g(x) - z_1 z_3), \tag{II.1b}$$

$$z_3' = f_3(x, \mathbf{z}) \equiv z_4, \tag{II.1c}$$

$$(x^3 z_4)' = f_4(x, \mathbf{z}) \equiv x^3 z_1^2. \tag{II.1d}$$

The boundary conditions (1.6, 1.9, 1.10) become

$$\begin{aligned} z_2(0) &= 0, \qquad & z_2(1) + hQz_1(1) &= 0, \\ z_4(0) &= 0, \qquad & z_3(1) - \lambda &= 0. \end{aligned} \tag{II.2}$$

To obtain this form of the problem, we have made the transformation $u = z_1$, $hu' = z_2$ $v = z_3$, $v' = z_4$. The differential equations (II.1) are approximated by the finite difference equations

$$hD_+(\mathbf{Z}_{j,1}) - f_1\left(x_{j+1/2}, \mathbf{Z}_{j+1/2}\right) = 0, \tag{II.3a}$$

$$hD_+({x_j}^3\mathbf{Z}_{j,2}) - f_2\left(x_{j+1/2}, \mathbf{Z}_{j+1/2}\right) = 0, \tag{II.3b}$$

$$D_+(\mathbf{Z}_{j,3}) - f_3\left(x_{j+1/2}, \mathbf{Z}_{j+1/2}\right) = 0, \tag{II.3c}$$

$$D_+({x_j}^3\mathbf{Z}_{j,4}) - f_4\left(x_{j+1/2}, \mathbf{Z}_{j+1/2}\right) = 0, \tag{II.3d}$$

with

$$\begin{aligned} \mathbf{Z}_{0,2} &= 0, \qquad & \mathbf{Z}_{m,2} + hQ\mathbf{Z}_{m,1} &= 0, \\ \mathbf{Z}_{0,4} &= 0, \qquad & \mathbf{Z}_{m,3} - \lambda &= 0 \end{aligned} \tag{II.4}$$

where

$$D_+(y_j) = \frac{y_{j+1} - y_j}{x_{j+1} - x_j}, \qquad y_{j+1/2} = \frac{y_{j+1} + y_j}{2}$$

and the points$\{x_j\}$, $j = 0, \ldots, m$ satisfy

$$0 = x_0 < x_1 < \ldots < x_m = 1.$$

For the annular plate or membrane we have $x_0 = a$. The difference scheme employed here is essentially the box scheme with the slight variation that we include the factor x^3 in the difference quotient of the second and fourth equations. This was found to decrease significantly the error in the finite difference approximation as compared to the usual box scheme.

For the plate equations, a uniform mesh is most frequently employed. However, if nearly singular membrane solutions are to be calculated, a fine mesh is necessary near the point of singularity. Using a uniform grid in this case would unnecessarily increase the computing effort required. Also, we have observed that the accuracy of the finite difference approximation for the circular membrane equations is enhanced with a fine mesh near the origin, independent of the smoothness of the desired solution. This may be attributed to the equation's (2.1) having a singular point at the origin; the linearization of this equation has a solution with a singularity of $O(x^{-2})$.

To define a nonuniform grid, a transformation of the independent variable is chosen to help resolve the difficulties we expect to encounter. A uniform grid is applied in the new variable; then the secant method is used to solve for the corresponding values in x. For example, the circular membrane solutions are calculated on a nonuniform mesh obtained from the transformation

$$s(x) = \frac{a}{(x + \delta_0)^3} + \frac{b}{(1 - x + \delta_1)^{\frac{1}{3}}}$$

where a and b are fixed constants and δ_0, $\delta_1 > 0$ are parameters that tend to zero as the mesh interval vanishes.

The left-hand side of the equations (II.3, II.4), depending on the unknowns $\mathbf{Z} = [\mathbf{Z}_{j,k}]$ and λ, is denoted by $G(\mathbf{Z}, \lambda)$ for the remainder of the chapter.

Iterations for Membrane Solutions. We first discuss the case where we wish to obtain a numerical solution of the circular membrane equations (2.1), satisfying

$$z_1(0) = \alpha > 0, \qquad z_2(0) = 0;$$

that is, we specify the stress at the center of the membrane. This can be considered as an initial value problem and solved accordingly. The only difficulty is that for the circular membrane the initial data are given at the singular point, and so the usual schemes are not valid for the first step. This is resolved by using the expansion about the origin to obtain values of z_1 and z_2 at a nearby point $x_1 > 0$.

Normally, this method is not used, but instead we use a form of constrained Newton's method. We take as an initial guess

$$\mathbf{Z}_{j,1} = \left(\tfrac{3}{4}x_j + \alpha^{\frac{3}{2}}\right)^{\frac{2}{3}},$$
$$\mathbf{Z}_{j,2} = \tfrac{1}{2}\left(\tfrac{3}{4}x_j + \alpha^{\frac{3}{2}}\right)^{-\frac{1}{3}}.$$

This initial guess contains certain aspects of the behavior of the membrane solutions at both ends of the compressive solution branch:

$$z_1(x) \sim \alpha, \qquad z_2(x) \to 0 \qquad \text{as } \alpha \to +\infty,$$
$$z_1(x) \sim \left(\tfrac{3}{4}x\right)^{\frac{2}{3}}, \quad z_2(x) \sim \tfrac{1}{2}\left(\tfrac{3}{4}x\right)^{-\frac{1}{3}}, \qquad \text{as } \alpha \to 0^+,\ x \to 0.$$

Letting G be the set of finite difference equations for the membrane equation, then the iterations are as follows:

$$G_{\mathbf{Z}}(\mathbf{Z}^n, \lambda^n)d\mathbf{Z}^n + G_\lambda(\mathbf{Z}^n, \lambda^n)d\lambda^n = -G(\mathbf{Z}^n, \lambda^n), \tag{II.5}$$

$$d\mathbf{Z}^n_{0,1} = 0. \tag{II.6}$$

The equation (II.5) is the usual linearization condition; the equation (II.6) is the condition that the stress remains fixed at the center. The equivalent problem for the annular membrane has the boundary conditions

$$z_1(a) = \eta > 0, \qquad z_2(a) = \alpha.$$

For the annular membrane we have instead of (II.6) the condition

$$d\mathbf{Z}^n_{0,2} = 0. \tag{II.7}$$

The procedure is observed to be convergent for both annular and circular membranes, provided the mesh is sufficiently fine.

Iterations from an Asymptotic Expansion for Plate Solutions. In Chapter 3 we compare the asymptotic expansions (3.34, 3.41) to plate solutions calculated numerically. We describe in this section the method by which these plate solutions are obtained. We take the asymptotic approximation evaluated at the grid points x_j as an initial guess and then apply an iterative method of constrained Newton type. The discretized plate equations are referred to as $G(\mathbf{Z}, \lambda)$. To determine the correction $d\mathbf{Z}^n$, $d\lambda^n$ to be applied to the nth iterate $\mathbf{Z}^n$, λ^n, we take the linearization condition (II.5) as well as the constraint

$$\langle c^n, d\mathbf{Z}^n \rangle + d\lambda^n = 0$$

where

$$G_{\mathbf{Z}}(\mathbf{Z}^n, \lambda^n)\mathbf{c}^n + G_\lambda(\mathbf{Z}^n, \lambda^n) = 0.$$

This equation implies that the correction will be orthogonal (in the sense of whatever inner product is chosen) to the level curve of G passing through the

nth iterate $\mathbf{Z}^n$, λ^n. The inner product we choose corresponds to quadrature over $x \in [0,1]$ using the trapezoidal rule; that is,

$$\langle \mathbf{y}, \mathbf{z} \rangle = \frac{1}{8} \sum_{k=1}^{4} \sum_{i=0}^{m-1} (x_{j+1} - x_j)(\mathbf{y}_{j+1,k}\mathbf{z}_{j+1,k} + \mathbf{y}_{j,k}\mathbf{z}_{j,k}). \tag{II.8}$$

Divergence is observed only near the points where the uniform asymptotic approximation breaks down; the condition for the breakdown is discussed in Chapter 3.

High-Order Continuation. Continuation is a numerical method for obtaining 1-parameter families of solutions of a set of equations. We will discuss the general problem

$$G(\mathbf{Z}, \lambda) = 0 \tag{II.9}$$

where $\mathbf{Z}$ is an n-vector, λ is a scalar and $G : \mathbb{R}^n \times \mathbb{R} \to \mathbb{R}^n$ is a smooth vector function. To construct a continuation step, we assume that a solution $\mathbf{Z}_0$, λ_0 of (II.9) is known. If this solution is a regular point of G, then a continuous branch of solutions of (II.9) exists passing through $\mathbf{Z}_0$, λ_0. The solution branch may be parameterized in terms of a scalar parameter s, $s \in [0, S]$, where $\mathbf{Z}(0) = \mathbf{Z}_0$, $\lambda(0) = \lambda_0$. For example, s may represent arclength or pseudo-arclength.[1,2] The continuation step gives an approximation $\mathbf{Z}_A$, λ_A to a point $\mathbf{Z}(s)$, $\lambda(s)$ for some s, $0 < s \leq S$. We prepare for the next continuation step by solving iteratively for a solution of (II.9), using $\mathbf{Z}_A$, λ_A as the initial guess.

The most frequently employed continuation methods are first-order accurate; that is, the approximate solution $\mathbf{Z}_A$, λ_A satisfies

$$G(\mathbf{Z}_A, \lambda_A) = O(s^2).$$

---

[1] H. B. Keller, *Applications of Bifurcation Theory*, 1977

[2] Ibid., *Recent Advances in Numerical Analysis*, 1979

The first-order continuation method is performed by finding nontrivial $\mathbf{Z}_1$, λ_1 such that

$$G(\mathbf{Z}_0 + \mathbf{Z}_1 s, \lambda_0 + \lambda_1 s) = O(s^2). \tag{II.10}$$

For example, in the Euler pseudo-arclength procedure we take

$$\mathbf{Z}_1 = -\frac{G_{\mathbf{Z}}^{-1}(\mathbf{Z}_0, \lambda_0) G_\lambda(\mathbf{Z}_0, \lambda_0)}{R}, \qquad \lambda_1 = \frac{1}{R} \tag{II.11}$$

where R is chosen such that $\langle \mathbf{Z}_1, \mathbf{Z}_1 \rangle + {\lambda_1}^2 = 1$ for some inner product $\langle \cdot, \cdot \rangle$ on $I\!R^n$. This formula is valid except for points where $G_{\mathbf{Z}}$ is singular; bifurcation theory[3] yields formulas for the coefficients $\mathbf{Z}_1$, λ_1 at some types of singular points. Then we let

$$\mathbf{Z}_A = \dot{\mathbf{Z}}_0 + \mathbf{Z}_1 s^{\cdot}, \qquad \lambda_A = \lambda_0 + \lambda_1 s^{\cdot},$$

where $s^{\cdot}$ is taken sufficiently small that the new solution is obtainable from the approximant by the chosen iterative method, usually within a prescribed number of iterations.

A natural generalization of this technique to obtain a higher order of accuracy in the continuation step is to let

$$\mathbf{Z}_A = \sum_{j=0}^{N} \mathbf{Z}_j s^{\cdot j}, \qquad \lambda_A = \sum_{j=0}^{N} \lambda_j s^{\cdot j}$$

where the coefficients $\mathbf{Z}_j$, λ_j are chosen such that

$$G\Big(\sum_{j=0}^{M} \mathbf{Z}_j s^j, \sum_{j=0}^{M} \lambda_j s^j \Big) = O(s^{M+1}) \quad \text{for } M = 1, \ldots, N. \tag{II.12}$$

Note that by letting $M = 1$, (II.12) reduces to the first-order condition (II.10).

---

[3] H. B. Keller and W. Langford, *Arch. Rat. Mech. Anal.* **48** (1972)

Let $\mathbf{Z}_1$, λ_1 be defined as in first-order pseudo-arclength continuation. We now derive the following formula for $\mathbf{Z}_M$, λ_M, $M \geq 2$:

$$\begin{aligned} G^0_{\mathbf{Z}}\mathbf{Z}_M + G^0_{\lambda}\lambda_M &= -\frac{1}{M!}\frac{d^M}{ds^M}G\Big(\sum_{j=0}^{M-1}\mathbf{Z}_j s^j, \sum_{j=0}^{M-1}\lambda_j s^j\Big)\Big|_{s=0} \\ &= F_M(\mathbf{Z}_0, \ldots, \mathbf{Z}_{M-1}, \lambda_0, \ldots, \lambda_{M-1}) \end{aligned} \tag{II.13}$$

where

$$G^0_{\mathbf{Z}} = G_{\mathbf{Z}}(\mathbf{Z}_0, \lambda_0), \qquad G^0_{\lambda} = G_{\lambda}(\mathbf{Z}_0, \lambda_0).$$

Let the sequences $\{\mathbf{Z}_M\}$, $\{\lambda_M\}$, $M = 2, 3, \ldots$, satisfy (II.13). We wish to show that (II.12) holds for $M \geq 1$. This may be verified by induction. Recall from (II.10) that

$$G(\mathbf{Z}_0 + \mathbf{Z}_1 s, \lambda_0 + \lambda_1 s) = O(s^2).$$

Thus, (II.12) holds for $M = 1$. Now suppose (II.12) has been verified for 1, $\ldots$, $M-1$. Then

$$\begin{aligned} G\Big(\sum_{j=0}^{M}\mathbf{Z}_j s^j, \sum_{j=0}^{M}\lambda_j s^j\Big) =& G\Big(\sum_{j=0}^{M-1}\mathbf{Z}_j s^j, \sum_{j=0}^{M-1}\lambda_j s^j\Big) + \\ &+ G_{\mathbf{Z}}\Big(\sum_{j=0}^{M-1}\mathbf{Z}_j s^j, \sum_{j=0}^{M-1}\lambda_j s^j\Big)\mathbf{Z}_M s^M + \\ &+ G_{\lambda}\Big(\sum_{j=0}^{M-1}\mathbf{Z}_j s^j, \sum_{j=0}^{M-1}\lambda_j s^j\Big)\lambda_M s^M + O(s^{M+1}). \end{aligned}$$

From the induction hypothesis we have

$$G\Big(\sum_{j=0}^{M-1}\mathbf{Z}_j s^j, \sum_{j=0}^{M-1}\lambda_j s^j\Big) = \frac{s^M}{M!}\frac{d^M}{ds^M}G\Big(\sum_{j=0}^{M-1}\mathbf{Z}_j s^j, \sum_{j=0}^{M-1}\lambda_j s^j\Big)\Big|_{s=0} + O(s^{M+1}).$$

Also, because G is smooth, we have

$$\begin{aligned} G_{\mathbf{Z}}\Big(\sum_{j=0}^{M-1}\mathbf{Z}_j s^j, \sum_{j=0}^{M-1}\lambda_j s^j\Big) &= G^0_{\mathbf{Z}} + O(s), \\ G_{\lambda}\Big(\sum_{j=0}^{M-1}\mathbf{Z}_j s^j, \sum_{j=0}^{M-1}\lambda_j s^j\Big) &= G^0_{\lambda} + O(s). \end{aligned}$$

Hence,

$$G\Big(\sum_{j=0}^{M}\mathbf{Z}_j s^j, \sum_{j=0}^{M}\lambda_j s^j\Big) = \frac{s^M}{M!}\frac{d^M}{ds^M}G\Big(\sum_{j=0}^{M-1}\mathbf{Z}_j s^j, \sum_{j=0}^{M-1}\lambda_j s^j\Big)\Big|_{s=0} + \\ + G^0_{\mathbf{Z}}\mathbf{Z}_M s^M + G^0_\lambda \lambda_M s^M + O(s^{M+1}).$$

From the formula (II.13) for $\mathbf{Z}_M$ and λ_M, we thus obtain

$$G\Big(\sum_{j=0}^{M}\mathbf{Z}_j s^j, \sum_{j=0}^{M}\lambda_j s^j\Big) = O(s^{M+1})$$

as desired.

The coefficients are not determined uniquely by the conditions (II.13). If we impose the additional constraints

$$\langle \mathbf{Z}_1, \mathbf{Z}_M\rangle + \lambda_1\lambda_M = 0 \qquad \text{for } M \geq 2, \tag{II.14}$$

then the coefficients are well-defined to all orders provided $\mathbf{Z}_0$, λ_0 is a regular or simple fold point of the solution branch.

In the implementation of this method, we solve for $\mathbf{Z}_M$, λ_M using the bordering algorithm.[4] Note that in determining each coefficent we must solve a linear system of the form

$$G^0_{\mathbf{Z}}\mathbf{a} = \mathbf{b}.$$

Thus, we perform one LU factorization on $G^0_{\mathbf{Z}}$; to calculate each coefficient we must perform one backsolve. The problems we wish to solve arise from the discretization of a differential equation; thus, $G^0_{\mathbf{Z}}$ is a band matrix. The LINPACK subroutine for LU factorization of a general band matrix is used as needed.

---

[4] H. B. Keller, *SIAM J. Sci. Stat. Comput.* **4** (1983)

The pseudo-arclength variable $\hat{s}$ is defined by

$$\hat{s} = \langle \mathbf{Z}_1, \mathbf{Z} - \mathbf{Z}_0 \rangle + \lambda_1(\lambda - \lambda_0).$$

We note that

$$\hat{s} = \sum_{j=1}^{M-1} \langle \mathbf{Z}_1, \mathbf{Z}_j \rangle \, s^j + \sum_{j=1}^{M-1} \lambda_1 \lambda_j s^j = (\langle \mathbf{Z}_1, \mathbf{Z}_1 \rangle + {\lambda_1}^2) s = s.$$

Thus, under the constraints (II.14), s is the pseudo-arclength parameter.

Implementation of HOC for the Plate Equations. The high-order continuation method described in the previous section is particularly effective for the von Kármán plate equations. The function G is obtained from the finite difference equations (II.3, II.4). The unknown $\mathbf{Z}$ is the discrete solution; λ is the specified value of $\mathbf{Z}_{m,3}$ and represents the edge load. The inner product we choose is given by (II.8).

To obtain a starting point for continuation, we use the large stress asymptotic expansions for the plate solutions. In the asymptotic limit $\lambda \to -\infty$ the boundary layer construction (1.15) becomes

$$v \sim \lambda, \qquad u \sim \frac{g(x)}{\lambda} - \frac{h\kappa}{\sqrt{-\lambda}} \exp - \frac{\sqrt{-\lambda}}{h}(1 - x) \tag{II.15}$$

where

$$\kappa = \frac{g'(1) + Qg(1)}{\lambda(1 + hQ/\sqrt{-\lambda})}.$$

For large compressive stress, the asymptotic expansion (1.16) may be used to obtain a starting point at which the stress is everywhere compressive.

Recalling the equations determining the expansion coefficients (II.13), we see that to implement the HOC procedure it is necessary to evaluate the function F_M at each order M. To illustrate, we take a particular element of

F_M corresponding to an element of G, where the nonlinear contribution has the form

$$(x_{j+1/2})^3 U_{j+1/2} V_{j+1/2}$$

where $U_j = \mathbf{Z}_{j,1}$ and $V_j = \mathbf{Z}_{j,3}$; This term appears in the discretization of the equilibrium equation (4.2a). Let the expansion for U_j and V_j

$$\sum_{k=0}^{M-1} U_{j,k} s^k, \qquad \sum_{k=0}^{M-1} V_{j,k} s^k$$

be known to order $M-1$ for $j = 0, \ldots, m$. Then the chosen element of F_M is given by

$$-(x_{j+1/2})^3 \sum_{k=1}^{M-1} U_{j+1/2,k} V_{j+1/2,M-k}.$$

Clearly, such formulas can be evaluated efficiently as long as the highest order of the expansion N is not too large. In practice, we choose $N \leq 10$.

We have seen that the plate solutions lie on an infinite number of distinct branches. To calculate several branches, we make use of the observation that as $\lambda \to +\infty$ on a particular branch, the solution approaches the purely buckled state, that is, the solutions of (4.2) for $g(x) \equiv 0$. When there is no pressure load on the plate, a symmetry exists with respect to the vertical deflection: the plate can buckle up as easily as it can buckle down. Thus, in the case of vanishing pressure load, if we have a buckled state $v(x)$, $u(x)$, then there also exists a buckled state given by $v(x)$, $-u(x)$. In the case of nonvanishing pressure load, when the applied edge load becomes large, the effect of the pressure load is of lower order. Thus, there are distinct branches n, $n+1$ that are related by

$$u_{n+1}(x) \approx -u_n(x), \qquad v_{n+1}(x) \approx v_n(x);$$

for λ sufficiently large, we may obtain an approximate solution on the $(n+1)$st branch from a solution on the nth branch.

Implementation of HOC for the Membrane Equation. In the implementation of the HOC method for the plate problem, the functions F_M could be easily expressed in closed form for arbitrary M. For the membrane problem the formulas are not simple, and so we choose to estimate F_M numerically. Recall from (II.13) that

$$F_M(\mathbf{Z}_0, \ldots, \mathbf{Z}_{M-1}, \lambda_0, \ldots, \lambda_{M-1}) = -\frac{1}{M!}\frac{d^M}{ds^M} G\Big(\sum_{j=0}^{M-1} \mathbf{Z}_j s^j, \sum_{j=0}^{M-1} \lambda_j s^j\Big)\Big|_{s=0}.$$

We could expand the derivative in terms of the partials of G with respect to $\mathbf{Z}$ and λ, but for numerical purposes we are better off not doing this. For if we have already calculated $\mathbf{Z}_1$, λ_1, ..., $\mathbf{Z}_{M-1}$, λ_{M-1}, then we can simply estimate the derivative using standard difference quotient methods for functions of a single real variable; the applicability of FFT methods[5] for numerical differentiation of functions of a single complex variable is under investigation.

As a starting point, a solution of $G(\mathbf{Z}, \lambda) = 0$ on the branch that we wish to calculate is obtained from the large stress asymptotic expansion

$$v(x) \sim \lambda \qquad \text{for } |\lambda| \gg 1.$$

True Arclength Parameterization. The choice of pseudo-arclength parameterization is found to be appropriate for continuation purposes; for other purposes the true arclength may be a better choice for the parameter. A series expansion can be used to obtain analytical information about the solution

[5] See B. Fornberg, *ACM-Trans. Math. Softw.* **7** (1981)

branch. Van Dyke[6] uses an exact series expansion in terms of the Dean number K for the problem of flow through a loosely coiled pipe to study the behavior of the solutions as $K \to \infty$. For this sort of application, it is necessary to obtain an expansion that is convergent at the point of interest. A first step toward obtaining such an expansion is to choose a parameterization so that there are no singularities on the real line between the origin of the expansion and the point of interest. After this expansion is obtained, manipulations such as the Euler transformation may be applied to try to get the required convergence properties. Parameterization in terms of true arclength along a smooth solution branch allows no singularities for real values of the parameter; thus, the true arclength may be a suitable parameter for analytical studies.

The coefficients $\mathbf{Z}_1$, λ_1 for true arclength parameterization are given by (II.11); they are identical to those of pseudo-arclength. The coefficients of $\mathbf{Z}_M$, λ_M for $M \geq 2$ are found by applying the condition (II.13) as well as the constraint

$$\langle \mathbf{Z}_1, \mathbf{Z}_M \rangle + \lambda_1 \lambda_M = -\frac{1}{M} \sum_{j=2}^{M-1} j(M+1-j)\Big(\langle \mathbf{Z}_j, \mathbf{Z}_{M+1-j} \rangle + \lambda_j \lambda_{M+1-j} \Big) \qquad \text{(II.16)}$$

for $M = 2, 3, \ldots$. Letting

$$\mathbf{Z}(s) = \sum_{j=0}^{N} \mathbf{Z}_j s^j, \qquad \lambda(s) = \sum_{j=0}^{N} \lambda_j s^j,$$

then the equation (II.16) implies that

$$\Big\langle \frac{d}{ds}\mathbf{Z}(s), \frac{d}{ds}\mathbf{Z}(s) \Big\rangle + \Big(\frac{d}{ds}\lambda(s) \Big)^2 = 1 + O(s^N).$$

Although the arclength parameterization will have no singularities on the real line when the solution branch is smooth, the singularities that appear

[6] *J. Fluid Mech.* **86** (1978)

for some complex values generally cause the radius of convergence to be less than that of the pseudo-arclength expansion; thus, true arclength is probably not a good parameter for high-order continuation purposes.

Operation Count. Many ODE's and PDE's arising from physical applications have polynomial nonlinearities of low degree. For example, the Navier-Stokes equations have quadratic nonlinearities. For such problems, the function F_M can be calculated in a manner similar to the calculation for the plate equations. We carry out an operation count for a typical PDE application of the HOC method. Let the domain of the independent variables be m-dimensional. With a mesh spacing of order $1/n$, the solution vector will have $O(n^m)$ components. For a PDE with polynomial nonlinearites of degree at most P, the operation count for the direct evaluation of F_M is $O(M^{P-1} \cdot n^m)$. Each coefficient evaluation requires a back-solve of the LU factorization of $G^0_{\mathbf{Z}}$. This requires $O(n^{2m-1})$ operations. The LU factorization itself requires $O(n^m \cdot n^{2m-2})$ operations, that is, the size of the solution vector times the square of the band width, which is typically $O(n^{m-1})$. The LU factorization is carried out an $O(1)$ number of times for each continuation step. Thus, we expect the operation count for one compete continuation step of order N, including the iterations for the new solution, to be $O(N^P \cdot n^m + N \cdot n^{2m-1} + n^{3m-2})$. It has been observed in our calculations that the length of a continuation step of order N is typically a multiple $R(N) \geq 1$ of the first-order continuation step, the factor R being essentially independent of the mesh size for a particular application. Thus, to calculate a given segment of the solution branch requires

$$O\left(\frac{1}{R(N)}(N^P \cdot n^m + N \cdot n^{2m-1} + n^{3m-2})\right) \tag{II.17}$$

operations.

For $m = 1$, the estimate (II.17) suggests that there is an optimal choice of N independent of the grid size for a particular application. For the membrane problem this is observed to be about 2, while for the plate problem the optimal value is about 7. For $m > 1$, (II.17) suggests that the optimal value of N will increase as n increases; in practice, it is not feasible to take N arbitrarily large because of storage considerations and round-off in the calculation of high-order coefficients. For fixed N, the extra work involved in calculating the expansion coefficients is of smaller order as $n \to \infty$ than the work involved in the iterations; the acceleration should approach the factor $R(N)$ as n increases. We cannot predict the magnitude of the factor $R(N)$; however, for the plate problem, $R(7)$ was frequently around 4 or 5. Thus, the prospect for application to other ODE's and also PDE's is very good. Application of this method to equations with more complicated nonlinearities may be feasible if numerical differentiation as described for the membrane problem is employed for the calculation of the functions F_M.

Bibliography

[1] Bender, C. M. and S. A. Orzag,
Advanced Mathematical Methods for Scientists and Engineers, McGraw-Hill, New York, 1978.

[2] Berger, M. S.,
"On von Kármán's equations and the buckling of a thin elastic plate, I, the clamped plate," *Comm. Pure Appl. Math.* **20**, 687–719 (1967).

[3] Berger, M. S. and P. C. Fife,
"On von Kármán's equations and the buckling of a thin elastic plate, II, plate with general edge condition," *Comm. Pure Appl. Math.* **21**, 227–241 (1968).

[4] Bodner, S. R.,
"The post buckling behavior of a clamped circular plate," *Q. Appl. Math.* **12**, 397–401 (1955).

[5] Bromberg, E.,
"Non-linear bending of a circular plate under normal pressure," *Comm. Pure Appl. Math.* **9**, 633–659 (1956).

[6] Callegari, A. J. and E. L. Reiss,
"Non-linear boundary value problems for the circular membrane," *Arch. Rat. Mech. Anal.* **31**, 390–400 (1968).

[7] Callegari, A. J., E. L. Reiss, and H. B. Keller,
"Membrane buckling: a study in solution multiplicity," *Comm. Pure Appl. Math.* **24**, 499–527 (1971).

[8] Dickey, R. W.,
"Nonlinear bending of circular plates," *SIAM J. Appl. Math.* **30**, 1–9 (1976).

[9] Fier, J. M.,
"Equilibrium chaos," Ph. D. Thesis: Part II, California Institute of Technology, 70–82, 1985.

[10] Fife, P.,
"Non-linear deflection of thin elastic plates under tension," *Comm.*

Pure Appl. Math. **14**, 81–112 (1961).

[11] Föppl, A.,
Vorlesungen über technische Mechanik, Vol. 5, Leipzig: Teubner, 1907.

[12] Fornberg, B.,
"CPSC: complex power series coefficients," *ACM-Trans. Math. Softw.* **7**, 542–547 (1981).

[13] Friedrichs, K. O. and J. J. Stoker,
"The non-linear boundary value problem of the buckled plate," *Amer. J. Math.* **63**, 839–888 (1941).

[14] Fröman, N. and P. O. Fröman,
JWKB Approximation; Contributions to the Theory, North-Holland Publishing Company, Amsterdam, 1965.

[15] Grabmüller, H. and H. J. Weinitschke,
"Finite displacements of annular elastic membranes," *J. Elast.* , to appear.

[16] Hoppensteadt, F.,
"Properties of solutions of ordinary differential equations with small parameters," *Comm. Pure Appl. Math.* **24**, 807–840 (1971).

[17] Huang, C. L.,
"Postbuckling of an annulus," *AIAA J.* **11**, 1608–1612 (1973).

[18] John, F.,
"Uniqueness of non-linear elastic equilibrium for prescribed boundary displacements and sufficiently small strain," *Comm. Pure Appl. Math.* **25**, 617–634 (1972).

[19] ——,
"Rotation and strain," *Comm. Pure Appl. Math.* **14**, 391–413 (1961).

[20] Keener, J. P. and H. B. Keller,
"Perturbed bifurcation and buckling of circular plates," in *Lecture Notes in Mathematics 280: Conference on the Theory of Ordinary and Partial Differential Equations*, 286–293, Springer, Berlin, New York, 1972.

[21] Keller, H. B.,
"Buckling of a circular plate under an unusual combined load," *SIAM J. Appl. Math.* **14**, 1275–1292 (1966).

[22] ——,
"Numerical solution of bifurcation and nonlinear eigenvalue problems,"

in *Applications of Bifurcation Theory*, P. Rabinowitz, editor, Academic Press, New York, 1977, pp. 359–384.

[23] ——,
"Global homotopies and Newton methods," in *Recent Advances in Numerical Analysis*, C. deBoor and G. H. Golub, editors, Academic Press, New York, 1979, pp. 73–94.

[24] ——,
"The bordering algorithm and path following near singular points of higher nullity," *SIAM J. Sci. Stat. Comput.* **4**, 573–582 (1983).

[25] Keller, H. B., J. B. Keller, and E. L. Reiss,
"Buckled states of circular plates," *Q. Appl. Math.* **20**, 55–65 (1962).

[26] Keller, H. B. and W. Langford,
"Iterations, perturbations and multiplicities for nonlinear bifurcation problems," *Arch. Rat. Mech. Anal.* **48**, 83–108 (1972).

[27] Kosecoff, M. A.,
"Some problems in nonlinear elasticity," Ph. D. Thesis, California Institute of Technology, 1975.

[28] Kreiss, H.-O.,
"Problems with different time scales for ordinary differential equations," *SIAM J. Numer. Anal.* **16**, 980–998 (1979).

[29] Majumdar, S.,
"Buckling of a thin annular plate under uniform compression," *AIAA J.* **9**, 1701–1707 (1971).

[30] Mansfield, E. H.,
The Bending and Stretching of Plates, Pergamon Press, New York, 1964.

[31] Perozzi, D. J.,
"Analysis of optimal step size selection in homotopy and continuation methods," Ph. D. Thesis, California Institute of Technology, 1980.

[32] Srubshchik, L. S.,
"On the existence of a solution to the membrane problem of the equilibrium of a circular membrane," *Prikl. Mat. Mekh.* **30**, 576–579 (1966). Translation in *J. Appl. Math. Mech.* **30**, 685–689 (1966).

[33] Srubshchik, L. S. and V. I. Yudovich,
"Asymptotic treatment of the equations for large bending of a symmet-

rically loaded circular plate," *Dokl. Akad. Nauk SSSR* **139**, 341–344 (1961). Translation in *Sov. Phys.-Dokl.* **6**, 634–637 (1962).

[34] Stoker, J. J.,
Nonlinear Elasticity, Nelson, London, 1968.

[35] Van Dyke, M.,
"Extended Stokes series: laminar flow through a loosely coiled pipe," *J. Fluid Mech.* **86**, 129–145 (1978).

[36] von Kármán, T.,
"Festigkeitsprobleme im Maschinenbau," *Encyk. Math. Wissen.*, Vol. IV-4, Teubner, Leipzig, 1910.

[37] Wan, F. Y. M. and H. J. Weinitschke,
"Boundary layer solutions for some nonlinear elastic membrane problems," *Tech. Rep.* **85-7**, Dept. Appl. Math., University of Washington, Seattle, W. A., 1985.

[38] Wolkowisky, J. H.,
"Existence of buckled states of circular plates via the Schauder fixed point theorem," in *Bifurcation Theory and Nonlinear Eigenvalue Problems*, J. B. Keller and S. Antman, editors, 1969, pp. 49–68.

[39] Yanowitch, M,
"Non-linear buckling of circular elastic plates," *Comm. Pure Appl. Math.* **9**, 661–672 (1956).